



Polytechnic University of Marche
Ph.D. School in Engineering Sciences
Curriculum in Civil, Environmental, Building Engineering and Architecture

Influence of FE modelling on typical and specific vulnerabilities of RC school buildings

Ph.D. Dissertation of:

Valentina Gazzani

Advisor:

Prof. Stefano Lenci

Co-Advisor:

Prof. Francesco Clementi

Curriculum supervisor:

Prof. Stefano Lenci

XXXI cycle

Polytechnic University of Marche
Department of Civil and Building Engineering and Architecture
Via Brezze Bianche 12 - 60131 - Ancona, Italy

Acknowledgements

I'm grateful to Professor Stefano Lenci, Professor Francesco Clementi, Professor Giuseppe Pace and Architect Stefano Ciarloni (municipality of Trecastelli) for their support and for giving me the opportunity to attend this Ph.D. course.

Abstract

The vulnerability assessment of existing school buildings against earthquakes represents a priority concern for the society in seismic countries.

Since structures belonging to the same type and construction period may share similar features, it was possible to point out typical and specific seismic vulnerabilities related to different school architectural layouts for buildings that host the lower levels of the Italian education system.

Firstly, to estimate the performance of buildings in a fast way, the vulnerability of each school building belonging to the municipality of Trecastelli was assessed, adopting a lumped plasticity approach and a nonlinear static procedure.

With the aim of quantifying the effective influence of these vulnerabilities detected on the global seismic behaviour, a RC school building was chosen and three different models were implemented correspond to as many different approaches affected by various limitations in the representativeness respect to the reality.

The different modelling technique used follow the lumped plasticity, the distributed plasticity (fibre model) and the 3D Continuum FE approaches.

Nonlinear static (pushover) analyses were performed to assess the global seismic behaviour of the structure.

The comparison of the numerical results has shown that the fibre model is the least suitable mean to represent the shear problems of the case study. Instead, the lumped plasticity model is closer to reality than the previous one but not precise enough to consider the concomitance of bending, shear and axial force and the interaction between them in the inelastic response.

Of course, the 3D Continuum model is much more accurate than other models to describe the mechanisms developed in the joint panels which are very complex and combined.

Finally, the effectiveness of a possible CFRP local strengthening intervention for the case study limited to confine the unconfined beam-column joints was also considered.

Keywords:

School buildings · Nonlinear static analyses · 3D Continuum FE model · Distributed plasticity model · Beam-column joints

Sommario

La valutazione della vulnerabilità degli edifici scolastici esistenti nei confronti dei terremoti è un'esigenza di primaria importanza per la società in Italia.

Poiché, generalmente, strutture dello stesso tipo e medesimo periodo di costruzione presentano caratteristiche simili, è stato possibile evidenziare le vulnerabilità tipiche e specifiche per differenti layout architettonici individuabili in scuole dell'infanzia, primarie e secondarie di I grado.

Inizialmente, per una stima rapida delle prestazioni degli edifici, è stata valutata la vulnerabilità sismica di ciascun edificio scolastico ubicato nel comune di Trecastelli, adottando modelli ad aste a plasticità concentrata ed analisi statiche non lineari.

Successivamente, per quantificare l'effettiva influenza delle vulnerabilità rilevate sul comportamento globale, è stato scelto un edificio scolastico in c.a. e realizzati tre modelli corrispondenti ad altrettanti approcci di modellazione affetti da diverse limitazioni di rappresentazione dei fenomeni reali.

Per tale scopo, sono stati impiegati approcci a plasticità concentrata, a plasticità diffusa (modellazione a fibre) e al continuo con elementi solidi.

Il confronto dei risultati numerici ottenuti da analisi pushover ha mostrato l'inadeguatezza del modello a fibre nella rappresentazione dei problemi di taglio del caso studio.

Diversamente, il modello a plasticità concentrata si è rivelato più aderente alla realtà di quello a fibre ma non abbastanza preciso da considerare sollecitazioni concomitanti di flessione, taglio e sforzo normale e l'interazione tra di esse nella risposta inelastica della struttura.

Naturalmente, il modello realizzato con elementi solidi 3D per il calcestruzzo e 1D per l'armatura risulta molto più accurato nella descrizione dei meccanismi complessi e combinati che si sviluppano nei nodi.

Infine, è stata valutata anche l'efficacia di un possibile intervento di rinforzo tramite CFRP limitandosi al confinamento dei nodi non confinati.

Contents

Acknowledgements	i
Abstract.....	iii
Sommario.....	vi
Contents.....	viii
List of Figures.....	xi
1 Chapter - Introduction	1
1.1 Teaching strategies and school typologies in Italy	2
1.2 Numerical modelling to assess of the seismic vulnerability of existing school buildings	9
1.3 Aims and thesis outline.....	10
2 Chapter - State of the Art – Seismic codes, technical and scientific literatures	11
2.1 National seismic code evolution.....	11
2.2 Technical documents for the design of school buildings.....	16
2.3 Scientific literature and main topics.....	18
3 Chapter - Vulnerabilities of school buildings and observed damages suffered during the Italian Seismic Events.....	23
3.1 Introduction	23
3.2 RC school buildings and vulnerabilities detected in the analysed building stock	24
3.3 Remarks on damage of school buildings after earthquakes.....	30
3.3.1 Molise Seismic Events (2002).....	30
3.3.2 Abruzzo Seismic Events (2009)	30
3.3.3 Central Italy Seismic Events (2016).....	31
4 Chapter - The school building stock: the case studies of the municipality of Trecastelli (AN).....	34
4.1 Historical seismology	34
4.2 Local soil conditions at the sites: the ground-type/soil-category	41

4.3	Acquisition of the appropriate level of knowledge of buildings, of the confidence factor FC and of the properties of materials.....	41
4.4	Description of case studies	48
4.4.1	IC Nori de' Nobili (Ripe).....	48
4.4.2	G. Marconi (Monterado).....	53
4.4.3	Peter Pan (Brugnetto - Ripe).....	58
4.4.4	Il Piccolo Principe (Castel Colonna).....	62
4.4.5	Il Girasole (Ripe).....	66
4.4.6	La Carica dei 101 (Ponte Rio - Monterado).....	68
5	Chapter - Numerical Modelling.....	72
5.1	Seismic performance evaluation	72
5.2	Lumped plasticity approach.....	74
5.2.1	Local safety verifications.....	74
5.2.2	Modelling the case studies of Trecastelli school building stock by adopting a lumped plasticity approach	79
5.3	Distributed Plasticity Model (Fibre Model)	84
5.3.1	Steel fibre constitutive model.....	86
5.3.2	Concrete fibre constitutive model	87
5.3.3	Distributed plasticity (fibre) model of Building C (G. Marconi school complex, Monterado)	89
5.4	3D Continuum FE model using a smeared approach for the fracture energy 91	
5.4.1	Concrete crack model	91
5.4.2	Steel model	96
5.4.3	3D Continuum FE model of Building C (G. Marconi school complex, Monterado).....	96
6	Chapter - Results.....	98
6.1	Overview of the structural performances of school buildings located in Trecastelli.....	98

6.2	Comparison of results for the three different models	100
6.3	General consideration and estimate of results for buildings not investigated in detail.....	115
7	Chapter - Reduction of seismic vulnerability of buildings by FRP local retrofit strengthening of RC Beam-Column Joints	118
7.1	Numerical model of the school building with FRP strengthening	120
7.2	Comparison of the numerical results of both unreinforced and reinforced models	123
8	Conclusions and Remarks	127
	References	131

List of Figures

Figure 1.1 Panoramic picture of the complex of San Francesco in Cagli (Italy).	3
Figure 1.2 The spatial complexity of a RC school building in the municipality of Trecastelli, originally designed as an elementary school, then readapted to a kindergartener school.	5
Figure 1.3 A masonry school building in the municipality of Trecastelli, later expanded with other structurally independent buildings.....	7
Figure 1.4 A RC school complex in the municipality of Trecastelli built in 70s.	8
Figure 2.1 Seismic classification of the Italian territory (a) 1981-2003 and (b) after 2003 (INGV2018).	14
Figure 2.2 A summary of the main topics related to rapid methods.	20
Figure 2.3 Summary of the main topics related to Infill walls and slab stiffness.	22
Figure 3.1 The basement floor (Ripe).	26
Figure 3.2 Irregular floor plans (Ripe).	27
Figure 3.3 Longitudinal strong direction and ribbon windows (Ripe).	27
Figure 3.4 Classrooms (Brugnetto-Ripe).	28
Figure 3.5 Strongly protruding cornices and shelters (Ripe).	29
Figure 3.6 Vulnerabilities of school buildings and earthquake damage observed.	32
Figure 4.1 List of Municipalities and fractions and parts of Municipalities in which the observance of the technical building standards for the seismic sites of the 1 st and 2 nd category was required.	35
Figure 4.2 Seismogenic Zonation ZS9 (App. 2 al Rapporto conclusivo, Meletti, Valensise 2004).	36
Figure 4.3 Seismic hazard map – Zone 2: a_g ranging between 0.175 – 0.200 g.	37
Figure 4.4 Annex 7 of OPCM n. 3907 - Contributions for seismic risk prevention interventions: list of municipalities and classification periods.	37
Figure 4.5 Seismic events related to Ripe.	38
Figure 4.6 Seismic events related to Monterado.	39
Figure 4.7 Seismic events related to Castel Colonna.	40
Figure 4.8 A concrete core test for strength (a) and a verification of rebars (b) (Ripe).	43
Figure 4.9 A pacometric test (a) and a concrete carbonatation testing (b) (Monterado).	44
Figure 4.10 A pacometric test on a RC wall to verify the positioning of steel bars (Brugnetto – Ripe).	45
Figure 4.11 Inspection holes in floors (a) and peripheral walls (b) (Castel Colonna).	46
Figure 4.12 Inspection to verify not complying steel reinforcements of beams (Ripe).	47
Figure 4.13 A magnetoscopic survey for the detection of defects (a) and the evaluation of the degradation on metallic elements (b) (Ponte Rio - Monterado).	48
Figure 4.14 Analysed buildings of the first school complex.	50
Figure 4.15 Photographic views of Building A.	51
Figure 4.16 Photographic views of Building B.	51
Figure 4.17 Photographic views of Building C.	52
Figure 4.18 Photographic views of Building D.	52
Figure 4.19 Analysed buildings of the second school complex.	53
Figure 4.20 Photographic views of Building A.	55
Figure 4.21 Photographic views of Building B.	56
Figure 4.22 Photographic views of Building C.	57

Figure 4.23 Analysed buildings of the third school complex.	59
Figure 4.24 Photographic views of Building A.	60
Figure 4.25 Photographic views of Building B.	61
Figure 4.26 Analysed buildings of the fourth school complex.	62
Figure 4.27 Photographic views of Building A.	63
Figure 4.28 Photographic views of Building B.	64
Figure 4.29 Photographic views of Building C.	65
Figure 4.30 Photographic views of Building D.	65
Figure 4.31 Analysed buildings of the fifth school complex.	66
Figure 4.32 Photographic views of the building.	67
Figure 4.33 Analysed buildings of the sixth school complex.	68
Figure 4.34 Photographic views of Building A.	69
Figure 4.35 Photographic views of Building B.	70
Figure 4.36 Photographic views of Building C.	71
Figure 4.37 Photographic views of Building D.	71
Figure 5.1 Adimensional force–deformation relationship adopted for a) bending and b) shear hinges.	76
Figure 5.2 Adimensional force-deformation relationship adopted for hinges for spandrel elements.	80
Figure 5.3 Adimensional force-deformation relationship for hinges for pier elements.	80
Figure 5.4 Models of IC Nori de’ Nobili school.	81
Figure 5.5 Models of G. Marconi school.	81
Figure 5.6 Models of Peter Pan school.	82
Figure 5.7 Models of Il Piccolo Principe school.	82
Figure 5.8 Models of Il Girasole school.	83
Figure 5.9 Models of La Carica dei 101 school.	83
Figure 5.10 Discretisation of a section in a fibre model [72]	85
Figure 5.11 Steel fibre constitutive model – Menegotto and Pinto	87
Figure 5.12 Concrete fibre constitutive model Kent & Park.	88
Figure 5.13 Model of G. Marconi school, Building C a), discretisation of each section by fibres b)	90
Figure 5.14 Concrete crack models.	92
Figure 5.15 Nonlinear tension softening.	94
Figure 5.16 Thorenfeldt compression curve.	95
Figure 5.17 Finite element models of the Building C of G. Marconi complex.	97
Figure 6.1 Global risk indexes for the school buildings of the municipality of Trecastelli.	99
Figure 6.2 Modal analyses results for the three models: a) LPM, b) FM, c) CM.	102
Figure 6.3 Pushover curves for the three models.	104
Figure 6.4 Brittle mechanisms due to the failure of the beams highlighted.	105
Figure 6.5 Failure of beam-column joints (red and pink dots for, respectively, the 1° floor and the 2° floor).	106
Figure 6.6 Pushover curves for the lumped plasticity model (LPM), the LPM only with axial-bending hinges and the Fibre Model (FM).	108
Figure 6.7 Pushover curves for the lumped plasticity model (LPM) and for the 3D Continuum Model (CM).	110
Figure 6.8 Modal pushover analyses for all directions: Crack patterns for 3D Continuum FE model with the smeared approach.	111

Figure 6.9 3D element strain for 3D Continuum FE model (+X, -X directions).....	113
Figure 6.10 3D element strains for 3D Continuum FE model (+Y, -Y directions).	114
Figure 7.1 Tensile and compressive behaviours of the CFRP strengthening a) and system details b)	121
Figure 7.2 3D Continuum FE Model with FRP strengthening on beam-column joints.....	122
Figure 7.3 Pushover curves for the lumped plasticity model (LPM) and for the 3D Continuum FE Model (CM) without/with FRP retrofit intervention.....	124
Figure 7.4 Crack patterns for 3D Continuum FE model before a), b) and after c), d) FRP strengthening intervention (+X direction).	125
Figure 7.5 3D element strain for 3D Continuum FE model before a), b) and after c), d) FRP strengthening intervention (+X direction).....	126

List of Tables

Table 2.1 Seismic code evolution (Part I).....	12
Table 2.2 Seismic code evolution (Part II)	13
Table 2.3 Seismic code evolution (Part III).....	14
Table 2.4 Seismic code evolution (Part IV).....	15
Table 2.5 Seismic code evolution (Part V).	16
Table 2.6 A review of technical documents – Part I.	17
Table 2.7 A review of technical documents – Part II.	18
Table 2.8 A review of the scientific literature: rapid methods.	19
Table 2.9 Review of the scientific literature: Infill walls and slab stiffness.....	21
Table 3.1 Typical vulnerabilities for existing school buildings built after World War II [39].....	25
Table 3.2 Specific vulnerabilities for existing school buildings built after World War II [39].....	25
Table 4.1 Definitions of site characteristics and ground responses for each school complex.....	41
Table 4.2 Properties of materials and KL for IC Nori de’ Nobili school complex (Ripe).	43
Table 4.3 Properties of materials and KL for G. Marconi school complex (Monterado).	44
Table 4.4 Properties of materials and KL for Peter Pan school complex (Brugnetto – Ripe).....	45
Table 4.5 Properties of materials and KL for Il Piccolo Principe school complex (Castel Colonna).	45
Table 4.6 Properties of materials and KL for Il Girasole school building (Ripe).	46
Table 4.7 Properties of materials and KL for La Carica dei 101 school complex (Ponte Rio).....	47
Table 4.8 Materials used for nonlinear analyses on Building C – G. Marconi (Monterado).	58
Table 5.1 G_{10} corresponding to D_{max} CEB-FIP 1990 [79].....	93
Table 5.2 Concrete parameters.	94
Table 5.3 Steel parameters for rebar.....	96
Table 5.4 Main characteristics of meshed elements.	96
Table 6.1 Periods and modal effective masses for transversal, longitudinal and vertical directions for the principal modes of Lumped plasticity model.	100
Table 6.2 Periods and modal effective masses for transversal, longitudinal and vertical directions for the principal modes of Fibre model.	100
Table 6.3 Periods and modal effective masses for transversal, longitudinal and vertical directions for the principal modes of 3D Continuum FE model.....	101

1 Chapter - Introduction

The vulnerability assessment of existing public constructions against seismic actions, which is the necessary pre-requisite for their successive protection, is a crucial issue in seismic prone countries.

Particularly, school buildings play a key role in the social and cultural life of people. In seismic regions, several school buildings were built before the development of modern seismic design provisions or not considering seismic provisions at all because seismic codes and seismic hazard classifications evolved.

It is also to be considered that the architectural layouts of school buildings, with their spatial configurations resulting from the different functions to be carried out within them, result in irregular structures with intrinsically unfavourable seismic behaviour [1].

In recent years, in several countries a significant effort has been dedicated to seismic rehabilitation projects of school buildings, including the allocation of funds to high seismic hazard regions [2].

Furthermore, several national and regional programs and activities have focused on the mitigation of the seismic risk of Italian public buildings. They promote the scheduling of the structural safety assessment of public buildings and, when needed, the design and execution of strengthening interventions.

Nevertheless, the strong earthquakes occurred in the last few decades in Italy, Molise (2002), Abruzzo (2009), Emilia (2012), and Central Italy (2016), confirmed the susceptibility of these types of buildings to extensive damage and therefore the need for a high level of safety against both vertical and horizontal loads and the social importance of their quick re-opening after a damaging earthquake.

First, the knowledge of construction typologies of school buildings is an essential prerequisite, which leads to the definition of the typical and specific building vulnerabilities associated.

In the following paragraph, the typologies of school buildings mainly found in Italy for what regards the lower levels of the Italian education system will be briefly examined.

As the school building stock is very large, the common outline of the existing works in literature is the rapid vulnerability assessment of school buildings for a prioritization scheme of intervention, based on the age of construction and location, visual inspections (type, configuration, quality and materials), and the simplified mechanics-based structural assessment [3].

Once the most problematic buildings were identified, they must be analysed with numerical models to accurately assess their behaviour by introducing the least possible amount of approximations.

Hence there is the need for refined models to evaluate the behaviour of school buildings and to identify the structural weaknesses of each school related to the vulnerabilities already found.

1.1 Teaching strategies and school typologies in Italy

The typologies of school buildings in Italy are strongly characterised by the construction period and the evolution of the teaching system [4].

Carrying out a typological study on school buildings means investigating the relationship between the shape of the building, the pedagogical method adopted and the reference legislative code framework. The evolution of teaching methods has determined the translation of educational principles into different architectural forms and layouts that can be grouped into various school typologies. School became a national institution in the post-unification period - when schooling and illiteracy were the main problems – and school buildings composed a new building typology.

After the schools located in noble palaces or religious institutions - available afterward Italian unification when many buildings lost their previous function becoming a municipal property adapted for teaching activities through renovation works (Figure 1.1) - a new type of school building was conceived on concepts of convenience, solidity and hygiene, follows the dictates of the Italian codes that defined its shape and size.

The first dispositions of 1888 defined a model by fixing the correct dimensioning of the classrooms space: the number, the type of lighting and ventilation, the sizing and the arrangement of the windows and the number and requirements of the toilet facilities.



Figure 1.1 Panoramic picture of the complex of San Francesco in Cagli (Italy).

Thus, the typology of school hosted in a noble palace was replaced by the corridor type. The plan was simply based on a series of classrooms with fixed dimensions that shows the best insolation connected by a long corridor.

The different functions within the school building were also outlined: the atrium space, the auditorium and the open spaces became important to give quality to the whole building.

In the 30s, when the main functions of the building were established, innovative elements were introduced, such as the outside staircase, the atrium space or the volume of the gym, to which the task of recognising and representing the building themselves, which delineate a volumetric specialisation at the base of every modern building.

Schools made up of small pavilions located inside urban parks - an emblematic case of the strict correspondence between pedagogical ideas and the architectural setting of school buildings - were originally intended for children predisposed to respiratory diseases. Therefore, the concept that the school environment actively interacts in the educational process was introduced, being an effective didactic tool through the practical learning of the space.

These principles were expanded in the Post-War period with the establishment in 1952 by the Ministry of Education of the Centre of Study for School Buildings, after the 40s, in which the war events and economic sanctions had reduced the school buildings to simple constructions made with the maximum possible volume but mostly lacking in quality.

Directed by Ciro Cicconcelli and composed of architects, pedagogues, doctors and administrators, this Centre fixed the new features of the school building of the

republican Italy, in a relationship with legislative activity and referred to the concepts of modern pedagogy [5].

Assuming importance the psychological factor of the child - to provide an experience as complete as possible from a spatial, visual and tactile points of view - the school typology evolved from the concept of teaching to that of education. It is not enough that the rooms were well lighted with suitable colours and appropriate hygienic characteristics to facilitate the development stages of the child.

There was a change in the concept of the school, meaning both the building and the function that took place there; it was a collective building with the task of transmitting the rules of behaviour to adapt the individual to society. The hierarchical space of the "corridor" type was eliminated, and a not authoritarian space was introduced, conceived regarding activities and no more than classrooms. From the "functionalist" school for which the building was a set of autonomously defined parts, the building became an "organism", characterised by the fluidity and elasticity and by the fusion between the rooms and the external spaces.

The new school was divided into "functional units" - aggregation of several classrooms distributed without corridors with a common area and toilets - whose combination and articulation depends on the typology of school. In 1954 the Centre of Study prepared a new regulation for the design of school buildings and published four books on kindergarten school, primary school and lower secondary school.

Between the 60s and 70s, the construction of new school buildings received a strong onrush and buildings were conceived giving greater importance to the direct experiences of children.

In 1970 new technical standards for school buildings were established: each school building was conceived as a homogeneous architectural organism and not as a simple addition of spatial elements, thus contributing to the development of the student sensitivity and becoming itself communication tool and therefore knowledge for those who use it.

The shape, the dimensions and the interactions of the school spaces were conceived according to the age of the students and the pedagogical units determined by the types of teaching and pedagogical methods, highlighting the close link between typology and teaching.

The themes of the flexibility of the school and the elasticity of the spaces were introduced to accommodate various activities, including extra-curricular activities, and new construction systems (including prefabricated ones) were designed to solve the strong demand for new schools due to population growth.

Since the environment can stimulate and encourage the development of the child in all phases of his education, different parameters to design spaces were defined for various education levels. For the kindergarten school, rooms were grouped into sections – each of which has rooms for different activities: classroom, changing room, toilets, rest - where they can carry out practical, orderly activities (activities performed on desk) and free (running, jumping, playing).

Since the child at this age needs to find places known as landmarks, the school environment must be as familiar as possible, but at the same time flexible, providing an articulation of spaces that allows different uses, stimulating to allow the child to recognise the environment. The main feature was a central space, naturally lit from above, around which are grouped the classrooms and the socialization activities took place.

The building shape of the primary school, which was divided into self-sufficient functional units united by a common room for collective activities, is given by different aggregations of these units and their relationship with the common spaces as well as the outside (Figure 1.2).



Figure 1.2 The spatial complexity of a RC school building in the municipality of Trecastelli, originally designed as an elementary school, then readapted to a kindergartener school.

An extreme attention was paid to lighting and the different height of the rooms as elements designed to diversify the various spaces without separating them even through the insertion of movable walls that allow a different configuration of the space, according to different needs.

For a lower secondary school, the best setting was to ensure a wide relationship between spaces in which the different activities were performed: the classrooms, the laboratories and the common areas that must be a whole fluid and linked, so the environments they blend dynamically integrating with each other and with external spaces.

These rules, defined in the 1960s, still establish the basic principles to which contemporary schools refer and on which the school buildings are designed.

Based on the considerations above, some different distributive typologies can be recognised, referring to different levels of education of the Italian system (kindergarten school, primary school and lower secondary school).

HISTORICAL OR MONUMENTAL BUILDINGS

Historical or monumental buildings (Figure 1.1) were built before 1900 and host a lot of educational activities, from primary school to university, or cultural activities. These buildings normally represent a part of a more complex urban environment and have a strong structural interaction with neighbouring buildings, often allowing for easy escape in case of an earthquake. The structural element typologies and material properties range widely because of centuries of architectural evolution and recent maintenance works. In this sense, the Cultural Heritage Ministry plays an important role in maintaining the original style of the buildings.

These buildings are often highly seismically vulnerable. Retrofitting can present problems due to the historical value of the buildings and/or the urban context. The most common vulnerability issues concern the weak stiffness of timber floors, composite rubble walls, poor level of material maintenance, structural form alterations, unrestrained roof planes and foundation settlements.

MASONRY BUILDINGS (STAND-ALONE OR LATER EXPANDED BY RC CONSTRUCTIONS)

Masonry buildings have timber roofs and two to three storeys, with a rectangular plan and regularly spaced windows (Figure 1.3). Most of these buildings built between 1900 and 1940 are primary schools owned by the town administration. Rooms are approximately 3.5 m tall, placed along two rows on the facade and connected by a central isle. Foundations are typically made of unreinforced concrete beams aligned under the main walls. Floors were originally constructed

using steel beams and hollow brick units, but due to school maintenance or widening, it is possible to find different constructions, often in the same building. Roofs, in general, do not present a rigid diaphragm and are composed of light timber elements. The mechanical properties of materials, though not very good, are usually similar in the different buildings of this category.

Stand-alone masonry buildings are characterised by a very low ductility, tall and large span, high shear stress peaks, and flexible floor slabs and roofs. One of the main vulnerability factors is the numerous and wide window openings, which introduces a stress amplification into the reduced width shear-resistant panels.



Figure 1.3 A masonry school building in the municipality of Trecastelli, later expanded with other structurally independent buildings.

The experimental evidence of damage in recent earthquakes shows that these panels fail in shear with a brittle behaviour. Other vulnerability factors are: out-of-plane instability due to the large-span rooms that have no adequate wall restraint, peripheral wall failures due to roof element pushing actions, failure of the links at orthogonal wall intersections, often weak due to construction sequences, weak connections between walls and slabs and poor-quality materials.

REINFORCED-CONCRETE FRAMED STRUCTURES

Reinforced-concrete framed structures (Figure 1.4), built after 1950, mainly serve as secondary schools owned by the province or regional administrations. They are completed with infilled masonry walls or prefabricated panels. Following “rational architecture”, these buildings are irregular in plan and elevation and usually have strip windows. Often the first floor is an open space. A wide range of details and quality of materials can be found in these structures as construction has been improved from 1950 to the present. Technical documentation is frequently lacking for these buildings, even for those recently constructed.

Reinforced-concrete framed structures do not adhere to the detailed rules now included in seismic codes. In addition, materials used between 1950 and 1970 were low-grade, and architectural shapes developed after 1970 were irregular, leading to poor seismic behaviours. The combination of low column ductility, due to the inadequate use of stirrups, and high shear forces, usually determined by torsional effects, result in brittle collapse susceptibility. In this typology, the infilled walls play an important role in global resistance and energy dissipation, the effect of which is significantly reduced by strip windows in school buildings.



Figure 1.4 A RC school complex in the municipality of Trecastelli built in 70s.

1.2 Numerical modelling to assess of the seismic vulnerability of existing school buildings

Numerical models of reinforced concrete (RC) structures within the framework of the finite element method (FEM) can be based either on beam elements or 3D continuum elements characterised by a nonlinear material model for concrete in combination with 1D elements for the reinforcement for steel bars.

The first approach is computationally cheaper if a lumped plasticity approach is used to modelling the inelastic resources and, thus, up to now it is preferred in earthquake engineering to simulate the structural behaviour due to earthquake excitation.

It offers noticeable advantages including the low computational cost, the simplicity to use, the correspondence to the reality in common situations the possibility to take into account nonlinear phenomena involving the reinforcement bars and shear failure but requires carefulness in the definition of plastic hinges and the shear span (see Chapters 5 and 6).

Otherwise, between the simplified and more accurate modelling strategies there is the distributed plasticity approach, where structural beam elements are considered by different sections discretised with fibres, which only deform axially.

The fibre approach generally gives an accurate picture of the structural behaviour, but considerable limitations affect the representativeness of the fibre model for constructions subject to shear problems (as shown in Chapter 6).

However, the concomitance of bending (M), shear (V) and axial force (N) and their interaction in the inelastic response remain the most relevant problem of both types of modelling, because they do not offer a detailed view of the structural response during an earthquake.

The Continuum model with 3D solid elements is computationally more expensive, but it provides information on the crack evolution in the concrete and of the stresses in the reinforcement.

Through this latter modelling typology is possible to evaluate together the states of stress, offering a representation of the strength and deformability of beam-column joints, and it also facilitates the evaluation of the effectiveness of any improvement interventions.

Hence, the application of computationally expensive 3D continuum FE-models will be of interest for the design of large-scale tests in earthquake engineering and for partially replacing such very time-consuming and expensive tests by numerical simulations [6].

1.3 Aims and thesis outline

The vulnerability assessment of existing school buildings against earthquakes represents a priority concern for the society in seismic countries, both for the function that these buildings are hosting and for a large number of buildings themselves characterised by inadequate seismic performances.

Since structures belonging to the same type and built in the same period may share similar features, the first purpose of this thesis was pointing out typical and specific seismic vulnerabilities related to the different school architectural layouts (Chapter 1-3).

To this aim, it was carried out a review of the seismic code evolution and technical documents for school design. The available scientific literature was also analysed, to understand if this issue was already addressed in other research projects (Chapter 2).

Mainly the vulnerability assessment of school construction was recently treated in order to obtain prioritization schemes of intervention by rapid procedures.

Since the type of buildings belonging to the upper secondary school level of education was recently analysed in another research contribution [7], this work considers only buildings that host the lower levels of the Italian educational system. A review of the main characteristics of the available modelling approach is reported in Chapter 5.

Firstly, to evaluate the performance of buildings in a fast way, the vulnerability of each school building belonging to the municipality of Trecastelli was assessed adopting a lumped plasticity approach and a nonlinear static procedure.

To perform these evaluations, surveys to acquire an appropriate level of knowledge of buildings were performed according to D.M. 14 January 2008 [8] along with geometric and photographic surveys (Chapter 4).

To evaluate the effects due to irregularities, misalignments, functional layouts and inadequate construction details, a RC school building was chosen to consider additional information provided by a more accurate modelling approach (which the mechanical nonlinearities are accurately represented) than a simpler one (Chapter 5-6)

Finally, the effectiveness of a possible retrofit intervention for the case study limited to beam-column joints was also assessed (Chapter 7).

2 Chapter - State of the Art – Seismic codes, technical and scientific literatures

This chapter focuses on the analysis of the state of the art to individuate codes and all technical documents realised to design, verify and individuate problems of school buildings. The first step was the study of state of the art relating to the theme of school buildings.

The reference legislation was then summarised, the scientific literature was examined to deal with the problems encountered in school buildings and issues examined in detail in the international scientific literature.

Furthermore, some works concerning the existing typologies of these structures and surveys of the damage recorded during the previous earthquakes are reported.

2.1 National seismic code evolution

Since mostly school buildings were built with an RC frame structure cast-in-place or masonry, the evolution of the Italian Code relating to them was analysed.

The seismic classification in Italy has evolved considerably over the last century (Tables 2.1, 2.2, 2.3, 2.4, 2.5). The first zonation – in which only the most damaged areas were classified – was made after the 1908 Messina earthquake, resulting in the first Italian Seismic Code in 1909 [9] and then implemented by the Decree of 1939 [10].

The municipalities falling within these areas had to comply with the code requirements but only 25% of the Italian territory – were classified into seismic zones [1].

In the mid-50s and late 60s (post war years), three measures were approved that incentivised the construction of new schools through funds and regulated the new projects. The design, execution and testing of the works did not refer to seismic zoning at all, only the urban planning and the assessment of the area.

The main considerations concerning seismic engineering started in the mid-70s, particularly in 1974 with Law n. 64 [11] that established rules for updating seismic codes; this means that buildings built before this period generally are not able to provide an adequate response to the earthquake.

From the law of '74 the declaration of works and projects must be notified both to the Civil Engineering Office and to the mayor of the municipality and the use license for RC buildings in seismic zones, conditioned to issue the certificate of the Civil Engineering office.

Code	Title	Main features
R.D.L. 22 Novembre 1937 n. 2105	<i>Norme tecniche di edilizia con speciali prescrizioni con speciali prescrizioni per le località colpite da terremoti</i>	Annex to the list of municipalities and fractions in which compliance with the special building technical standards for the seismic sites of the 1st and 2nd category was mandatory
R.D.L. 16 Novembre 1939 n. 2229	<i>Norme per l'esecuzione delle opere in conglomerato cementizio semplice od armato</i>	Chapter III Design standards - art. 18 Description of resistance to concrete and steel (design and construction indications quite thin)
L. 9 agosto 1954, n. 645	<i>Provvidenze straordinarie a favore dell'edilizia scolastica nonche' nuova misura delle tasse per gli istituti di istruzione media, classica, scientifica, magistrale e tecnica e disposizioni sugli esoneri dal pagamento delle tasse stesse e Istituzione di borse di studio.</i>	Funds for the construction of new school buildings
D.P.R. 1 dicembre 1956, n. 1688	<i>Approvazione di nuove norme per la compilazione dei progetti di edifici ad uso delle scuole elementari e materne.</i>	Judgment of suitability of the area of competence of civil engineering but without references to seismic zoning, only with respect to the provisions of urban planning instruments
Circolare Ministero LL.PP. del 23 maggio 1957 n.1472	<i>Armature delle strutture in cemento armato</i>	Steels Aq 42-50-60 and with improved adhesion
L. 25 Novembre 1962 n. 1684	<i>"Provvedimenti per l'edilizia, con particolari prescrizioni per le zone sismiche"</i>	List of municipalities in seismic areas (Ancona) art. 7 identification features buildings in 1st and 2nd category art. 12 stability calculations - design of structures with a horizontal force equal to 0.10% corresponding weights building mass (1st cat.) and 0.07% matching weights building mass (2nd cat.)
L. 5 Novembre 1964 n.1224	<i>"Integrazioni della legge 25 novembre 1962, n. 1684, concernente provvedimenti per l'edilizia con particolari prescrizioni per le zone sismiche"</i>	Integration of previous law, reiterated mandatory compliance with technical standards for listed municipalities
L. 28 luglio 1967 n. 641	<i>Nuove norme per l'edilizia scolastica e universitaria e piano finanziario dello intervento per il quinquennio 1967-1971</i>	The provisions relating to the design, execution and testing of the works did not refer to any seismic zoning.

Table 2.1 Seismic code evolution (Part I).

In 1975 a law [12] and a decree [13] relating to school buildings were also approved: the decree concerned the association between learning requirements, functional distributions and shapes of the building and the law mentioned among the safety conditions for habitability also safety concerning earthquakes.

Until 1980, similar seismic zone regulations were enforced after each damaging earthquake.

In 1981, after the 1980 Irpinia earthquake, a more comprehensive and rational seismic zonation was proposed [14], taking into account the Italian seismic history of the past several centuries. At the time, about the 45% of the Italian territory was classified as seismic zones 1, 2 and 3, although no seismic provision was made for constructions in the remaining 55% of the country.

In 1984 a regional law of Marche Region [15] defined the modalities of control on buildings in the municipalities or declared seismic portions. Technical regulations were followed by introducing the possibility of calculation with limit states and the control of the story drift (a limit to flexibility). Regarding the specific law for school buildings in 1996 [16], it does not directly mention the adaptation of buildings to seismic regulation.

Code	Title	Main features
L. 5 Novembre 1971 n.1086	"Norme per la disciplina delle opere di conglomerato cementizio armato, normale e precompresso ed a struttura metallica"	Law containing indications of an administrative nature. Technical requirements in the implementing decrees
D.M.30/05/1972	Norme Tecniche alle quali devono uniformarsi le costruzioni in conglomerato cementizio, normale e precompresso ed a struttura metallica	Introduction of further steel types FeB22, FeB32, A38, A41, FeB44
L. 2 Febbraio 1974 n.64	"Provvedimenti per le costruzioni con particolari prescrizioni per le zone sismiche"	art. 9 seismic actions - introduction of two horizontal orthogonal force systems art. 17 Reporting of the works, presentation and examination of the projects: in the seismic areas referred to in art. 3 notice simultaneously with the mayor and the civil engineering office. art. 28 For the use it is necessary the use license for reinforced concrete constructions and the certificate of practicability of the municipalities is conditioned (in seismic zones) to the certificate of the Civil Engineering Office
D.M. 30 maggio 1974	Norme tecniche per la esecuzione delle opere in cemento armato normale e precompresso e per strutture metalliche	Introduction possibility of calculation to limit states (poor description)
D.M. 3 Marzo 1975 n. 39	Approvazione delle "Norme tecniche per le costruzioni in zone sismiche"	Introduction of equivalent static analysis and dynamic analysis
L. 5 Agosto 1975 n.412	"Norme sull'edilizia scolastica e piano finanziario d'intervento"	Functional distribution of environments in relation to pedagogical utility
D.M. 18 dicembre 1975	"Norme tecniche aggiornate relative all'edilizia scolastica, ivi compresi gli indici di funzionalità didattica, edilizia ed urbanistica, da osservarsi nella esecuzione di opere di edilizia scolastica funzionale didattica, edilizia ed urbanistica, da osservarsi nella esecuzione di opere di edilizia scolastica"	
Decreto Ministeriale 3 Ottobre 1978	"Criteri generali per la verifica della sicurezza delle costruzioni e dei carichi e sovraccarichi"	5. Rules relating to living conditions: guaranteeing safety conditions (static construction, defense of external atmospheric agents, fires, earthquakes) operating loads, snow, wind, accidental overloads

Table 2.2 Seismic code evolution (Part II)

Over the next 20 years, the understanding of the concept of seismic hazard advanced rapidly and it resulted in a new seismic classification proposal (the Italian State delegated the adoption of a new classification of the territory to Regions in 1998 [17], whereby about 70% of the territory was classified into these three seismic zones. In 2003 (following Molise earthquake), based on this proposal, the new national classification was officially implemented (Figure 2.1). The classification recognised that all Italian territory is subject to seismic hazard and it introduced a new, low seismicity zone to cover the remaining unclassified 30% of the territory.

OPCM 3274/2003 [18] subdivided Italian territory into four seismic zones and provided for the assessment of infrastructures and strategic constructions.

Code	Title	Main features
D.M. 3 giugno 1981 n.515	<i>Classificazione sismica del territorio basata su uno studio del CNR</i>	Valid until 2003
L. R. 3 Novembre 1984 n. 33	<i>Norme per le costruzioni in zone sismiche nella Regione Marche</i>	defines the modalities for the control on the constructions on zones of the regional territory declared seismic according to the art. 3 of the law of 2 February 1974, n. 64. rules for training and for the adaptation of urban planning instruments for the prevention of seismic risk
D.M. 19 Giugno 1984	<i>Norme tecniche relative alle costruzioni sismiche</i>	
D.M. LL PP 24 gennaio 1986	<i>Norme tecniche relative alle costruzioni antisismiche</i>	
D.M. 9 gennaio 1987 D.M. 20 novembre 1987	<i>Norme tecniche per la progettazione, esecuzione e collaudo degli edifici in muratura e per il loro consolidamento.</i>	2.4.1 Security checks with the method of the admissible tensions 2.4.2 Security checks with the method of semiprobabilistic to the limit states
L.R. 27 marzo 1987, n. 18	<i>Modifiche della L.R. 3 novembre 1984, n. 33 riguardante "Norme per le costruzioni in zone sismiche".</i>	changes to Law previous one
D.M. 9 gennaio 1996	<i>"Norme tecniche per il calcolo, l'esecuzione ed il collaudo delle strutture in cemento armato, normale e precompresso e per le strutture metalliche"</i>	Section II: indications to follow for the verification of normal and pre-stressed reinforced concrete structures and steel structures. Section III: permitted for the application of the European experimental standards Eurocode (indications for use)
L. 11 gennaio 1996, n. 23	<i>Norme per l'edilizia scolastica</i>	Cited interventions of restructuring and extraordinary maintenance aimed at adapting the buildings to the current norms in terms of practicability, safety, hygiene. No direct reference to seismic.
D.M. 16 gennaio 1996	<i>"Norme tecniche per le costruzioni in zone sismiche"</i>	C.9 Interventions on existing buildings: adaptation and improvement There remains a portion of the Italian territory that is not classified as seismic
Circ. M. LL.PP. n.65/AA.GG. del 10 Aprile 1997	<i>"Istruzioni per l'applicazione delle "Norme tecniche per le costruzioni in zone sismiche" di cui al D.M. 16/01/1996"</i>	ANNEX 1 Constructional indications for reinforced concrete structures Annex 2: interaction between frames and walling panels
D.P.R. n.380 del 6 giugno 2001	<i>Testo unico delle disposizioni legislative e regolamentari in materia edilizia</i>	Administrative provisions, resumed and modified the previous ones

Table 2.3 Seismic code evolution (Part III)

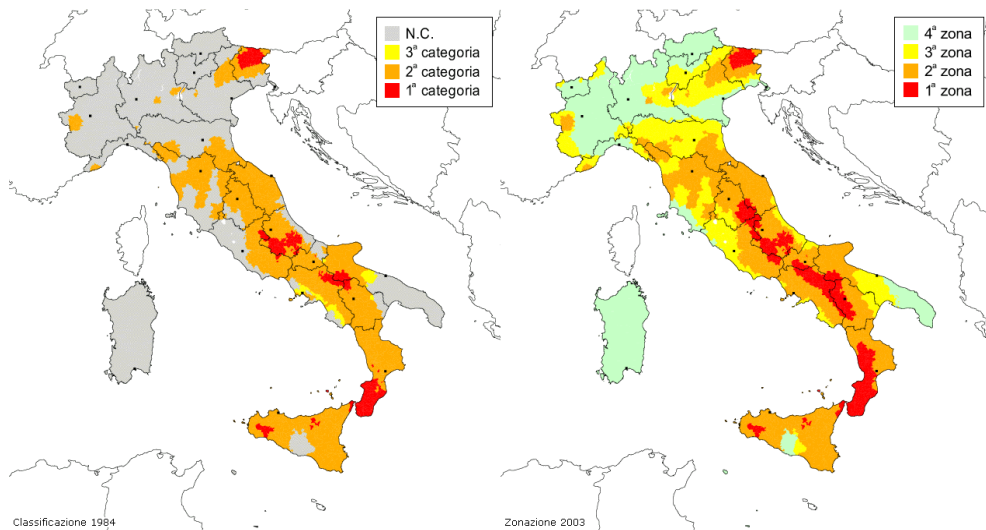


Figure 2.1 Seismic classification of the Italian territory (a) 1981-2003 and (b) after 2003 (INGV2018).

An update of the national seismic hazard study, foreseen by OPCM 3274/03, was adopted with OPCM n. 3519 of 28 April 2006 [19].

After the seismic event of L'Aquila in 2009, NTC08 [8] came into force with the relative Circular 2009 [20], which are nothing more than the national appendix of Eurocodes.

Legislative activity for school buildings following the numerous earthquakes is currently aimed at reducing seismic risk, with the allocation of funds for the safety of school buildings, interventions, construction of new buildings and seismic risk prevention [21] [22] [23] [24] [25] [26].

Code	Title	Main features
O.P.C.M. 20 Marzo 2003 n.3274	"Primi elementi in materia di criteri generali per la classificazione sismica del territorio nazionale e di normative tecniche per le costruzioni in zona sismica"	Annex 1 - Criteria for the identification of seismic zones - identification, training and updating of the lists in the same areas Annex 2 - Technical standards for the design, evaluation and seismic upgrading of buildings
O.P.C.M. 2 ottobre 2003 n. 3316	Modifiche ed integrazioni all'ordinanza del Presidente del Consiglio dei Ministri n. 3274 del 20 marzo 2003, recante "Primi elementi in materia di criteri generali per la classificazione sismica del territorio nazionale e di normative tecniche per le costruzioni in zona sismica"	Modifications and additions to the O.P.C.M. n. 3274 of March 20, 2003
D.P.C.M. 21 ottobre 2003 n.3685	Disposizioni attuative dell'art. 2, commi 2, 3 e 4, dell'ordinanza del Presidente del Consiglio dei Ministri n. 3274 del 20 marzo 2003, recante «Primi elementi in materia di criteri generali per la classificazione sismica del territorio nazionale e di normative tecniche per le costruzioni in zona sismica»	
O.P.C.M. del 3 Maggio 2005 n.3431	Ulteriori modifiche ed integrazioni all'OPCM n. 3274 del 20 marzo 2003 recante "Primi elementi in materia di criteri generali per la classificazione sismica del territorio nazionale e di normative tecniche per le costruzioni in zona sismica"	
D.M. 14/09/2005	"Norme Tecniche per le Costruzioni"	
D.M. 14 Gennaio 2008	"Norme Tecniche per le Costruzioni"	Requirements relating to works in concrete, masonry, new-built wood and existing existing buildings. Recall Eurocodes (EC2 - UNI EN 1992-1-1: 2005 Part 1-1, EC8 - UNI EN 1998-1: 2005 Part 1 and 3)
Circolare 02 febbraio 2009 n. 617	Istruzioni per l'applicazione delle «Nuove norme tecniche per le costruzioni»	
D.L. 28 aprile 2009 n. 39 e L. 24 giugno 2009 n. 77	Interventi urgenti in favore delle popolazioni colpite dagli eventi sismici nella regione Abruzzo nel mese di aprile 2009 e ulteriori interventi urgenti di protezione civile	art. 11 Verifications and interventions for the reduction of seismic risk

Table 2.4 Seismic code evolution (Part IV).

Code	Title	Main features
L. 12 novembre 2011, n. 183	<i>Disposizioni per la formazione del bilancio annuale e pluriennale dello Stato. (Legge di stabilità 2012)</i>	art. 33, paragraph 3, allocation of resources for the development and cohesion fund for the securing of school buildings
D.L. 6 dicembre 2011, n. 201	<i>Disposizioni urgenti per la crescita, l'equità e il consolidamento dei conti pubblici, convertito con modificazioni dalla legge 22 dicembre 2011, n. 214. Interventi urgenti in favore delle popolazioni colpite dagli eventi sismici che hanno interessato il territorio delle province di Bologna, Modena, Ferrara, Mantova, Reggio Emilia e Rovigo, il 20 e il 29 maggio 2012, convertito con modificazioni dalla legge 1° agosto 2012, n. 122.</i>	art. 33, paragraph 8, institution fund for the securing of school buildings art. 30, paragraph 5-bis, adoption of acts necessary for the provision of resources for safety interventions and anti-seismic adaptation of schools
D.L. 6/6/2012, n. 74	<i>Disposizioni urgenti per il rilancio dell'economia, convertito con modificazioni dalla legge 9 agosto 2013, n. 98.</i>	art. 5, paragraph 1-bis, new appropriations for the construction of new school buildings
D.L. 21-6-2013, n. 69	<i>Ministero dell'istruzione, dell'università e della ricerca - Procedura di cofinanziamento di interventi di edilizia scolastica e messa in sicurezza delle scuole, in attuazione di quanto disposto dalla direttiva 1° agosto 2013.</i>	art. 18, paragraph 8-8-septies, INAIL fund destinations for the plan to make school buildings safe and to build new school buildings
D.M. 10 ottobre 2013, n.267	<i>Ministero dell'istruzione, dell'università e della ricerca - Assegnazione delle risorse destinate all'attuazione di misure urgenti di riqualificazione e di messa in sicurezza delle istituzioni scolastiche statali. (Decreto n. 906).</i>	Co-financing procedure for school buildings and safety measures for schools
D.M. 5-11-2013, n. 906	<i>Misure urgenti per la competitività e la giustizia sociale, convertito con modificazioni dalla legge 23 giugno 2014, n. 89.</i>	Assignment of resources for securing schools
D.L. 24-4-2014, n. 66	<i>Misure urgenti per l'apertura dei cantieri, la realizzazione delle opere pubbliche, la digitalizzazione del Paese, la semplificazione burocratica, l'emergenza del dissesto idrogeologico e per la ripresa delle attività produttive</i>	art. 48, paragraph 1, exclusion from the internal stability pact of the expenses incurred by the municipality for school building works art. 48, paragraph 2, allocation of new funds for the securing of school buildings
D.L. 12-9-2014, n. 133		art. 9 Extremely urgent interventions concerning hydrogeological constraints, anti-seismic regulations and safety measures for school buildings and artistic, musical and dance training - AFAM
Legge di Bilancio 2017		Fund for the financing of: public housing (including the scholastic building); seismic risk prevention; seismic emergency measures: contributions for public reconstruction.

Table 2.5 Seismic code evolution (Part V).

2.2 Technical documents for the design of school buildings

Over the years, rapid assessment of the behaviour of existing buildings was carried out, gradually more accurate, through projects funded for seismic risk assessment since the mid-1960s and then developed in the 1990s.

Forms of 3 levels were obtained, from 0 to 2 (from the least accurate and fast to the most articulate) to classify buildings [27] [28] [29]. Recently, questionnaires related to school buildings were also made. From the project *Strumenti Aggiornati per la Vulnerabilità patrimonio Edilizio* a large inventory of the public buildings of the South was derived [30]. Finally, in 2003 the CNR produced guidelines for assessing the vulnerability of school buildings (Table 2.6).

Since the observation of the events and the assessment of the state of the schools are essential tasks, the post-earthquake reports of the ReLUIIS consortium [31] were

also considered with the description of the buildings and the damage reported after the earthquake and also Legambiente reports [32].

Investigations - catalogs	
1966	National survey on the state of school buildings - Institute for the Development of Social Housing - Ministry of Education
1996	Project LSU Form "LEVEL 0 " Form "LEVEL 1 "
1999	Form of vulnerability 2° Level (masonry) GNDT Form of vulnerability 2° Level (R.C.)
2002/14	Form AeDES - Pres. del Consiglio dei Ministri, Dip. Protezione Civile
2004	Questionnaires of the school building and the school institution - MIUR
2005	SAVE: Inventory and vulnerability of public and strategic buildings in central and southern Italy - INGV - GNDT, M. Dolce, A. Martinelli
CNR	
2003	Guidelines for the evaluation of the vulnerability of school buildings - Vulnerability of public, strategic and cult buildings in the municipalities affected by the earthquake of 31/10/2002 - Reg. Molise, Dept. of Civil Protection, University of the Studies of Basilicata, ITC - CNR
ReLUIS Report	
2009	Report of the damage caused by the earthquake of 6 April on the school buildings of the historical center of L'Aquila - University of Pisa - W. Salvatore, S. Caprili, V. Barberi
2012	Emilia Romagna earthquake - May 2012 Preliminary report on the damage found in some public buildings - Reliability surveys and verification - University of Naples "Federico II" A. Formisano, G. Florio & F. Gamardella

Table 2.6 A review of technical documents – Part I.

Finally, there are ministerial and manual publications referring to functional layouts of buildings according to pedagogical needs of different periods (Table 2.7). One of the main causes of vulnerability of school buildings is the architectural (and structural) layout. Schools are composed of different areas deriving from teaching activities, then the building results irregular and/or articulated in shape, both in plan and in elevation.

Current typical vulnerabilities in the past were well-defined design criteria.

Legambiente Reports

2015	School Ecosystem - XVI Report LEGAMBIENTE REPORT on the quality of school buildings
2016	School Ecosystem - XVII Report LEGAMBIENTE REPORT on the quality of school buildings

Ministerial publications

	Books of the study center for school buildings: <i>Middle school: studies, schemes, examples</i>	
1953 -	<i>Prefabrication in school buildings</i>	Ministry of
1965	Kindergartens: study examples schemes Elementary schools: study examples schemes Minimum schools: studies, schemes, projects	Education

Manuals

1958	Kindergartens, elementary and secondary schools - C. Cicconcelli
1964	Industrialization and prefabrication in school buildings - Various authors "The Italian cement industry" A.I.T.E.C.
1969	Prefabrication in industrialized buildings: Building and constructions in prefabricated buildings of c. to. - R. von Halász, I.T.E.C.
1975	Developmental lines of school buildings - F.E. Leschiutta
1976	School building, Model approach, Development for functional units - RDB Information desks Prefabricated school buildings
1982	School building manual - R. Airoldi

Table 2.7 A review of technical documents – Part II.

2.3 Scientific literature and main topics

Since it is impossible to analyse the entire Italian school building stock using sophisticated mechanical models, the rapid methodologies (on several levels) were treated by many studies, adopting the visual information provided by the forms to define intervention priorities, therefore on already available datasets.

A review of the scientific literature on rapid methods is available in Table 2.8 and a summary of the main topics related to rapid methods is reported in Figure 2.2.

VULNERABILITY OF SCHOOL BUILDINGS		
year	Research Group and Article	Note
2004	N. Cosentino, G. Manieri, A. Benedetti - A brief review of school typologies in Italy: specific vulnerability and possible strategies for seismic retrofitting [33]	Description of four types of school buildings in Italy, characteristics and vulnerabilities, possible retrofitting strategies
	M. Dolce, A. Masi, C. Moroni, A. Martinelli, A. Mannella, L. Milano, A. Lemme, C. Miozzi - Sisma Molise 2002 : Il progetto "scuola sicura": dall'indagine di vulnerabilità sismica alle esecuzioni degli interventi	Activities for SHM school buildings Simplified models for vulnerability assessment (schede GNDT 2° level)
2004	M. Dolce - Seismic safety of schools in Italy [1]	Lack of adequate classification of seismic areas until 2003 Functional and structural school layouts, low construction standards, poor materials and changes to the original layout
2004	N. Augenti, E. Cosenza, M. Dolce, G. Manfredi, A. Masi, L. Samela - Performance of School Buildings during the 2002 Molise, Italy, Earthquake [34]	Damage distribution comparison with vulnerability classes - Molise school buildings - San Giuliano
2006	D. N. Grant, J. J. Bommer, R. Pinho, G. M. Calvi, A. Goretti, F. Meroni - A Prioritization Scheme for Seismic Intervention in School Buildings in Italy [3]	Three step procedure (different degrees of detail) by definition of intervention priority
2006	R. Pinho, G. M. Calvi, H. Crowley, M. Colombi, A. Goretti, F. Meroni - Strumenti speditivi per la definizione di priorità di intervento per edifici non adeguati sismicamente	1 - PGA deficit assessment (Current-Design) for buildings inventory 2 - vulnerability index assessment 3 - structural evaluation with a simplified mechanical method
2006	B. Borzi, R. Pinho, H. Crowley - Simplified pushover-based vulnerability analysis for large-scale assessment of RC buildings [35]	Structural evaluation with a simplified mechanical method
2008	H. Crowley, M. Colombi, G.M. Calvi, R. Pinho, F. Meroni, A. Cassera - Application of a prioritization scheme for seismic intervention in schools buildings in Italy - 14 th WCEE 2008 Cina	Modification of the methodology proposed in the previous work (masonry) Application to case studies of Friuli Venezia Giulia and Marche regions
2009	A.M. Ceci, A. Contento, L. Fanale, D. Galeota, V. Gattulli, M. Lepidi, F. Potenza - Structural performance of the historic and modern buildings of the University of L'Aquila during the seismic events of April 2009 [36]	Identification of possible causes of structural collapses - mechanisms Buildings contextualization, attention to the local amplification effects and to the vertical component of acceleration Fundamental role for the dissipation of non-structural components
2010	N. Augenti, F. Parisi - Learning from Construction Failures due to the 2009 L'Aquila, Italy, Earthquake [37]	Damage to structural and non-structural elements, mechanisms, elements of vulnerability
2012	J.E. Rodgers - Why Schools are Vulnerable to Earthquakes - 15 WCEE Lisbona 2012 [38]	Physical and organizational characteristics of schools that cause vulnerability - table with dataset characteristics
2013	B. Borzi, P. Ceresa, M. Faravelli, E. Fiorini, M. Onida - Seismic Risk Assessment of Italian School Buildings	Fast method with dataset usage from catalogues Fragility curves
2015	F. Clementi, E. Quagliarini, G. Maracchini, S. Lenci - Post-World War II Italian School building: typical and specific seismic vulnerabilities [39]	Considerations to improve knowledge of post-war school buildings: typical and specific vulnerabilities, standard architectural principles from manuals and legislation Application to a case study with different configurations (modeling elements of vulnerability) with nonlinear static analysis and I.D.A.

Table 2.8 A review of the scientific literature: rapid methods.



Figure 2.2 A summary of the main topics related to rapid methods.

Moreover, observing the consequences of earthquakes, another topic of research involves the evaluation of the behaviour of non-structural elements, which can heavily affect the performance of buildings (Table 2.9).

A review of the scientific literature on infill walls and slab stiffness is available in Table 2.9 and a summary of the main topics related to infill walls and slab stiffness is reported in Figure 2.3.

INFLUENCE OF WALLS AND FLOORS ON THE BUILDING				
year	Research team	UNIVERSITY	Article	Note
2002	G.Al-Chaar	US Army Corps of Engineers Center	Evaluating Strength and Stiffness of Unreinforced Masonry Infill Structures [40]	resistance evaluation stiffness of non-reinforced infill panels subjected to lateral loads - frame with eccentric equivalent struts
2004	L. Decanini, F. Mollaioli, A. Mura, R. Saragoni	Università di Roma "La Sapienza" Università del Cile	Seismic performance of masonry infilled RC frames [41]	Effects of infill panels on the performance of multi-level frames in c.a. Compression-resistant diagonal struts with hysteretic effects of masonry subject to repeated loads (resistance and stiffness reduction)
2012	A.Fiore,F.Porco,D .Raffaele,G.Uva	Polytechnic of Bari	About the influence of the infill panels over the collapse	

			mechanisms activated under pushover analyses: two case studies	Parameters involved in the definition of equivalent struts in models used for nonlinear static analysis
2012	A. Fiore, A. Netti, P. Monaco	Polytechnic of Bari	On the role of equivalent strut models in the seismic assessment of infilled RC buildings [42]	Macromodel -> equivalent struts
2012	C.Z. Chrysostomou, P.G. Asteris	Cyprus University of Technology Sch. of Ped. and Tech. Education Athens Greece	The influence of masonry infill on the seismic behaviour of RC frame buildings [43]	Review methodologies macro-modelling masonry panel in the frame Double diagonal strut-connecting rod subjected to cyclic loads FEMA 273 - FEMA 306 - FEMA 356 Properties of materials, modelling, breaking mode Considerations effect of the panel in the frame on the structure and uncertainties
2013	P.G. Asteris, D.M. Cotsosvos, C.Z. Chrysostomou, A. Mohebkah, G.K. Al-Chaar	School of Ped. and Tech. Education Athens School of the Built Env. UK Cyprus Un. of Technology Malayer University Constr. Eng. Research Laboratories (CERL) USA	Mathematical micromodeling of infilled frames: State of the art [45]	Overview of methodologies for micro-modelling of the masonry panel FE modelling: masonry as a 1, 2 or 3 phases material FEM, BEM, DEM FE-BE model: Boundary Element panel - Finite Element frame Frame - panel interface: springs or Interface el. Cracking: smeared crack approach
2015	Fabio Di Trapani	University of Palermo	Masonry infills and RC frames interaction: Literature overview and state of the art of macromodeling approach [46]	Review literature available macro-modelling approach
2016	P.G. Asteris, L. Cavaleri, F. Di Trapani, A.K. Tsaris	School of Pedagogical and Technological Education Athens University of Palermo	Numerical modelling of out-of-plane response of infilled frames: State of the art and future challenges for the equivalent strut macromodels [47]	macro-modelling: buffering behaviour OOP outside the plane (arc effect) OOP (arc effect) and IP combined fibre model with diffused plasticity of the strut connecting rod building modelling three elevations in plan
2008	R. Pinho, C. Bhatt, S. Antoniou, R. Bento	University of Pavia Technical University of Lisbon, Portugal SeismoSoft Greece	Modelling of the horizontal slab of a 3d irregular building for nonlinear static assessment	non linear and non linear dynamic static analyses fibre modelling structural elements floor modelled as a rigid diaphragm and rigid link poor ductility, deformable floors high displacements imposed
2009	J. A. Rivera, R. Pinho	IUSS Pavia, Università di Pavia	On the Development of Seismic Design Forces for Flexible Floor Diaphragms in Reinforced Concrete Wall Buildings	Review modelling types (modelling pin-pin beams, slabs) plan of buildings with arms, significant irregularities due to the deformability of the floors, not uniform distribution of resistance and stiffness

Table 2.9 Review of the scientific literature: Infill walls and slab stiffness.

✓ **MACRO-MODELLING OF FRAME + INFILL WALLS -> InPlane**

✓ **MICRO-MODELLING OF FRAME + INFILL WALLS -> InPlane**

✓ **InPlane+OutOfPlane MODELS**



INFLUENCE OF INFILL PANELS ON THE GLOBAL RESPONSE OF SCHOOL BUILDINGS

✓ **PIN-PIN BEAM E SLABS**



INFLUENCE OF THE FLOOR STIFFNESS

Figure 2.3 Summary of the main topics related to Infill walls and slab stiffness.

For example, in a lot of articles the macro-modelling of infill walls in reinforced concrete frames was treated, evaluating both behaviours in plane and out of plane. The micro-modelling of the infill panels was also analysed, where the interface between the frame and the panel has been appropriately considered. Another interesting aspect treated in literature is the evaluation of the behaviour of the structure in relation to different type of models and slab stiffness. Finally, the vulnerability assessment using both numerical models with 1D elements, such as [48], and 3D solid elements [6] is a very interesting issue. Although it is not possible to carry out extensive surveys on a large number of buildings (due to the calculation burden), numerical models with a continuum approach offer the possibility to obtain very important information regarding the typical and specific vulnerabilities found in school buildings, to better understand the effects introduced by irregularities in structures [49] and verify the significance of the results obtained with less refined methodologies and models.

3 Chapter - Vulnerabilities of school buildings and observed damages suffered during the Italian Seismic Events

3.1 Introduction

Buildings belonging to the same type and built in the same period may share similar geometrical and spatial characteristics. When these features also affect the seismic response of the buildings, they are referred to as typical seismic vulnerabilities. When a building presents one or more of these typical vulnerabilities, some general and qualitative considerations on its seismic behaviour can be made a priori, considering their actual influence on the seismic behaviour of other similar cases [39].

Most recent seismic events (e.g. Molise 2002, L'Aquila 2009, Emilia 2012 and Central Italy 2016) have shown the high seismic vulnerability of the Italian existing RC buildings, which often provide an inadequate safety level against seismic actions.

This high vulnerability is due to a lot of aspects, mostly related to the age of the buildings, the low standards of construction and maintenance, and the legislation in force at the time that did not effectively deal with the seismic problem, even allowing the design for gravity loads in some earthquake prone areas, erroneously considered as non-seismic zones.

For this reason, existing RC framed buildings are today characterised by poor quality concrete [50], inefficient construction details - especially in the joints – a lack of the fundamental principle of the capacity design and low column ductility mainly due to an inadequate use of stirrups.

The evaluation of the seismic vulnerability of these RC structures has a key role in the determination and reduction of earthquake impact.

For this reason, after the tragic collapse of a school building during the 2002 Molise earthquake [34], the Italian Government started a mitigation policy issuing the Ordinance of the President of the Ministers' Council n. 3274 [18]. More specifically, an important national plan was set up with the aim of assessing and mitigating the risk of those buildings and infrastructures designed without earthquake resistant criteria, and whose integrity during earthquakes is of vital importance for communities (e.g. hospitals) or which is significant in view of the consequences associated with their collapse (e.g. schools).

One of the main purposes of this thesis is to improve the knowledge of the school buildings built in Italy before NTC2008 by pointing out typical and specific seismic vulnerabilities related to their architectural layout and construction characteristics and the assessment of the seismic vulnerability of six school complexes, paying attention to reinforced concrete buildings.

For existing buildings that show similar spatial configurations and follow the same construction and architectural principles, some general and qualitative considerations on their seismic behaviour might be made a priori, before in situ investigations, due to the possibility of observing the seismic performance of other similar buildings. This is the case of homogeneous building typologies, in which common structural features are present and whose seismic response can be related to the common typological aspects shared by the whole class of buildings [1] [38]. The basic idea is that some kind of buildings can have seismic vulnerabilities that could be the same for the entire typological class. These vulnerabilities are referred to as typical vulnerabilities. They substantially differ from another type of vulnerability, the specific vulnerabilities, which instead are related to methods of construction, materials quality and peculiarities of every single building that may vary from case to case. The presence of specific vulnerabilities usually worsens the seismic damage related to the typical ones.

3.2 RC school buildings and vulnerabilities detected in the analysed building stock

Most of the school buildings are spatially organised in the same way: the classrooms are placed next to each other in front of a corridor or a hallway [38]. This layout supports school functions but increases inevitably seismic vulnerability. Then, the design of this type of building is strongly correlated with their structural behaviour.

Based on the information gathered in Chapter 2 about the evolution of school typology, it was possible to define common aspects that are shared between all school buildings and important suggestions on the distributive and functional characteristics that make these buildings, or at least some of them, very similar. Referring to the work of [39], two lists of typical (Table 3.1) and specific vulnerabilities (Table 3.2) for RC primary school buildings built after World War II are reported below.

Typical vulnerabilities
Different infill panels distribution for the basement floor (in elevation irregularity)
In plan irregularity due to: alignment of the classrooms and common hall
Large classrooms
In plan shape irregularity
Eccentric position of the stairs
Tall windows for the common hall
Double height spaces in the common hall
Frames in one direction only
Flexible floor

Table 3.1 Typical vulnerabilities for existing school buildings built after World War II [39].

Specific vulnerabilities
Low standards of construction execution
Weak column – strong beam
Inadequate construction details (especially in the joints)
Low-grade materials
Degradation of the materials (no maintenance)
“Strong” infill panels
Undersized column

Table 3.2 Specific vulnerabilities for existing school buildings built after World War II [39].

It was possible to identify most of these critical aspects in the analysed building stock of the municipality of Trecastelli, also built after the time interval considered by the authors of the above-mentioned work.

For example, the Lower Secondary School of Ripe “IC Nori De 'Nobili” is composed of four buildings designed as a sum of “functional units” according to the analogous architectural concept.

Moreover, one of these buildings (see Figure 3.1) is a multi-storey structure mainly realised with a connection function in plane and in height (by stairs), with a semi-embedded basement floor devoted to the complementary functions i.e. heating system and storage area (designed for school bus parking).

Since the basement storey could not contain classrooms, it has got a different in plan distribution of infill panels from the upper level, triggering possible soft storey mechanisms.

The same building hosts school offices and laboratory on the first floor and a library and a common hall on the ground floor.



Figure 3.1 The basement floor (Ripe).

The ground floor of another building of the same complex and the first floor of a further building host teaching activities with large square shaped classrooms while the ground floor of the last building mentioned includes the gym locker rooms. The building in Figure 3.2 (on the left) shows a “L-shaped” floor plan. Thus, typically stiffness distribution is not symmetric in both principal directions in plan. Shape irregularity, which often results in structural irregularity, is an unfavourable feature of buildings in seismic areas, as the shape determines the concentration of damage in specific parts or storeys of a building and may even cause collapse. Furthermore, for constructions built during the Seventies (designed for vertical loads and with few indications regarding horizontal loads) frames are usually in one direction, generally the longer one (longitudinal), identifying a strong direction, whilst in the orthogonal direction the frames are present on the external sides only as in the Lower Secondary School of Ripe (Figure 3.3).

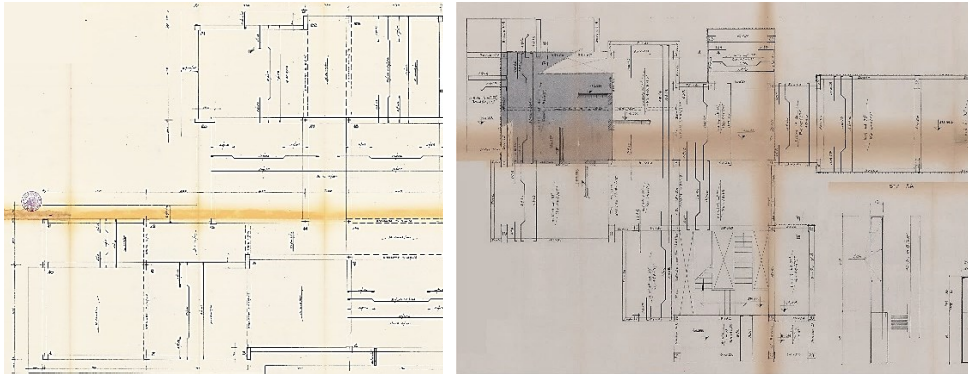


Figure 3.2 Irregular floor plans (Ripe).

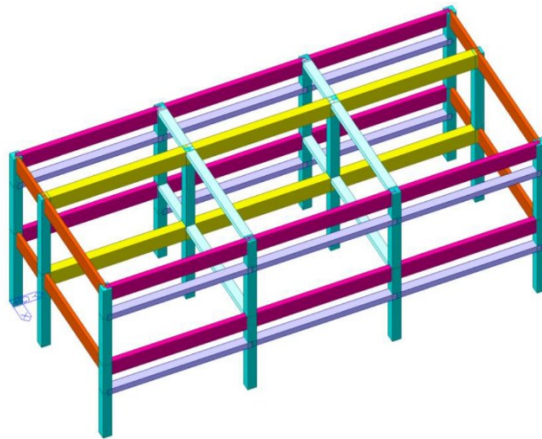


Figure 3.3 Longitudinal strong direction and ribbon windows (Ripe).

Another striking example of an assemblage of several units is the kindergarten school “Peter Pan” of Brugnetto (Ripe). It is made up of functional units recognisable from the outside, as volumes emerging from the corridors. There is an accessible central courtyard destined to be an aggregation space and as a source of solar lighting for connecting spaces (completely closed only on one side). The canteen has larger dimensions both in plan and height compared to other spaces while classrooms are emerging blocks equipped with large windows and glass doors to encourage lighting and the contact with the outside garden (Figure 3.4).



Figure 3.4 Classrooms (Brugnetto-Ripe).

Slabs with one-way RC ribs and hollow blocks, also defined as “composite masonry and concrete joists slabs”, are commonly used in school buildings. This type of floor structure is made by several parallel ribs placed or cast along a specific direction (one way), generally made of reinforced cast-in-place concrete and hollow blocks used to reduce the floor weight. These slabs cannot be considered as rigid because solid concrete plates were designed without the minimum thickness (40 mm) and necessary reinforcements to assure a rigid behaviour as required by the Italian Standards [51], and/or they are made of poor quality concrete.

Consequently, this feature can be considered as an additional typical vulnerability of the examined building typology. Also, due to the flexibility of slabs, the infill masonry panels distributed at the perimeter and at the centre of building do not cooperate to the global behaviour like structural cross bracing. Such action is then bounded to the single frame and, consequently, the soft storey mechanism is triggered where there is no structural cross bracing to limit transversal displacement.

Specific vulnerabilities are usually related to the methods of construction and to the quality of the materials, i.e. peculiarities of the single building that may vary from case to case.

Reinforcement steel generally used until the 70s consists of smooth bars and the mechanical properties of the concrete have a very big in-situ variability with low cubic resistances.

The poor prescriptions provided by codes up to 1971 (1939 and 1957) (e.g. about minimum member dimensions and reinforcement detailing), might be compensated making references to the most prominent handbooks and to the current design practice (typical construction drawings) of the various periods. According to these, it was seen that in the 50s, 60s and 70s, the distribution of stirrups within structural elements was typically poor and ineffective, particularly within column-beam nodes, where they are completely absent.

Furthermore, in old RC buildings columns are often undersized, with different stiffness and strength in the two main directions calculated without taking into account the three-dimensional effects. It should also be noted that the seismic behaviour of such structures can be strongly affected by the effect of masonry infills, especially in those cases in which the external unreinforced infill masonry walls are made with “strong” infill panels.

In addition to the vulnerabilities detected in [39], in the case studies located in Trecastelli it was found the presence of heavy loads deriving from strongly protruding cornices and shelters of considerable size (Figure 3.5).



Figure 3.5 Strongly protruding cornices and shelters (Ripe).

Furthermore, it is possible to find recent school buildings (designed with DM96 [52,53]) characterised by typical and specific vulnerabilities that greatly worsen their structural behaviour under horizontal loads, as the case study chosen in Chapter 5.

3.3 Remarks on damage of school buildings after earthquakes

3.3.1 Molise Seismic Events (2002)

The damage caused by the Molise earthquake in 2002 drew attention to a serious problem in Italy with regard to seismic vulnerability: many of the municipalities at the beginning of the 2000s hit by the earthquake were not classified as seismic areas yet, and structures were built without seismic provisions [54]. Therefore, the damage exceeded that which would be expected in an earthquake of moderate magnitude. The collapse of the primary school Iovene in San Giuliano, where 27 children and one teacher died, alerted the country to the vulnerability of critical structures.

There are several reasons why most Italian schools are vulnerable, or highly vulnerable, to earthquakes. It is possible to recognise these reasons in the case of San Giuliano Primary School.

First, the area of San Giuliano was not classified as a seismic zone, although recent studies indicate that earthquakes with 0.165 g maximum peak ground acceleration (PGA) (MMI = VIII-IX) are expected with a 475-year return period. Therefore, seismic criteria were not considered in the building design. In addition, recent works – such as the partial addition of one storey – completed in August 2003 did not require any seismic upgrading, only verification for vertical loads. According to the new 2003 seismic zonation, San Giuliano is now classified in Zone 2 (Ordinance 3274).

Moreover, the low standard of construction execution also contributed to the collapse. The school was constructed using poor quality masonry and with a heavy reinforced-concrete roof [34].

Finally, the increase of masses caused by the addition of a second storey may have contributed to the collapse of this school.

3.3.2 Abruzzo Seismic Events (2009)

On Monday, the 6th of April 2009, at 03:32:39 a.m. local time, a devastating earthquake struck the city of L'Aquila and surrounding villages in the Abruzzo Region of Central Italy. The earthquake caused about 300 fatalities, more than a thousand injuries, and extensive and severe damage to buildings and other engineering structures.

The magnitude of the event was estimated to be $ML = 5.8$ (Richter magnitude scale), and $MW = 6.2$ (moment magnitude scale), according to the Italian INGV. The main shock was followed by a swarm of aftershocks, giving rise to a long-lasting seismic sequence, including more than 30 aftershocks with magnitude $3.5 < ML < 5.0$, and several thousand events of lower magnitude.

This earthquake which struck the city of L'Aquila caused a disaster of vast proportions, from both social and economic viewpoints, which will affect the entire region for many years to come. The large number of human casualties and great economic losses can be largely attributed to the high levels of damage suffered by many buildings, especially in the historical centre of L'Aquila, where many full or partial collapses were recorded [37] [55] [56].

An example of the damaged school structure in this earthquake is the building stock owned by the University of L'Aquila, located mainly in three zones of the town, which represents a significant sample of the different architecture typologies, construction dates and structural systems to be found in the region. The University of L'Aquila plays a central role in the life of this town from both cultural and economic perspectives and it constitute a significant sampling of the different architecture typologies coexisting in the area, including examples of traditional masonry buildings together with modern constructions of architectural value [57].

3.3.3 Central Italy Seismic Events (2016)

The recent Central Italy earthquake consisted of a sequence of events. The first earthquake of the sequence ($M=6.0$) hit several central Italy regions (i.e., Abruzzo, Lazio, Umbria, Marche regions) on August 24, 2016, at 01:36:32 GMT; the quake epicentre was close to Amatrice, Accumoli, and Arquata del Tronto and caused diffuse building collapse and about 300 casualties. Two months later, on October 26, 2016, two events, $M=5.4$ (17:10:36 UTC) and $M=5.9$ (19:18:06 UTC), extended the seismogenic volume to the NW. Four days later, on October 30, 2016, at 06:40:18 UTC, an event of $M=6.5$, struck the area corresponding to the Sibillini mountains, with epicentre located close to Norcia, Umbria region. The quakes that occurred after the first event caused extensive damage, especially to many historical buildings, but no deaths were registered [58].

The progressive damage of the Amatrice civic clock tower, symbol of the destruction of 2016 Central Italy seismic sequence, was investigated by Poiani et al. [59] with an advanced numerical model.

Another study that assess the effects of a real earthquake belonging to Central Italy seismic sequence is proposed by Gazzani et al. [60] considering the case of Pomposa Abbey belfry.

In this Section the results of the visual inspections of damages occurred on many school buildings in the aftermath of the 2016 Central Italy earthquake sequence are reported in the photographic survey (Figure 3.6), joined with the vulnerabilities of the school buildings observed.

RC buildings showed significant damage or, in several cases, the collapse of partition walls and ceilings; the observed behaviour for each building confirms the relevance of the performance of non-structural elements in the overall response of the structure, which becomes critical if the building is a school with large population exposure and a possible emergency management role.

Moreover, RC school complexes may suffer from insufficient technical joints between different buildings, especially for very irregular in-plane configuration. In this case, damage may occur to structural joints with a seismic pounding effect between buildings, which may lead to out-of-plane behaviour of infill walls.

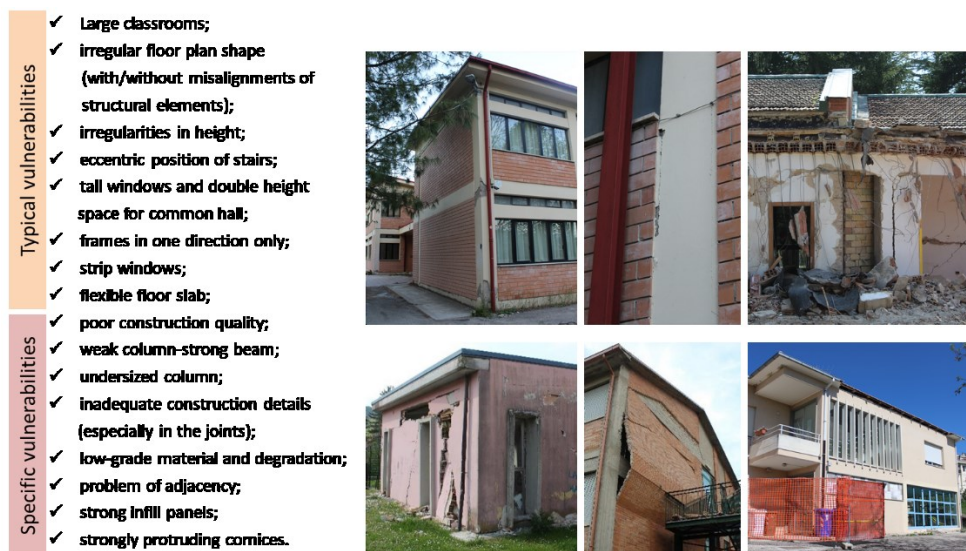


Figure 3.6 Vulnerabilities of school buildings and earthquake damage observed.

From the results obtained for masonry case study buildings, it was possible to observed that:

- the plaster expulsion from masonry walls may lead to the unusability of schools because of non-structural damage on electrical, plumbing, and heater systems and/or other;
- old masonry school buildings may have damage due to insufficient transverse connection between orthogonal masonry walls, with triggering of the façade-overturning mechanism. In the case of strong motion, false vault collapse may occur.

4 Chapter - The school building stock: the case studies of the municipality of Trecastelli (AN)

4.1 Historical seismology

The seismic characterisation of the area of the municipality of Trecastelli is articulated through the historical-seismological classification and the evaluation of the local seismic response.

The Marche region has been affected for centuries by a widespread and frequent seismic activity, with maximum intensity equal to the X degree of the MCS scale.

In particular, the seismic activity is concentrated in well-defined bands (fault lines) from the geological and physiographic point of view:

- a more internal one corresponding to the area of the Apennine zone, characterised by frequent earthquakes and intensity equal to the X degree of the MCS scale and where the seismogenic activity takes place within the first 12 km of depth;
- an intermediate line corresponding to the pedeappenninic area, characterised by a moderate but widespread seismic activity;
- the periadriatic lineament characterised by moderate seismic activity and, generally, the seismic activity is limited to the first 10 km of depth.

The earthquakes that periodically affect the regional territory are the expression of a still active tectonic faults.

The municipalities of Ripe, Monterado and Castel Colonna were classified as seismic locations since 1935 due to the Royal Decree L.25 March 1935, n. 640 (GU n. 120 del 22/05/1935) following the seismic events occurred, where it was necessary to follow more stringent building standards and regulations (Figure 4.1).

This Decree: 1) forced municipalities to prepare their codes; 2) limited the heights of the buildings according to the width of the roads and the construction techniques and 3) introduced a coefficient of reduction of the loads.

ELENCO dei Comuni e frazioni di Comune nei quali è obbligatoria l'osservanza delle speciali norme tecniche di edilizia per le località sismiche della 1ª e della 2ª categoria.

(Elenco allegato al R. decreto-legge)

1ª categoria	2ª categoria	Annotazioni
PROVINCIA DI ANCONA.		
Agugliano (per la frazione Castel d'Emilio) Ancona Camerano Castel Colonna Castelidardo Chiaravalle Corinaldo Monsano Montemarcellano Monterado Monte San Vito Morro d'Alba Numana Offagna Osino (per le frazioni Abbazia, Aspigo, Campo Cavallo, San Biagio Gallo e Stazione) Ostra Polverigi Ripe San Marcello Senigallia		

Figure 4.1 List of Municipalities and fractions and parts of Municipalities in which the observance of the technical building standards for the seismic sites of the 1st and 2nd category was required.

The Working Group for the drafting of the seismic hazard map (OPCM n.3274 of 20.03.2003 – INGV) proposed a seismogenic zonation ZS9 that integrates the previous information levels with the latest developments in the studies in the geological-structural and seismogenic fields (Figure 4.2).

For the eastern Marche region, the Zone n. 917, in which the municipal territory of Trecastelli falls, the ZS9 model identifies a soft compressive tectonic regime, with alignments along the coast or towards the sea and an effective depth class included between 5 and 8 km, representative of most seismic events.

The OPCM n. 3274 of 20 March 2003 and subsequent modification and additions, implemented by the Marche Region Decree D.G.R. n. 1046 of 29.07.2003, classifies the municipality of Trecastelli in Zone 2 (Figure 4.3).

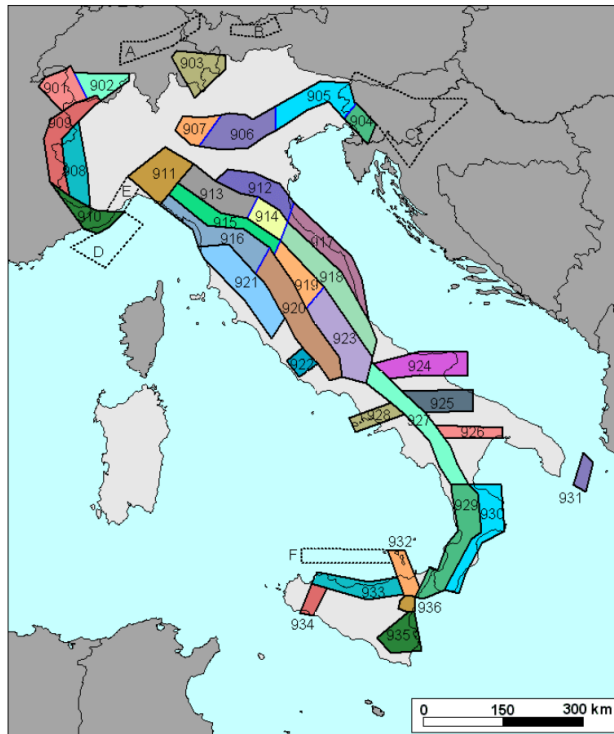


Figure 4.2 Seismogenic Zonation ZS9 (App. 2 al Rapporto conclusivo, Meletti, Valensise 2004)

The subsequent OPCM n.3519 of 2006 defines the seismic hazard of the national territory, expressed in terms of maximum acceleration to the ground.

In this context, the municipal territory is characterised by a seismic hazard defined in terms of maximum horizontal expected acceleration a_g in free field conditions on a rigid site of reference with horizontal topographic surface (A T1) equal to:

TR 475: $a_g = 0.185 \text{ g}$ (Ripe, Monterado and Castel Colonna)

TR 712 anni: $a_g = 0.214 \text{ g}$ (Monterado and Castel Colonna) - 0.215 g (Ripe)

The Annex 7 of OPCM n. 3907/2010 (Contributions for seismic risk prevention interventions) includes a list of municipalities and classification periods (Figure 4.4).

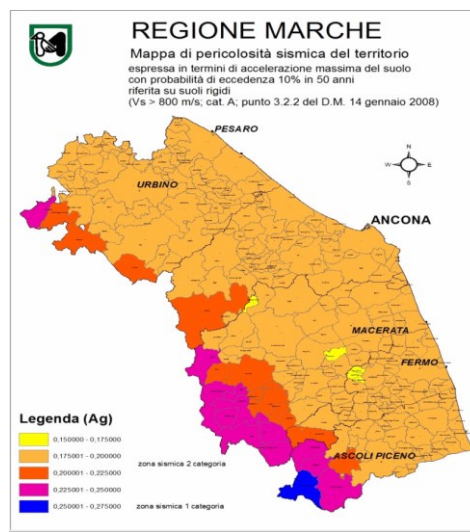
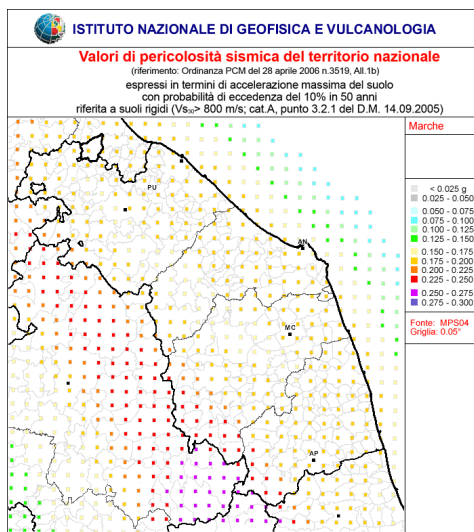


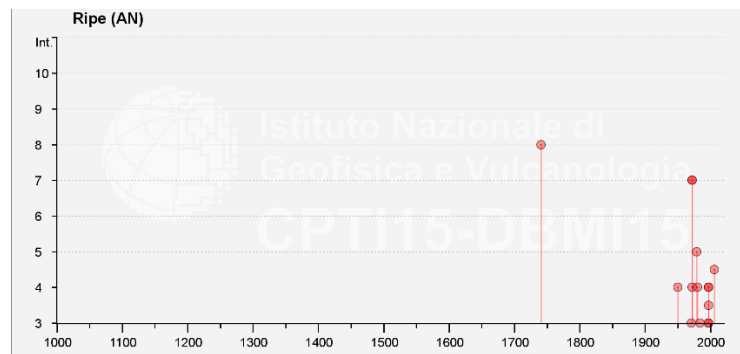
Figure 4.3 Seismic hazard map – Zone 2: a_g ranging between 0.175 – 0.200 g.

Allegato 7: elenco dei comuni con $a_g > 0.125 g$ e periodi di classificazione

Codice Istat	Provincia	Comune	a_g	Data di prima classificazione dell'intero territorio comunale	Periodo di declassificazione
11042001	042	Agugliano	0.183579	1983*	
11042002	042	Ancona	0.182759	1935	
11042003	042	Arcevia	0.177204	1983	
11042004	042	Barbara	0.181873	1983	
11042005	042	Belvedere Ostrense	0.185198	1983	
11042006	042	Camerano	0.180549	1935	
11042007	042	Camerata Picena	0.183124	1958	
11042008	042	Castellbellino	0.180545	1983	
11042009	042	Castel Colonna	0.184821	1935	
11042010	042	Castelfidardo	0.182431	1935	
11042011	042	Castelleone di Susa	0.181611	1983	
11042012	042	Castelplanio	0.178957	1983	
11042013	042	Cerreto d'Esi	0.17834	1983	
11042014	042	Chiaravalle	0.183229	1935	
11042015	042	Corinaldo	0.185688	1935	
11042016	042	Cupramontana	0.178906	1983	
11042017	042	Fabriziano	0.210939	1983	
11042018	042	Falconara Marittima	0.182167	1958	
11042019	042	Filottrano	0.183834	1983	
11042020	042	Genga	0.175793	1983	
11042021	042	Jesi	0.184627	1983	
11042022	042	Loreto	0.181455	1983	
11042023	042	Marilati Spontini	0.180495	1983	
11042024	042	Merigo	0.175421	1983	
11042025	042	Monzano	0.184003	1935	
11042026	042	Montecarotto	0.178976	1983	
11042027	042	Montemarciano	0.18334	1935	
11042028	042	Monterado	0.184765	1935	
11042029	042	Monte Roberto	0.180685	1983	
11042030	042	Monte San Vito	0.183871	1935	
11042031	042	Morro d'Alba	0.184437	1935	
11042032	042	Numana	0.179472	1935	
11042033	042	Offagna	0.182805	1935	
11042034	042	Osimo	0.183589	1983*	
11042035	042	Ostra	0.185007	1935	
11042036	042	Ostra Vetere	0.185285	1983	
11042037	042	Poggio San Marcello	0.177945	1983	
11042038	042	Polverigi	0.183628	1935	
11042039	042	Ripe	0.185035	1935	
11042040	042	Rosora	0.175751	1983	

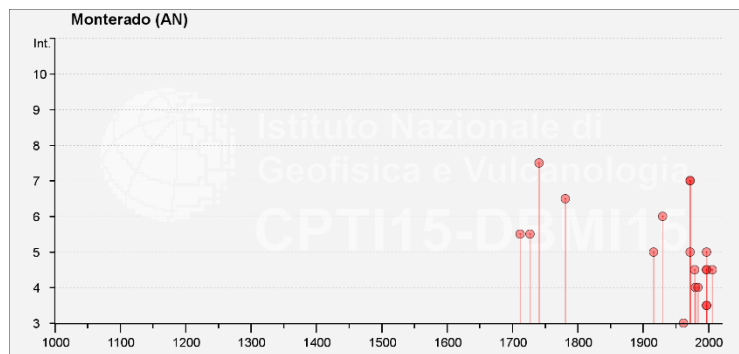
Figure 4.4 Annex 7 of OPCM n. 3907 - Contributions for seismic risk prevention interventions: list of municipalities and classification periods.

The analysis on the historical seismicity of the municipal territory considered the macroseismic data reported in the Italian macroseismic database, the latest version DBMI 2015 (<https://emidius.mi.ingv.it>), from which the most important events affected the territory of Trecastelli were selected, referring to the fractions of Ripe (Figure 4.5), Monterado (Figure 4.6) and Castel Colonna (Figure 4.7). These three municipality denominations existed until 1st January 2014, when the municipality of Trecastelli, in the province of Ancona, was established by merging these adjacent territories, following the Regional Law n.18, 22th July 2013.



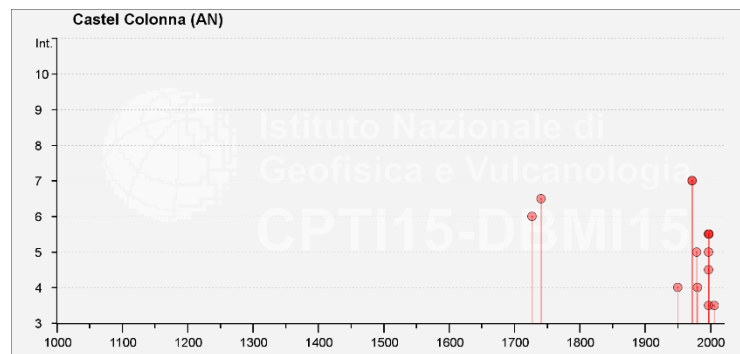
Effetti	In occasione del terremoto del									
Int.	Anno	Me	Gi	Ho	Mi	Se	Area epicentrale	NMDP	Io	Mw
8	1741	04	24	09	20		Fabrianese	135	9	6.17
NF	1906	01	29	15	05		Valle del Tronto	50	5	4.28
NF	1948	06	13	06	33	3	Alta Valtiberina	142	7	5.04
4	1950	09	05	04	08		Gran Sasso	386	8	5.69
NF	1971	02	11	18	49	2	Valle del Chiascio	71	6	4.61
3	1971	10	04	16	43	3	Valnerina	43	5-6	4.51
7	1972	02	04	02	42	1	Costa anconetana	75		4.57
7	1972	02	04	09	18	3	Costa anconetana	56		4.36
4	1972	11	30	11	25	2	Costa pesarese	30		4.52
5	1979	09	19	21	35	3	Valnerina	694	8-9	5.83
4	1980	11	23	18	34	5	Irpinia-Basilicata	1394	10	6.81
3	1984	04	29	05	02	5	Umbria settentrionale	709	7	5.62
2-3	1986	10	13	05	10	0	Monti Sibillini	322	5-6	4.46
NF	1993	06	05	19	16	1	Valle del Topino	326	6	4.72
4	1997	09	26	00	33	1	Appennino umbro-marchigiano	760	7-8	5.66
4	1997	09	26	09	40	2	Appennino umbro-marchigiano	869	8-9	5.97
3	1997	10	03	08	55	2	Appennino umbro-marchigiano	490		5.22
3-4	1997	10	06	23	24	5	Appennino umbro-marchigiano	437		5.47
3	1997	10	14	15	23	1	Valnerina	786		5.62
NF	2006	04	10	19	03	3	Maceratese	211	5	4.06
4-5	2006	10	21	07	04	1	Anconetano	287	5	4.21

Figure 4.5 Seismic events related to Ripe.



Effetti	In occasione del terremoto del									
Int.	Anno	Me	Gi	Ho	Mi	Se	Area epicentrale	NMDP	Io	Mw
5-6	1712	03	28				Appennino umbro-marchigiano	3	6-7	4.86
5-6	1727	12	14	19	45		Valle del Metauro	32	7	5.24
7-8	1741	04	24	09	20		Fabrianese	135	9	6.17
6-7	1781	06	03				Cagliese	157	10	6.51
5	1916	08	16	07	06	1	Riminese	257	8	5.82
6	1930	10	30	07	13		Senigallia	268	8	5.83
2	1957	11	11	21	40		Costa anconetana	50	5	4.50
3	1962	01	23	17	31		Costa pesarese	49	5	4.35
7	1972	02	04	02	42	1	Costa anconetana	75	4	4.57
7	1972	02	04	09	18	3	Costa anconetana	56	4	4.36
5	1972	11	30	11	25	2	Costa pesarese	30	4	4.52
4-5	1979	09	19	21	35	3	Valnerina	694	8-9	5.83
4	1980	11	23	18	34	5	Irpinia-Basilicata	1394	10	6.81
4	1984	04	29	05	02	5	Umbria settentrionale	709	7	5.62
4-5	1997	09	26	00	33	1	Appennino umbro-marchigiano	760	7-8	5.66
5	1997	09	26	09	40	2	Appennino umbro-marchigiano	869	8-9	5.97
3-4	1997	10	03	08	55	2	Appennino umbro-marchigiano	490	5	5.22
3-4	1997	10	06	23	24	5	Appennino umbro-marchigiano	437	5	5.47
4-5	1997	10	14	15	23	1	Valnerina	786	5	5.62
4-5	2006	10	21	07	04	1	Anconetano	287	5	4.21

Figure 4.6 Seismic events related to Monterado.



Effetti	In occasione del terremoto del									
Int.	Anno	Me	Gi	Ho	Mi	Se	Area epicentrale	NMDP	Io	Mw
6	1727	12	14	19	45		Valle del Metauro	32	7	5.24
6-7	1741	04	24	09	20		Fabrianese	135	9	6.17
4	1950	09	05	04	08		Gran Sasso	386	8	5.69
7	1972	02	04	02	42	1	Costa anconetana	75		4.57
7	1972	02	04	09	18	3	Costa anconetana	56		4.36
5	1979	09	19	21	35	3	Valnerina	694	8-9	5.83
4	1980	11	23	18	34	5	Irpinia-Basilicata	1394	10	6.81
NF	1986	10	13	05	10	0	Monti Sibillini	322	5-6	4.46
NF	1993	06	05	19	16	1	Valle del Topino	326	6	4.72
5	1997	09	26	00	33	1	Appennino umbro-marchigiano	760	7-8	5.66
5-6	1997	09	26	09	40	2	Appennino umbro-marchigiano	869	8-9	5.97
5-6	1997	10	03	08	55	2	Appennino umbro-marchigiano	490		5.22
4-5	1997	10	06	23	24	5	Appennino umbro-marchigiano	437		5.47
3-4	1997	10	14	15	23	1	Valnerina	786		5.62
5-6	1998	03	26	16	26	1	Appennino umbro-marchigiano	409		5.26
NF	2006	04	10	19	03	3	Maceratese	211	5	4.06
3-4	2006	10	21	07	04	1	Anconetano	287	5	4.21

Figure 4.7 Seismic events related to Castel Colonna.

The lists highlight the main events, from 1741 to 2006, with the parameters relating to the intensity of the effects in the sites [MCS], the epicentral area of the earthquake, the epicentral intensity and the moment magnitude.

In the municipal territory the most important seismic events occurred both in epicentral areas of the mountain zone (Fabrianese occurred on 1741 and Valnerina on 1979) and the coastal area (Costa Anconetana on 1972), which they have produced macroseismic intensity effects ranging from 5 to 8 degrees of MCS scale.

4.2 Local soil conditions at the sites: the ground-type/soil-category

The geological reports made specifically for this study of seismic vulnerability in accordance with NTC 2008 include:

- Descriptions of the survey program;
- Seismic investigations by MASW method;
- Passive seismic surveys performed with the horizontal-to-vertical spectral ratio (HVSr) method;
- geognostic surveys;
- Plans with survey locations;
- Lithological and stratigraphic profiles of the subsoil with the groundwater level;
- Geological-stratigraphic columns.

The subsoil of the municipality of Trecastelli is substantially composed of a compact and consistent clayey-marly substratum.

The site characteristics and ground responses for each school complex are summarised in the following Table 4.1.

School	Altitude above sea level (m a.s.l.)	Latitude / Longitude	Ground type
IC Nori de' Nobili - Lower secondary school (Ripe)	120-140	43.66969/13.10639	C T3
G. Marconi (Monterado)	163	43.69610/13.09202	C T3
Peter Pan (Brugnetto - Ripe)	48	43.65953/13.15237	C T1
Il Piccolo Principe (Castel Colonna)	150	43.68061/13.10429	B T3
Il Girasole (Ripe)	130	43.67224/13.10392	C T1
La Carica dei 101 (Ponte Rio – Monterado)	39	43.72641/13.098997	C T1

Table 4.1 Definitions of site characteristics and ground responses for each school complex.

4.3 Acquisition of the appropriate level of knowledge of buildings, of the confidence factor FC and of the properties of materials

In European countries, most of the old existing RC framed buildings are usually characterised by poor quality materials with highly dispersed mechanical properties [61] [62].

In particular, for concretes, this feature is ascribable to the limited knowledge of the concrete mix design and to the lack of curing quality in casting operations that in the past characterised the construction of these buildings.

Moreover, different seasoning phases and material decay, which are quite common for these buildings, as well as stress conditions and loading history, may have further accentuated this state. In the field of the seismic assessment of existing RC buildings, an accurate estimation of the concrete and reinforcement mechanical properties is fundamental to provide a reliable prediction of the seismic behaviour of buildings. The compressive strength of concrete is the most used parameter for the characterisation of concrete mechanical properties, from which stiffness values can be also derived. In some cases, carbonation tests can be added with the aim of assessing the state of degradation of the structural elements.

Similarly, masonry is a composite material obtained joining bricks by means of mortar layers. The non-uniformity of the mixture is due to the variability of both the components, mortar and bricks, by the part of the country considered and then the final values of the stiffness and resistances have great variability in the territory. For this reason, it is very limited to characterise the masonry material of old constructions only by the Tables C8A.2.1 and C8A.2.2 without in situ surveys[20].

The surveys to acquire an appropriate level of knowledge of the buildings for the analyses were performed according to Chapter 8 of the D.M. 14 January 2008 and of the Chapter C8 of the related Explanatory Circular No. 617 of 2 February 2009.

The investigation also consisted in a geometrical survey aimed at a quality check-up of wall-to-wall and wall-to roof connections, and the characterisation of masonry texture.

National codes and standards provide clear rules and testing procedures for the material properties evaluation. The concrete core testing, which is a destructive test that consists of the extraction of concrete cores from structural elements and the execution of laboratory compression tests on them, is the most reliable tool and it is exactly that used in the present work.

The mechanical properties of masonry school building analysed in the municipality of Trecastelli were obtained by a double flat jack testing method.

The available data obtained by surveys allowed to achieve a normal Knowledge Level (KL), classified in the Italian Seismic Code (NTC2018) as KL2, corresponding to a Confidence Factor (CF) equal to 1.20.

Otherwise, the evaluations of the most recent buildings are considered only a preliminary study only for the purpose of this research to have a picture of the behaviour of all school complexes of the municipality.

For these buildings, a level of knowledge KL1 was assumed and further investigations are necessary to achieve a level of knowledge appropriate to the analysis method as indicated in the NTC08 and related Circular. The results of the in situ investigations and of the inspections carried out are summarised below in Tables 4.2, 4.3, 4.4, 4.5, 4.6, 4.7.

IC Nori de' Nobili (Ripe)	Materials	Surveys	KL
BUILDING A	The cement type is "730" and the smooth steel rebar type is Aq42.	<ul style="list-style-type: none"> • Concrete core test for strenght and carbonatation testing (Figure 4.8a); • tensile test of steel bar; • pacometric test to localise reinforcement in RC elements; • video-endoscope survey for floor inspection 	2
BUILDING B	The cement type is "425", the concrete type is R _{bk} 300 and the ribbed steel rebar type is FeB44k.		2
BUILDING C			2
BUILDING D			2
Remarks: Considering the inspections and in situ surveys carried out, there is a moderate correspondence between the conditions of the places and what is reported in structural design documents. With regard to the original design documents of Building A, the absence of original test certificates on the materials was found. With regard to B and C buildings, the lack of RC reinforcement drawings was found (only in table format).			

Table 4.2 Properties of materials and KL for IC Nori de' Nobili school complex (Ripe).

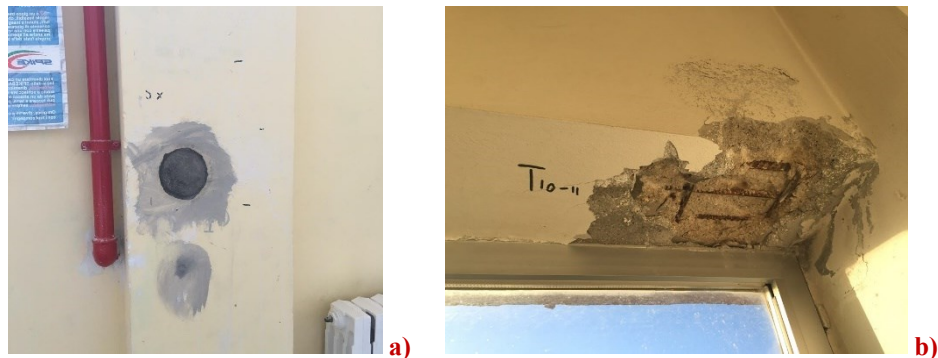


Figure 4.8 A concrete core test for strength (a) and a verification of rebars (b) (Ripe).

G. Marconi (Monterado)		Materials	Surveys	KL
BUILDING A		Solid bricks and lime mortar.	<ul style="list-style-type: none"> • Flat jack testing method for masonry properties; • video-endoscope survey for floor inspection; • inspection holes in floors and peripheral walls. 	2
BUILDING B		The cement type is “425” and the steel rebars are smooth instead of the ribbed steel rebar type written on project (FeB44k).	<ul style="list-style-type: none"> • Concrete core test for strenght and carbonatation testing (Figure 4.9a); • tensile test of steel bar; • pacometric test to localise reinforcement in RC elements (Figure 4.9b); • video-endoscope survey for floor inspection 	3
BUILDING C		The cement type is “425”, the concrete type is R_{ck} 350 and the ribbed steel rebar type is FeB44k.		3
<p>Remarks:</p> <p>Considering the inspections and in situ surveys carried out, there is a moderate correspondence between the conditions of the places and what is reported in structural design documents (documents are not available for the masonry building).</p> <p>Building A is a structurally independent unit separated from B and C buildings by joints. It is difficult to evaluate the interaction with adjacent buildings (other properties); for this reason, three possible situations were taken into account, with different constraints between buildings.</p> <p>In Building C there is a floor slab with a thickness of 20+4 cm instead of 16+4 cm (project).</p>				

Table 4.3 Properties of materials and KL for G. Marconi school complex (Monterado).

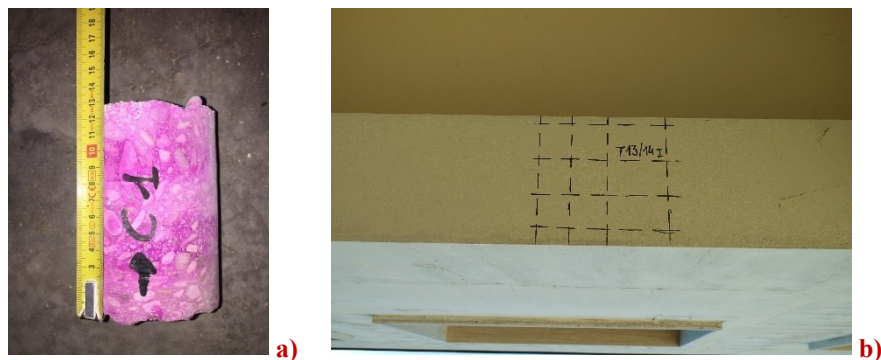


Figure 4.9 A pacometric test (a) and a concrete carbonatation testing (b) (Monterado).

Peter Pan (Brugnetto - Ripe)		Materials	Surveys	KL
BUILDING A	The cement type is "425" and the smooth steel rebar type is Aq50.	The concrete type is C28/35, the ribbed steel rebar type is B450C and the glued laminated timber type is GL24h.	<ul style="list-style-type: none"> • Concrete core test for strength and carbonation testing; • tensile test of steel bar; • pacometric test to localise reinforcement in RC elements (Figure 4.10). 	2
BUILDING B				2
Remarks: Considering the inspections and in situ surveys carried out, there is a moderate correspondence between the conditions of the places and what is reported in structural design documents for Building A (some differences regarding the dimensions of the rectangular column of the patio and the non-naming of some beams); otherwise, a good correspondence can be seen for Building B.				

Table 4.4 Properties of materials and KL for Peter Pan school complex (Brugnetto – Ripe).



Figure 4.10 A pacometric test on a RC wall to verify the positioning of steel bars (Brugnetto – Ripe).

Il Piccolo Principe (Castel Colonna)		Materials	Surveys	KL
BUILDING A	Solid bricks and lime mortar.	The concrete type is R_{bk} 300 and the ribbed steel rebar type is FeB44k.	<ul style="list-style-type: none"> • Flat jack testing method for masonry properties; • inspection holes in floors and peripheral walls (Figure 4.11). • Concrete core test for strength and carbonation testing; • tensile test of steel bar; • pacometric test to localise reinforcement in RC elements. 	2
BUILDING B				2
BUILDING C				2
BUILDING D				2
Remarks: Considering the inspections and in situ surveys carried out, there is a moderate correspondence between the conditions of the places and what is reported in structural design documents for Building A. Only intervention projects (not the design project) of Building A were found. In Building A there is a heavy ceiling made by hollow clay blocks hanging from the roof. Finally, it is possible to see openings on peripheral walls closed only with hollow bricks and mortar instead of solid bricks and lime mortar.				

Table 4.5 Properties of materials and KL for Il Piccolo Principe school complex (Castel Colonna).



Figure 4.11 Inspection holes in floors (a) and peripheral walls (b) (Castel Colonna).

Il Girasole (Ripe)	Materials	Surveys	KL
BUILDING A	The concrete type is Rbk 300 and the ribbed steel rebar type is FeB44k.	<ul style="list-style-type: none"> • Concrete core test for strength and carbonatation testing; • tensile test of steel bar; • pacometric test and inspections to localise reinforcement in RC elements (Figure 4.12). 	2
Remarks: Considering the inspections and in situ surveys carried out, there is a moderate correspondence between the conditions of the places and what is reported in structural design documents (some differences regarding the reinforcement of RC beams).			

Table 4.6 Properties of materials and KL for Il Girasole school building (Ripe).



Figure 4.12 Inspection to verify not complying steel reinforcements of beams (Ripe).

La Carica dei 101 (Ponte Rio - Monterado)	Materials	Surveys	KL
BUILDING A	The concrete type is Rbk 300 and the ribbed steel rebar type is FeB44k. There are also tubular profile made by Fe 37 B and steel columns (Fe 360).	<ul style="list-style-type: none"> • Concrete core test for strength and carbonation testing; • tensile test of steel bar; • pacometric test to localise reinforcement in RC elements; • magnetoscopic survey for the detection of defects on metallic elements (Figure 4.13a); • evaluation of the degradation on metallic elements (Figure 4.13b). 	2
BUILDING B	The cement type is "425", the concrete type is Rbk 300 and the ribbed steel rebar type is FeB44k.	Limited visual inspections.	1
BUILDING C			1
BUILDING D			1
Remarks: Considering the inspections and in situ surveys carried out, there is a good correspondence between the conditions of the places and what is reported in structural design documents.			

Table 4.7 Properties of materials and KL for La Carica dei 101 school complex (Ponte Rio).



Figure 4.13 A magnetoscopic survey for the detection of defects (a) and the evaluation of the degradation on metallic elements (b) (Ponte Rio - Monterado).

4.4 Description of case studies

The school complexes assessed in this work are located in areas belonging to the Municipality of Trecastelli in the province of Ancona.

For the analyses of these structures, documents were found at the offices of Ex Genio Civile of Ancona and in situ surveys were performed to define the material properties as described in Section 4.3.

4.4.1 IC Nori de' Nobili (Ripe)

The first school complex evaluated is the Lower Secondary School of Ripe "IC Nori De 'Nobili" (Figure 4.14) located in the municipality of Trecastelli in Viale Umberto I 18 60012 (AN).

The school complex consists of four RC framed structures built in different periods and characterised by different floor plans and number of storeys.

The four buildings are structurally independent as they are separate from each other, so the performance of each individual building was evaluated.

These structures are characterised by one-way hollow block slabs 16 + 4 cm high, with RC joists ($i = 33$ cm), considered for their characteristics as "flexible floor diaphragms".

Moreover, there are heavy infill panels made by semi-hollow bricks and mortar often interrupted in elevation by windows placed under beams.

Building A (Figure 4.15) was built in 1970: although the original project envisaged an additional elevation with an external staircase, only a 1-storey L-shaped

structure was built, characterised by irregularities in the floor plan and in the distribution of structural elements (beams and columns).

It has got a RC frame structure with columns (arranged at variable distances between 2.60 m and 7.40 m) and beams.

B and C Buildings (Figures 4.16-4.17) were built in 1977 and realised simultaneously, excluding the raising of the second building, already planned in the 1977 project but realised during the construction of the Building D.

Building B hosts the gym, it has a rectangular floor plan and a regular scan of the structure elements while the Building C links the gym with the other buildings of the complex.

The columns of RC framed structure of Building B are arranged at distances of 5.20 m in X-direction and 5.30 and 10.60 m in Y-direction).



Figure 4.14 Analysed buildings of the first school complex.

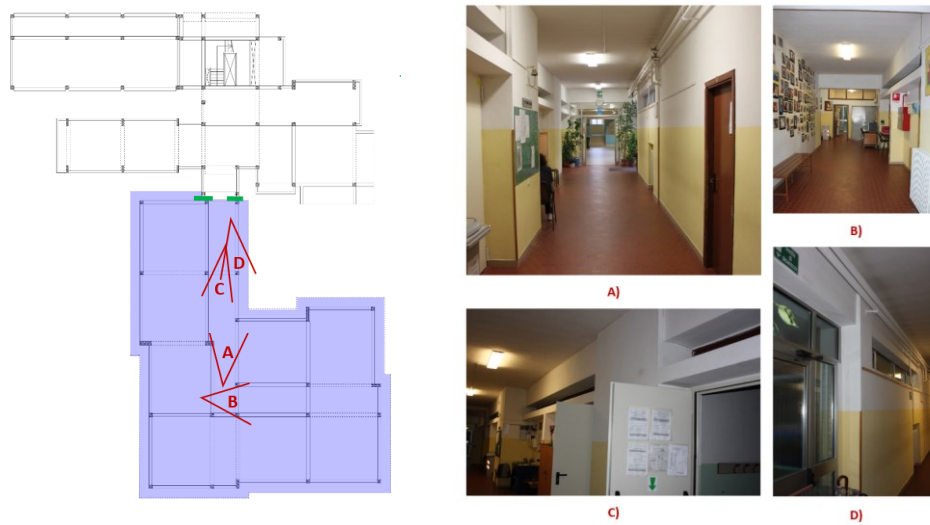


Figure 4.15 Photographic views of Building A.

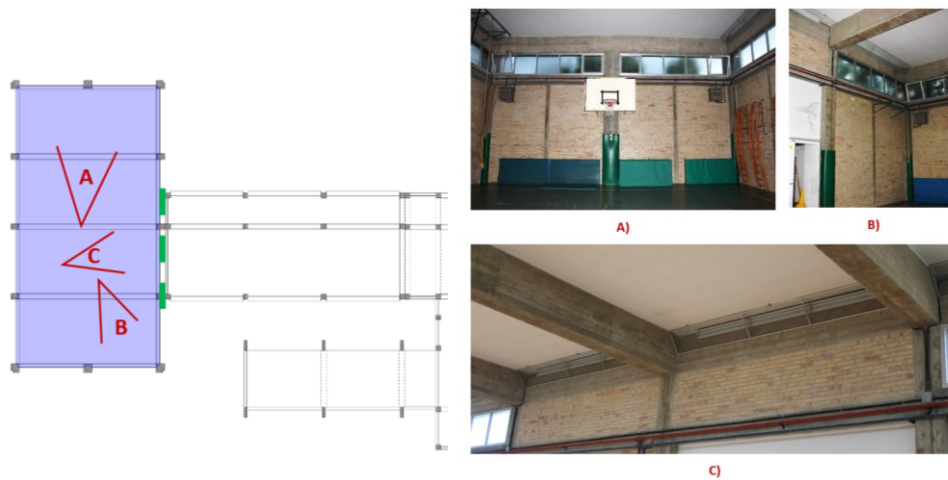


Figure 4.16 Photographic views of Building B.

Building C has a rectangular floor plan and a RC framed structure with columns (arranged with distances of 2.30 m and 5.10 m in X-direction and 5.70 m in Y-direction) and beams.

Finally, the last part of the complex is Building D (Figure 4.18), whose project dates back to the year 1980 and is characterised by many structural irregularities both in floor plan and in elevation than the other buildings. It consists of four storeys and the last elevation hosts only the stairs leading to the not practicable roof.

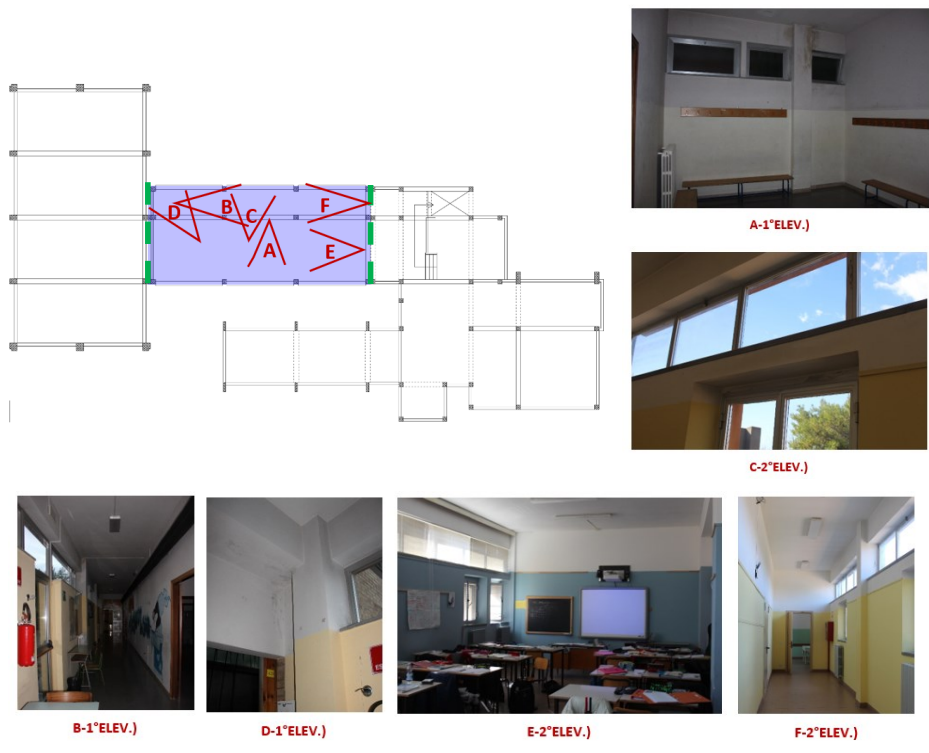


Figure 4.17 Photographic views of Building C.

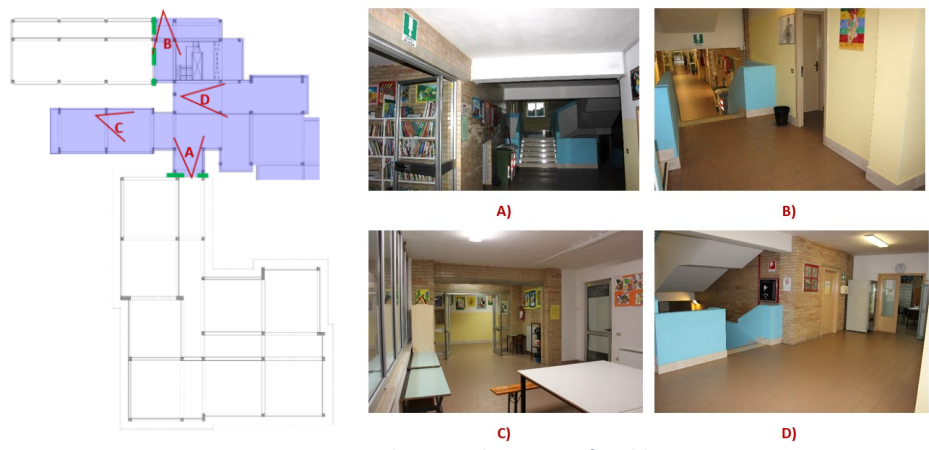


Figure 4.18 Photographic views of Building D.

4.4.2 G. Marconi (Monterado)

The second school complex analysed is the Primary School and Lower Secondary School “G. Marconi” of Monterado (Figure 4.19) located in the municipality of Trecastelli in via E. Paci 44 60012 (AN).



Figure 4.19 Analyzed buildings of the second school complex.

The school complex consists of three independent buildings of different structural and material types: the first construction with masonry walls and one-way hollow block slabs, the second 1-storey RC building realised to optimize the functional distribution and the third 2-storey RC framed structure recently built as an extension for teaching functions.

Building A (Figure 4.20) presumably was built in the '30s following a change in use at school; for this structure the original project was not available, but it was possible to characterise it through in-situ surveys and laboratory tests.

This masonry building consists of two storeys above the ground plus the garret and a basement extended for a small portion of the overall dimensions of the first floor. Moreover, it shows a "U" shape floor plan with maximum dimensions of approximately 30.5 m x 22.3 m.

The bearing structure is made by masonry with solid bricks and lime mortar and floor diaphragms are composed by hollow blocks and a 12 cm-RC slab except for the garret, characterised by "Varese" beams (21 cm high) or by a simple ceiling depending on the different areas.

In Building A, there are different types of roof: a pavilion roof, a simple timber roof with purlins and a flat RC roof. The intermediate floor was considered as "rigid floor diaphragm" and roof floors as "flexible floor diaphragms".

Building B (Figure 4.21) was built in 1979 and denotes a connecting function while Building C was built in 2008.

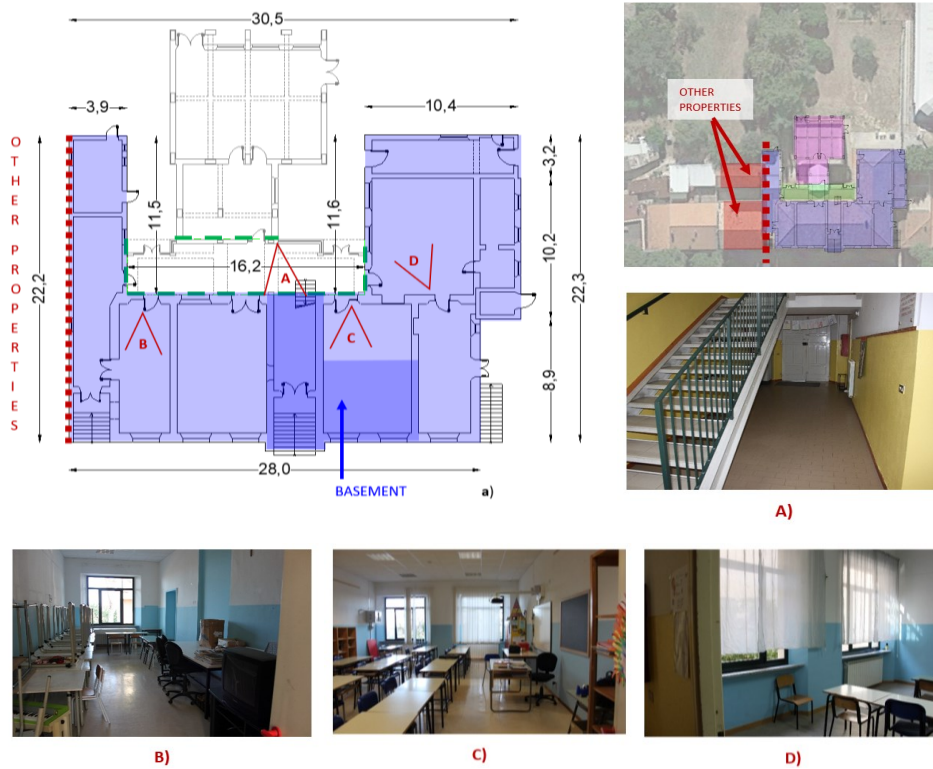


Figure 4.20 Photographic views of Building A.

Building B has a regular rectangular floor plan and it is characterised by a RC structure with columns (arranged at distances of 3.00 m, 3.45 m and 6.35 m in X-direction and 3.15 m and 4.00 m in Y-direction), beams and slab. The maximum dimensions in plan are 16.10 m x 4.00 m. This cast-in-place RC slab, which represents the roof of this building, is 15 cm high and considered as "rigid floor diaphragm".

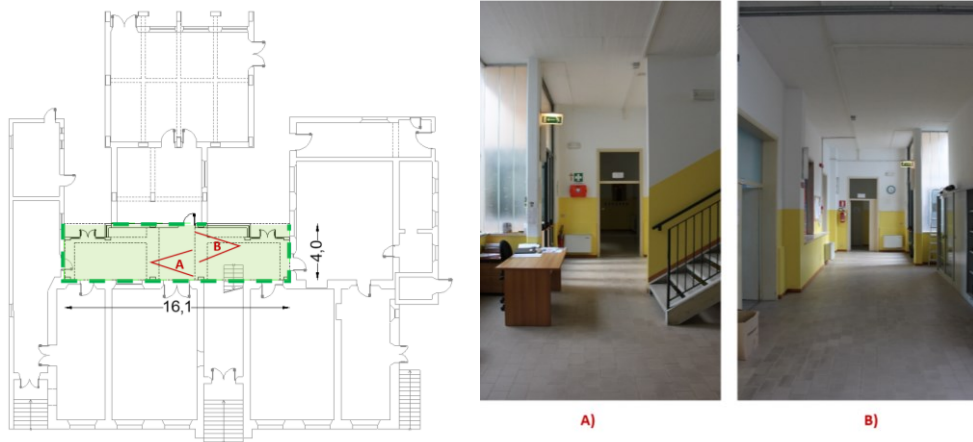


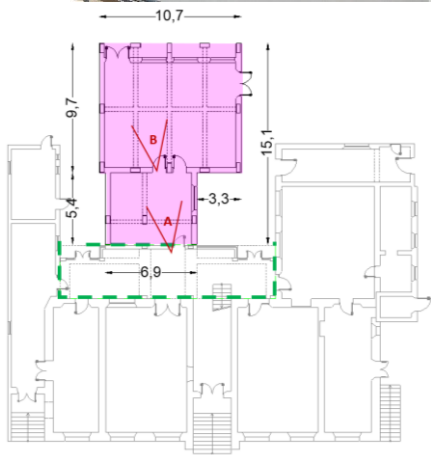
Figure 4.21 Photographic views of Building B.

Building C (Figure 4.22) is characterised by a floor plan consisting of two rectangles (among which there is a misalignment of the bearing structure) and it is made up of RC framed structure with columns (arranged with distances from 2.65 m to 3.92 m in X-direction and 3.85 m and 4.80 m in Y-direction) and beams.

The intermediate floor and the roof are one-way hollow block slabs 20 + 4 cm and 16 + 4 cm high cast-in-place with RC joists ($i = 50$ cm) and they are considered for their characteristics as "rigid floor diaphragms".

The infill walls are made by a double layer hollow blocks with mortar, insulation and plaster.

The three buildings are structurally independent, so the seismic vulnerability of each building was evaluated.



A)



B)

Figure 4.22 Photographic views of Building C.

To evaluate the effects due to the slight irregular floor plan shape (with misalignments of structural elements), to the design of large classrooms for greater functional flexibility, to the inadequate construction details (lack of stirrups in beam-column joints and to the heavy infill walls, the Building C of G. Marconi (Monterado) school complex was chosen for comparison between different types of modelling (see Chapter 5).

This example shows also some discrepancies between in situ survey with deposited project.

Table 4.8 below shows the material values used for non-linear analyses on Building C.

MATERIAL FOR NONLINEAR ANALYSES												
	CONCRETE								STEEL			
	f_{cm} [MPa]	f_{cm} MODEL [MPa]	f_{cm} DUCTILE CHECK [MPa]	f_{cm} BRITTLE [MPa]	E_m [MPa]	E_m cracked concrete [MPa]	ν [-]	ν cracked [-]	f_{ym} [MPa]	f_{ym} MODEL [MPa]	f_{ym} DUCTILE CHECK [MPa]	f_{ym} BRITTLE CHECK [MPa]
COLUMN	34.58	34.58	34.58	23.05	31920.54	23940.40	0.20		543.49	543.49	543.49	472.60
BEAM	34.58	34.58	34.58	23.05	31920.54	15960.27	0.20		543.49	543.49	543.49	472.60
KL	1.00											

Table 4.8 Materials used for nonlinear analyses on Building C – G. Marconi (Monterado).

4.4.3 Peter Pan (Brugnetto - Ripe)

The third school complex evaluated is the kindergarten school “Peter Pan” of Brugnetto Ripe (Figure 4.23) located in the municipality of Trecastelli in Via Pio IX 60012 (AN).

The school complex consists of two one-storey independent buildings, which differ for structural and material types: the first with RC walls and one-way hollow block Slabs and the second with RC framed structure and glued laminated timber beams. Building A was built between 1970 and 1971, with the final project version of 1972, while Building B was built between 2010 and 2011.

Building A (Figure 4.24) has an irregular floor plan with maximum dimensions of approximately 33.2 m x 30.4 m and a basement extended for a small portion of the overall dimensions of the first floor.

The structure consists mainly of thin walls of reinforced concrete (15 and 20 cm thick and intersecting at distances of about 7 m) and of six RC columns around the inner patio, while the roof is made of one-way hollow block slabs 20 + 4 cm high, with RC joists, considered for their features as "flexible floor diaphragms".

The complex has sloping roofs placed on different heights on classrooms, on toilets and on canteen, with volumes visible compared to the hallway characterised by flat roof.



Figure 4.23 Analysed buildings of the third school complex.

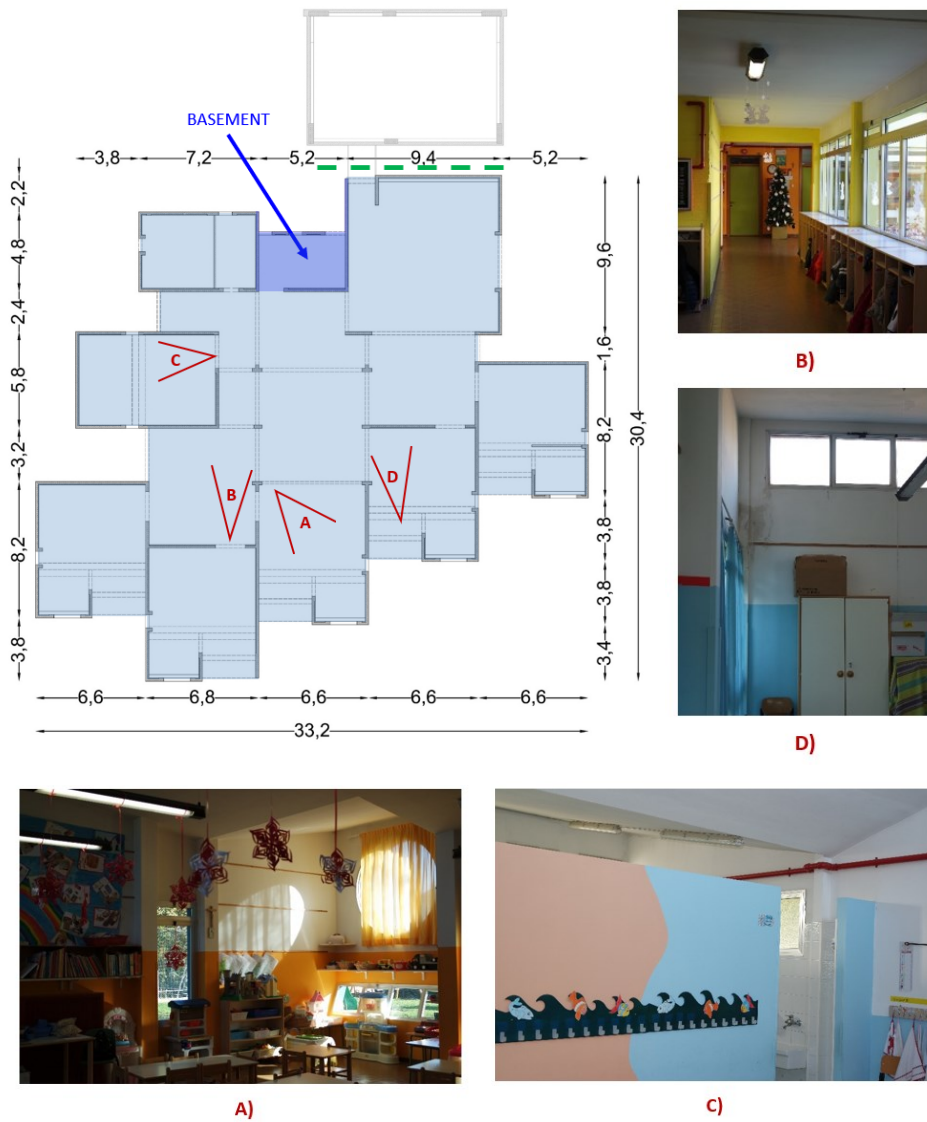


Figure 4.24 Photographic views of Building A.

Building B (Figure 4.25) has a rectangular floor plan and a RC structure with columns and beams and glued laminated timber beams with 35 mm thick wooden deck. The maximum dimensions in plan are 12.2 m x 8.15 m.

There are two types of infill walls: the first made of different layer, lightened hollow blocks (filled with insulation inside the holes) with mortar and plaster, thermal insulation and solid bricks, and the second made with hollow blocks with mortar and a double layer of plaster (both inside and outside). The two buildings are structurally independent, for this reason the seismic vulnerability of each individual building was assessed.

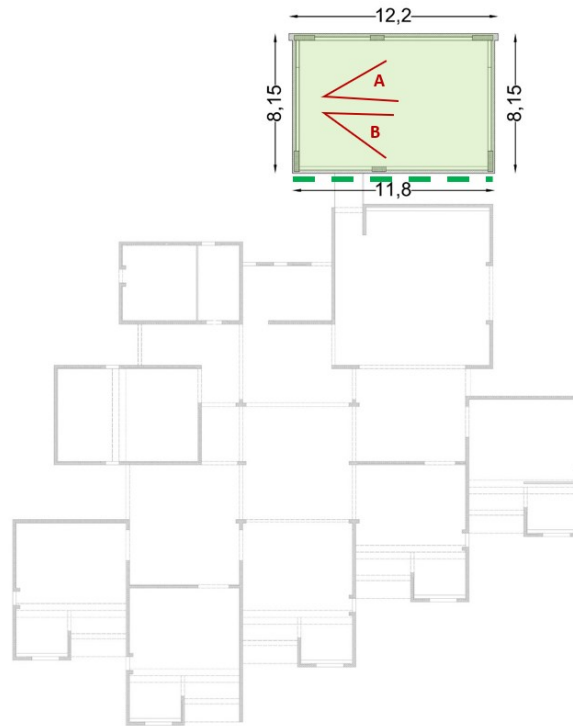


Figure 4.25 Photographic views of Building B.

4.4.4 Il Piccolo Principe (Castel Colonna)

The fourth school complex analysed is the kindergarten school “Il piccolo Principe” of Castel Colonna (Figure 4.26) located in the municipality of Trecastelli in Via Marconi 18 60012 (AN).



Figure 4.26 Analysed buildings of the fourth school complex.

The school complex consists of four independent buildings of different structural and material types: the first construction with masonry walls and one-way hollow block slabs, the second one-storey RC building realised to host the kitchen, the third two-storeys RC building built as an extension for didactic functions and the fourth RC building to optimise the functional distribution by hosting a staircase.

Probably, Building A (Figure 4.27) was built before 1967: the original project was not found in this masonry structure, but it was possible to characterise it through in-situ surveys and laboratory tests.

Building A is a masonry building consisting of two storeys and it has a "T" symmetrical shaped plan in one direction and with maximum sizes of approximately 21.5 m x 9.7 m.

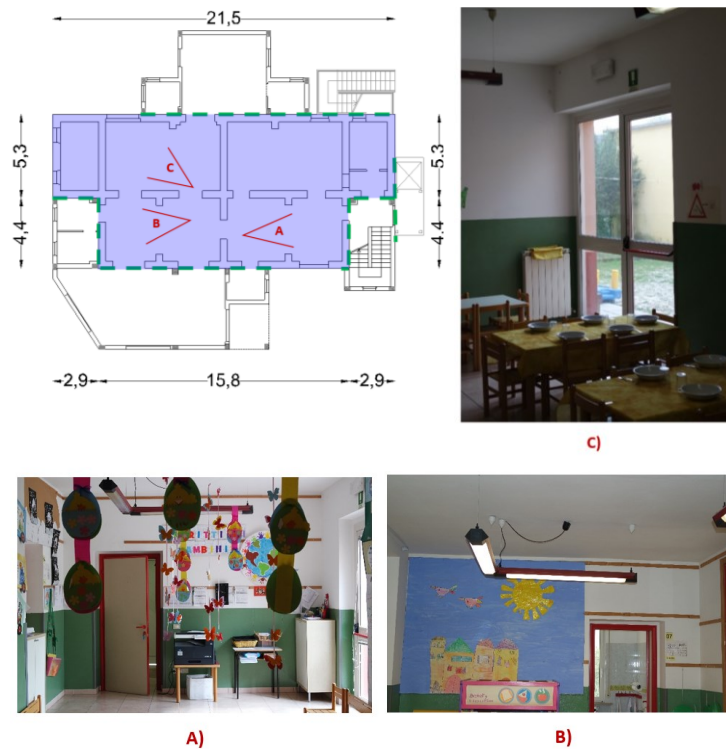


Figure 4.27 Photographic views of Building A.

The bearing structure is made by masonry with solid bricks and lime mortar and floor diaphragms are composed by hollow blocks and RC joists.

The garret is delimited by a heavy ceiling (therefore without a structural slab and considered only as a load on the top of the construction) made by hollow clay blocks hanging from the roof.

The roof is composed of one-way hollow block slabs (16 cm thick) and RC joists, considered for their features as "flexible floor diaphragms".

The three most recent RC buildings (B, C and D) were designed together with the intervention to improve the foundation of the masonry building, they have one-way hollow block slabs with RC joists ($i = 50$ cm) considered as "flexible floor diaphragms" and double layer infill walls with hollow block and mortar, insulation and plaster.

Building B (Figure 4.28) has a "T" symmetrical shaped plan (in one direction) with a RC framed structure with columns (arranged with distances of 2.30 m and 5.55 m in X-direction and 1.92 m and 4.87 m in Y-direction) and beams.

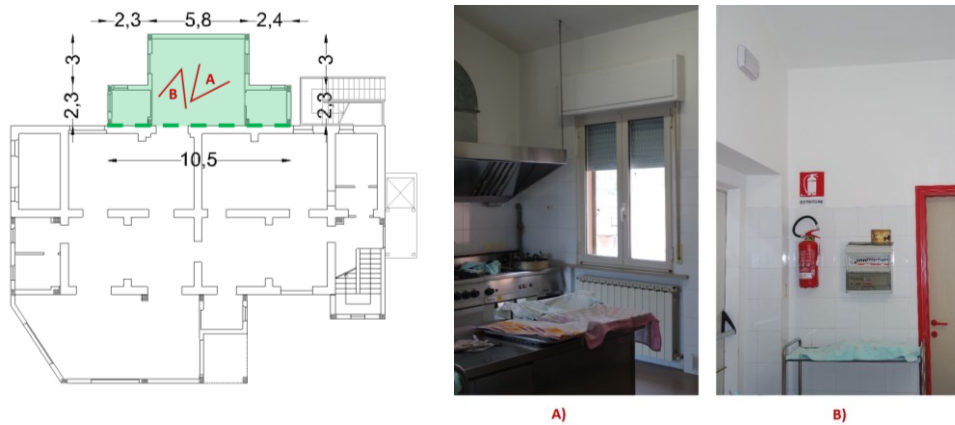


Figure 4.28 Photographic views of Building B.

Building C (Figure 4.29) is characterised by a L-floor plan and it has a RC framed structure with columns (arranged with distances of 2.50 m and 4.70 m in X-direction and 4.10 m and 4.80 m in Y-direction) and beams.

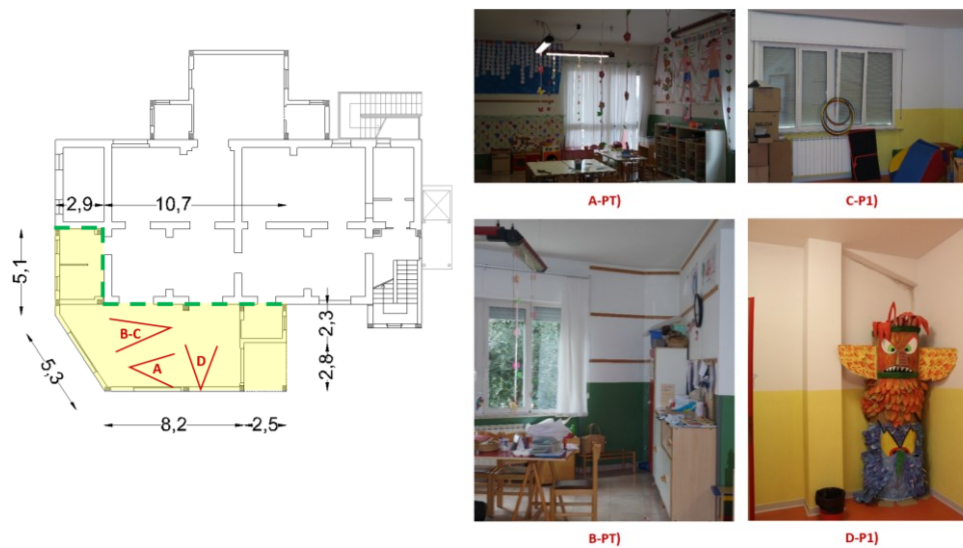


Figure 4.29 Photographic views of Building C.

Building D (Figure 4.30) has a rectangular floor plan with an irregularity at the corner of Building A and a RC framed structure with columns (arranged with distances of 2.50 m and 2.85 m in X-direction and 5.50 m in Y-direction) and beams. Moreover, it is a two-storey building with a sloping roof and with two flights of stairs supported by 15 cm RC slabs.

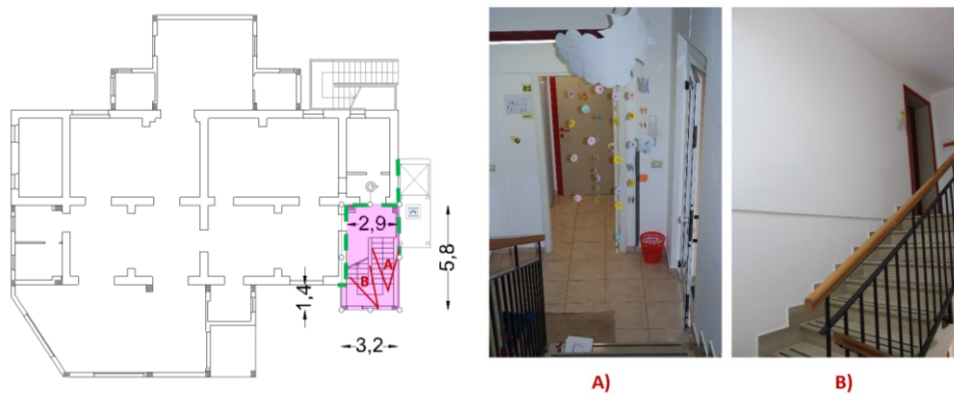


Figure 4.30 Photographic views of Building D.

The four buildings are structurally independent, so their performances were assessed separately.

4.4.5 Il Girasole (Ripe)

The fifth school complex evaluated is the kindergarten school of Ripe “Il Girasole” (Figure 4.27) located in the municipality of Trecastelli in via Mattei, 32 - 60012 (AN).



Figure 4.31 Analyzed buildings of the fifth school complex.

The school complex (Figure 4.28) is formed by a one-storey single RC framed structure with columns (arranged at distances between 2.70 m and 5.40 m) and beams. It was built in 1992 and it is characterised by a trapezoidal shape in plan. The roof is a one-way hollow block slab with a thickness of 20 + 4 cm and RC joists ($i = 50$ cm) considered as a "deformable deck". The infill panels are composed by a double layer of hollow blocks, solid bricks and thermal insulation interposed. This building is an isolated structure from the surrounding building whose seismic vulnerability was assessed.

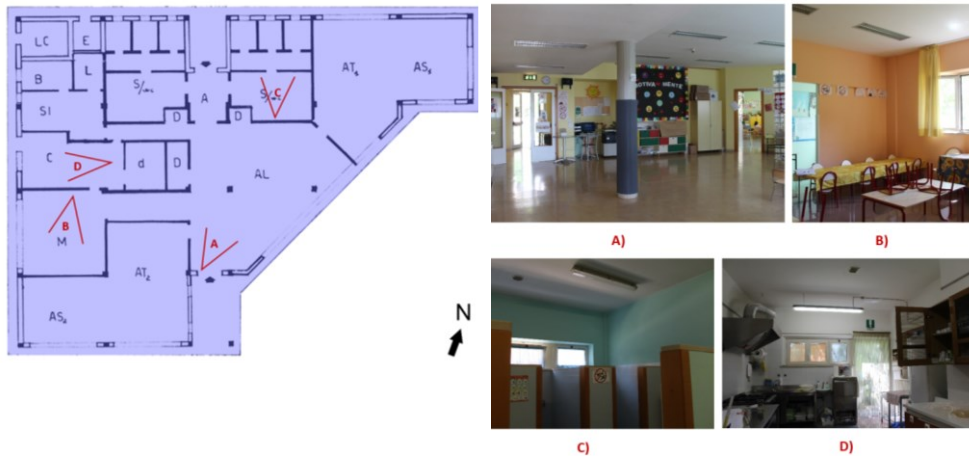


Figure 4.32 Photographic views of the building.

4.4.6 La Carica dei 101 (Ponte Rio - Monterado)

The last school complex evaluated is the kindergarten school “La Carica dei 101” of Ponte Rio - Monterado (Figure 4.29) located in the municipality of Trecastelli, in via I Maggio, 26 – 60012 (AN).



Figure 4.33 Analyzed buildings of the sixth school complex.

The school complex consists of four RC framed structures built in different periods and characterised by different floor plan shapes and only one storey.

The four buildings are structurally independent and separate from each other, so the performance of each individual building was evaluated.

Building A (Figure 4.30) was built in 1983, it has an irregular floor plan and a RC framed structure with columns (arranged with distances of 4.00 m in X-direction and 4.35 m and 4.65 m in Y-direction) and beams.

In Building A, there are two types of roof: a flat RC roof 16+4 cm high cast-in-place with RC joists ($i = 50$ cm) and a steel roof with a corrugated sheet of the thickness of 10/10, both considered as "flexible floor diaphragm" and roof floors as "flexible floor diaphragms".

Infill walls are composed of hollow concrete blocks and mortar, thermal insulation and plaster.

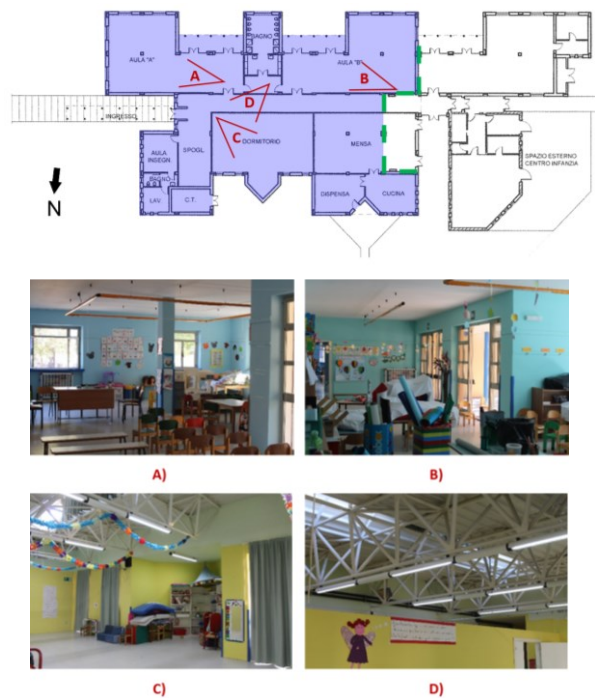


Figure 4.34 Photographic views of Building A.

The three most recent RC buildings (B, C and D) were designed to expand the first building.

They have one-way hollow block slabs (16 + 4 cm thick) with RC joists ($i = 50$ cm) considered as "rigid floor diaphragms" and double layer infill walls with hollow bricks and mortar, insulation, hollow blocks and mortar and plaster.

Buildings B and C were built in 2008 and they show an irregular distribution of structural elements (beams and columns) probably due to the need to maintain the functional and architectural continuity of spaces and, at the same time, to avoid the interaction of the structure.

The building B (Figure 4.31) is an extension of the canteen of Building A, it has a rectangular floor plan but also irregular distances between columns of RC frames while the Building C represents hosts educational function and services.



Figure 4.35 Photographic views of Building B.

Building C (Figure 4.32) has an irregular floor plan and a RC framed structure with columns (arranged with distances of 2.25 m and 5.20 m in X-direction and ranging between 3.67 m and 4.77 m in Y-direction) and beams. Also, there are some steel columns at the cantilever roof.

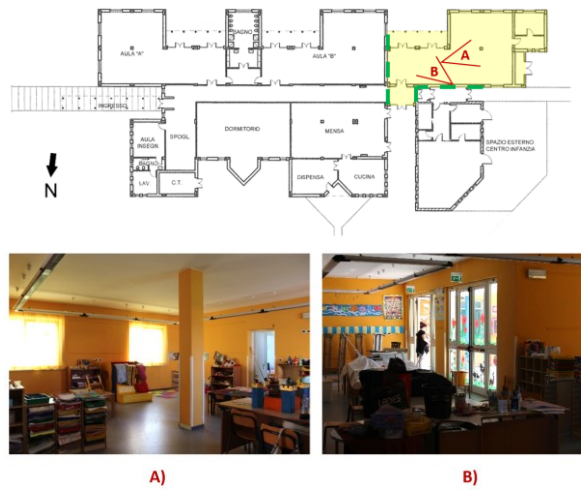


Figure 4.36 Photographic views of Building C.

Finally, the last portion of the complex - Building D (Figure 4.33) - was built in 2009 and it is characterised by a greater structural regularity in plan compared to the other buildings. It has a trapezoidal floor plan and a RC framed structure with columns arranged at interaxis of 4.09 m and 4.15 m in x-direction and ranging between 4.04 m and 4.55 m in y-direction and beams. The building part adjacent to the Building C consists of a RC slab of a thickness of 20 cm.

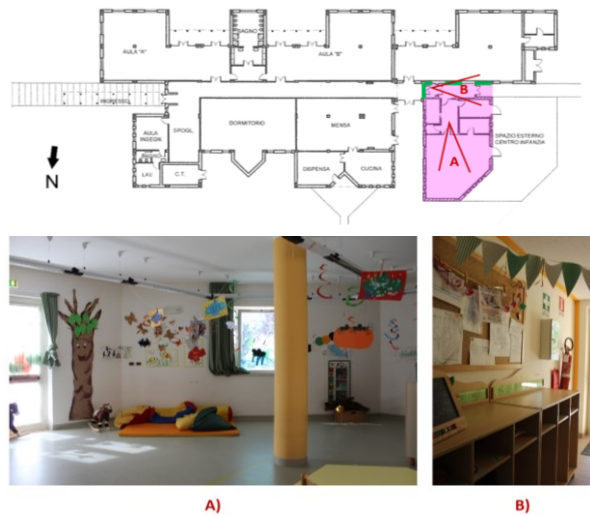


Figure 4.37 Photographic views of Building D.

5 Chapter - Numerical Modelling

5.1 Seismic performance evaluation

The study of the overall response of the building can be performed with frame models, which are the practice for RC buildings, but which allow to represent, sometimes, also the regular masonry buildings through the "equivalent frame" scheme.

The global seismic analysis must use, as far as possible, methods of analysis that allow to evaluate appropriately both resistance and ductility, taking into account the possibility of developing resistant mechanisms both "ductile" and "brittle" and adopting material parameters diversified according to the type of verification.

In national Codes (Ministerial Circular No. 617, 2009, Minister of Public Works and Transport, 2008) and International (CEN, 2005), or in Guidelines (CNR, National Research Council, 2013) it is clarified that in existing structures the capacity of elements with both "ductile" and "brittle" resistant mechanisms can be activated.

The analysis of structures subject to seismic action can be linear or nonlinear. With reference to RC structures, the NTC 2008 affirm that linear analyses can always be used even with limited information on construction details and material strengths (KL1 level); otherwise, nonlinear analyses can be used if the knowledge is adequate, or a level of intermediate knowledge is reached, i.e. equal to LC2 (Ministerial Circular No. 617, 2009 [20]).

Nonlinear analyses are certainly the most appropriate to describe the inelastic process, but they do not always represent the optimal solution. Among these it is possible to include the nonlinear dynamic analysis which, although it is the best choice compared to current knowledge, it is not an easy tool and therefore it is currently relegated to the academic world. On the other hand, nonlinear static analysis - also known as "pushover" - is easier to use but it must be used with extreme care in the presence of strong irregularities in plan and height.

The nonlinear static (pushover) analysis has developed over the last two decades and it has become the most suitable procedure for design and seismic performance evaluation, as it is relatively simple, and it considers the post-elastic behaviour. The construction of the capacity curves for RC structures requires a certain computational effort. It also requires a careful – and demanding – check of the input data, since the results are very sensitive to the geometric and material modelling [63].

The nonlinear static analysis is performed following the N2 method, originally proposed by [64], with two distributions, one proportional to the fundamental modes and the other to the mass. In the following, the two distributions will be identified with the labels "PushMode" (proportional to the modes) and "PushMass" (proportional to the mass).

These procedures are displacement-based when considering the ductile mechanisms, and force- (strength-) based when considering the brittle mechanisms. In particular, the ductile modes should be checked in terms of the so-called "chord rotation", while the brittle ones should be assessed in terms of shear strength.

As the irregularities in plan and height of the structure increase, the degree of accuracy of the analysis may decrease, being sensitive to the applied load profile, leading to underestimation or overestimation of the structural strength and ductility. In these situations, as also highlighted by the current seismic regulations, it is possible to replace the previous profiles with those deriving from the overlapping of the most significant modal forms of the structure (multimodal pushover analysis).

Then, the investigation of the structural behaviour of the case study was carried out also with an improved pushover analysis procedure called *multimodal pushover analysis (MPA)* [65].

This analysis method is based on structural dynamics theory, which retains the conceptual simplicity and computational attractiveness of current procedures with invariant force distribution now common in structural engineering practice.

The standard response spectrum analysis for elastic multistorey buildings can be reformulated as a multimodal pushover analysis (MPA). The peak response of the elastic structure due to its n -th vibration mode can be exactly determined by pushover analysis of the structure subjected to lateral forces distributed over the height of the building according to $\mathbf{s}_n^* = \mathbf{m}\Phi_n$, where \mathbf{m} is the mass matrix and Φ_n its n -th mode, and the structure is pushed to the roof displacement determined from the peak deformation D_n of the n -th mode elastic SDF system; D_n is available from the elastic response (or design) spectrum. Combining these peak modal responses by an appropriate modal combination rule leads to the MPA procedure.

The modelling types available for the determination of the nonlinear response of structural systems in the most common computational codes belong mainly to three categories: Lumped Plasticity Models (LPM), i.e. "plastic hinges", Distributed Plasticity Model (i.e. "fibre model") and 3D Continuum FE Model that they use a smeared approach for the fracture energy by three-dimensional elements.

5.2 Lumped plasticity approach

Lumped plasticity models are usually associated with a phenomenological approach available when the possibility of formation of plasticized areas inside the element can be excluded.

The inelastic resources are lumped in "plastic hinges" located at the end of linear elements (modelled as an elastic part) and they are usually synthesized by a hysteretic behaviour, which differs according to the axial-bending-shear failure.

The advantages of this modelling are: 1) a very low computational cost; 2) the possibility to take into account nonlinear phenomena such as buckling of rebars and bond strength between bars and concrete, poor confinement, shear deformability, etc.; 3) the simplicity and correspondence to the reality as long as there are no particular situations (e.g. the sections must be rectangular in shape).

On the other hand, the positioning of the plastic hinges requires a certain experience of the operator, as well as the shear span definition and the force-deformation relationship assigned to them.

The major problem with this approach is the absence of interaction between the axial, bending and shear forces during the transversal loading increment. For the most common approach, at present, the interaction is purely numeric and is delegated to the Finite Element solver. Furthermore, these quantities are a function of the shear span, which is always constant during the loading increment: this assumption can lead to under- or over-estimate the capacity of the element. This means that the capacity curve is not enough to evaluate the capacity of the structure and this explains the need for local checks.

In lumped plasticity models it is also possible to consider more sophisticated models such as the one of [66] which takes into account axial force, bending and shear behaviours and their interactions by single plastic hinge.

5.2.1 Local safety verifications

The ductile mechanisms are assessed at the member level, through the evaluation of the chord rotation demand, i.e. ϑ_D , and the corresponding capacity, i.e. ϑ_u , at the ends of each structural element (beams and columns).

The chord rotation capacity depends on both the geometrical and mechanical properties of the considered member and on the seismic input (the shear span length is defined as the ratio of bending moment demand to shear demand and the curvature capacity is influenced by the amount of axial load). The chord

rotation capacity, hence, may not be defined as an intrinsic property of a member since the same member may develop different values of capacity as the seismic action changes.

The empirical expression for chord rotation capacity at flexural failure is based on cycling load results and developed on the basis of statistical methods. According to both Eurocode 8 [67] and Italian Seismic Code:

$$\theta_u = \frac{1}{\gamma_{el}} 0.016 \cdot (0.3^v) \left[\frac{\max(0.01; \omega')}{\max(0.01; \omega)} f_{cm} \right]^{-0.225} \left(\frac{L_v}{h} \right)^{0.35} 25^{\left(\alpha \rho_{sx} \frac{f_{yw}}{f_{cm}} \right)} (1.25^{100\rho_d}) \quad (5.1)$$

where $\gamma_{el} = 1.5$ as prescribed by Eurocode 8 for primary elements; h is the cross-section depth; $v = N/(A_c f_{cm})$ is the axial load normalized with respect to the cross section; ω and ω' are the mechanical reinforcement ratios of the longitudinal reinforcement in tension and in compression zone respectively; f_{cm} , f_{ym} and f_{ywm} are, respectively, the average concrete compressive strength and the steel yield strength obtained as already specified; $\rho_{sx} = A_{sx}/b_w s_h$, where A_{sx} is the area of transverse steel parallel to the X-direction loading, s_h is the stirrups spacing and b_w is the web width; $\rho_d = 0$ is the ratio of diagonal reinforcement; α is the confinement effectiveness factor equal to

$$\alpha = \left(1 - \frac{s_h}{2b_o} \right) \left(1 - \frac{s_h}{2h_o} \right) \left(1 - \frac{\sum b_i^2}{6h_o b_o} \right) \quad (5.2)$$

In the case of RC members without details for earthquake resistance, both Codes require multiplying the above expression of ϑ_u by a reduction factor (0.825 for Eurocode 8, 0.85 for the Italian Seismic Code). Therefore, the only difference between the two Codes in the evaluation of ϑ_u consists in the value proposed for this reduction factor.

The elastic part may be considered equal to the yielding chord rotation, ϑ_y , defined as for beams and columns:

$$\theta_y = \phi_y \frac{L_v}{3} + 0.0013 \left(1 + 1.5 \frac{h}{L_v} \right) + 0.13 \phi_y \frac{d_{bL} f_{ym}}{\sqrt{f_{cm}}} \quad (5.3)$$

The beam and column elements are characterized by the nonlinear properties, that for lumped plasticity models, are usually elastoplastic curves for bending moments with nonlinear constitutive laws suggested by the Eurocode 8 provisions [67] and limited ductility behaviour (Figure 5.1). For ductile members, in order to consider the complex interaction between the bending moments about two axes and the axial force, during the transversal load increment a biaxial bending with axial

interaction (PMM, that is axial force P and biaxial bending moments M_x, M_y) is usually adopted in the FEM programs.

According to Eurocode 8 and Italian Seismic Code the beam and column verifications for the LSSD (Limit State of Significant Damage) consist in checking that the displacement demand could be achieved by the structure without the elements reaching their ultimate deformation (ductile mechanism). The check is satisfied if $\theta_b \leq \theta_c$, where θ_c is the chord rotation capacity computed with θ_u , which for LSSD is equal to $\frac{3}{4}\theta_u$.

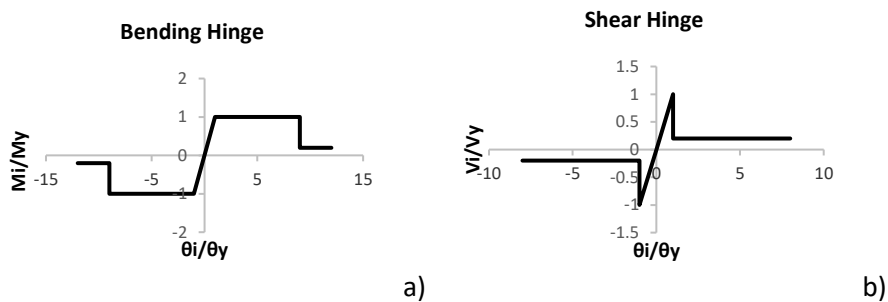


Figure 5.1 Adimensional force–deformation relationship adopted for a) bending and b) shear hinges.

The brittle mechanisms are assessed at the section level, through the evaluation of shear demand and corresponding capacity at the two ends of each structural member. If a nonlinear analysis is carried out, the values of the internal forces at each step will correctly represent the actual distribution of the demand in structural members: the shear demand is, hence, assumed to be equal to the values obtained directly from the analysis.

The procedure to assess the shear capacity proposed in the Italian Seismic Code is the same as Eurocode 2, and it differs from that recommended in Eurocode 8 and in CNR-DT 212 [68]. In the following sections, the first procedure is shown.

The resisting model is the classical Mörsh-Ritter truss, with 45% inclined compressed concrete struts. The resistance V_R is, hence, the minimum between the value of shear that causes the transverse reinforcement to yield in tension and the one that leads to the diagonal compression failure of the concrete web:

$$V_R = \min(V_{R,s} + V_{Rc,t}; V_{Rc,max}) \quad (5.4)$$

where the shear that causes the transverse reinforcement to yield in tension is calculated as $V_{Rc,t} + V_{R,s}$.

V_{Rc} is the concrete contribution to shear resistance:

$$V_{R,ct} = \left\{ 0.18 \cdot k \cdot (100 \cdot \rho_1 \cdot f_{cm})^{1/3} / \gamma_c + 0.15 \cdot \sigma_{cp} \right\} \cdot b_w \cdot d \geq (v_{min} + 0.15 \cdot \sigma_{cp}) \cdot b_w \cdot d \quad (5.5)$$

where $k = 1 + (200/d)^{1/2} \leq 2$, $v_{min} = 0.035k^{3/2}f_{ck}^{1/2}$, d is the effective depth of the section (in mm); $\rho_1 = A_{s1}/(b_w \cdot d)$ is the geometrical ratio of longitudinal reinforcement (≤ 0.02); $\sigma_{cp} = N_{Sd}/A_c$ is the average compressive stress in the section ($\leq 0.2f_{cd}$); b_w is the section minimum width (in mm).

$V_{R,s}$ is the resisting force due to transverse reinforcement:

$$V_{R,s} = 0.9 \cdot d \cdot f_{yw} \frac{A_{sw}}{s} \cdot \sin \alpha (\cot \theta + \cot \alpha) \quad (5.6)$$

The shear that causes diagonal compression failure of the concrete web is computed, according to the Moërsch-Ritter truss model, as:

$$V_{Rc,max} = 0.9 \cdot d \cdot \alpha_c f'_{cd} \cdot b_w \cdot (\cot \theta + \cot \alpha) \sin^2 \theta \quad (5.7)$$

where f'_{cd} is the reduced compressive strength of the concrete core ($f'_{cd} = 0.5 \cdot f_{cm}$); α_c is a coefficient that takes into account the compression.

Finally, it must be carried out the capacity evaluation of beam-column joints.

As for the European Code EC8, both for new and existing buildings, the evaluation of the horizontal maximum shear acting in the joint panel (shear demand) can be performed through the following two expressions, respectively for external and internal joints:

$$V_{jhd} = \gamma_{Rd} \cdot A_{s1} \cdot f_{yd} - V_C \quad (5.8)$$

$$V_{jhd} = \gamma_{Rd} \cdot (A_{s1} + A_{s2}) \cdot f_{yd} - V_C \quad (5.9)$$

where A_{s1} is the area of the beam top reinforcement, A_{s2} is the area of the beam bottom reinforcement, V_C is the column shear force, obtained from the analysis in the seismic design situation, γ_{Rd} is a factor to account for over-strength due to steel strain-hardening and should be not less than 1.2.

The EC8 formulation for predicting the joint shear capacity is made up of two separated steps.

Firstly, there is an expression to evaluate the compression capacity of the strut that can be recognised in the joint panel under seismic actions and, then, an expression devoted to verifying the tensile strength of the joint in order to avoid diagonal cracking.

The horizontal shear demand should not exceed a value that could cause the compression failure of the joint:

$$V_{jhd} \leq \eta f_{cd} \sqrt{1 - \frac{v_d}{\eta}} b_j \cdot h_{jc} \quad (5.10)$$

where $\eta = 0.60$ ($1 - f_{ck}/250$) for interior joints and $\eta = 0.48$ ($1 - f_{ck}/250$) for exterior joints, practically meaning that the strength of exterior joints is 0.8 (0.48/0.60) times that one of interior joints (assuming the same joint materials and detailing); v_d is the normalised axial force in the column above the joint, f_{ck} is given in MPa, h_{jc} is the distance between the extreme layers of column reinforcement, b_j is the effective width of the joint. Further, EC8 provides an expression to evaluate the joint transverse reinforcement needed to avoid the diagonal cracking caused by the achievement of the concrete tensile strength f_{ctd} , as follows:

$$\frac{A_{sh} \cdot f_{ywd}}{b_j \cdot h_{jw}} \geq \frac{(V_{jhd}/b_j \cdot h_{jc})^2}{f_{ctd} + v_d f_{cd}} - f_{ctd} \quad (5.11)$$

where, A_{sh} is the total area of the horizontal hoops in the joint, V_{jhd} is the horizontal joint shear demand, h_{jw} is the distance between top and bottom reinforcement of the beam.

The Italian Code IC (Ministry of Infrastructures, 2008) deals separately with joints belonging

to new and existing buildings, the former ones being evaluated as in EC8. As for existing buildings, IC contains two expressions devoted to verify beam-column joint without seismic provisions, that is without hoops in the panel (paragraph C8.7.2.5). These expressions allow to calculate the maximum diagonal compression (5.12) and tensile (5.13) stresses in the concrete joint core that must be below given values related to the concrete strength f_c :

$$\sigma_{nc} = \frac{N}{2A_g} + \sqrt{\left(\frac{N}{2A_g}\right)^2 + \left(\frac{V_n}{A_g}\right)^2} \leq 0.5f_c \quad (5.12)$$

$$\sigma_{nt} = \left| \frac{N}{2A_g} - \sqrt{\left(\frac{N}{2A_g}\right)^2 + \left(\frac{V_n}{A_g}\right)^2} \right| \leq 0.3\sqrt{f_c} \quad (f_c \text{ in MPa}) \quad (5.13)$$

where N is the axial force acting on the upper column, A_g is the gross area of the joint panel horizontal section and V_n the horizontal shear acting in the joint panel evaluated accounting both the column shear and the shear transmitted by the beam reinforcing bars.

5.2.2 Modelling the case studies of Trecastelli school building stock by adopting a lumped plasticity approach

Using the structural layout and material property information identified during the building surveys, a nonlinear numerical model of each school building was developed to identify both modal properties and seismic response characterisation outlined later.

By a finite element approach, eighteen different spatial models of the case studies were adopted for the analyses of the building stock, each one characterised by specific and typical vulnerabilities individuated after the assessments done on Chapter 3.

In these models the frame structure was taken into account modelled by beam elements (Figures 5.4, 5.5, 5.6, 5.7, 5.8, 5.9).

Wall elements were used (Figures 5.6 h), 5.9 q)) to model RC walls with proper plastic hinges.

Plate elements were used to reproduce stairs (Figure 5.4 d)) and shelters (Figures 5.5 f), 5.9 q)-r)-s)-t)), in order to better understand the influence of these rigid elements on the seismic behaviour.

All models consider flexible or rigid floors according to the features show on Chapter 4.

The classical parabola-rectangle diagram for the concrete under compression was implemented along with an elastic-hardening diagram for the reinforcement steel. As already mentioned, in order to describe the nonlinear behaviour of columns and beams it was adopted a lumped plasticity approach with default plastic hinges assigned to the elements: axial force and biaxial bending (i.e., PMM 3D status determination which take into account the variation of axial force during the analysis) for columns, and pure bending (i.e., M3 pure uniaxial bending for a fixed value of axial force) for beams. The hinge nonlinear constitutive laws mentioned above (Figure 5.1) were utilised.

Given that existing RC buildings have usually low concrete strength (except for the recent buildings) and an insufficient amount of transverse steel (stirrups), the shear failure of members were taken into account by the introduction of shear hinges (Figure 5.1 b).

Similarly, the unreinforced masonry school buildings (see Figure 5.5 e) – 5.7 l)) were modelled using the equivalent frame approach for the evaluation of global seismic response of URM buildings.

To define the equivalent frame model, the steps required are summarised below.

A generic masonry wall with openings is idealised by identifying two main structural components: the piers and the spandrels. Piers are the main vertically resisting elements while spandrels couple the response of two adjacent piers. This methodology was developed from the observation of typical damage during past earthquakes.

The nonlinear macro-element model implemented allows the two main failure modes governing the response of masonry walls to be reproduced with a limited number of degrees of freedom. In terms of flexural behaviour, rocking and crushing mechanisms are considered, whereas diagonal cracking and shear sliding are taken into account for shear failure.

The hinge nonlinear constitutive law suggested by the FEMA provisions [69] were adopted (see Figure 5.2 and Figure 5.3).

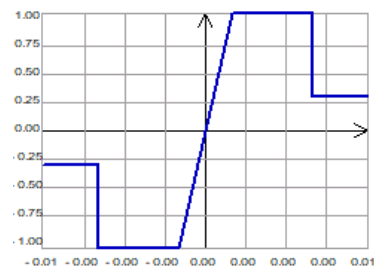


Figure 5.2 Dimensional force-deformation relationship adopted for hinges for spandrel elements.

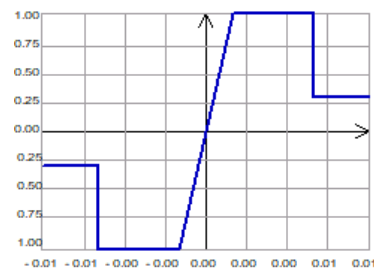


Figure 5.3 Dimensional force-deformation relationship for hinges for pier elements.

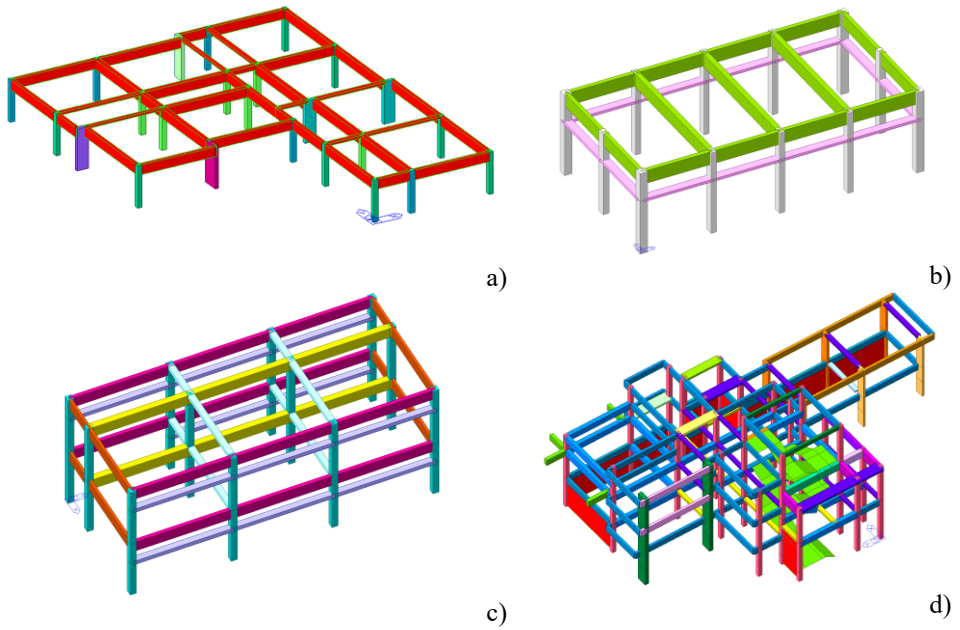


Figure 5.4 Models of IC Nori de' Nobili school.

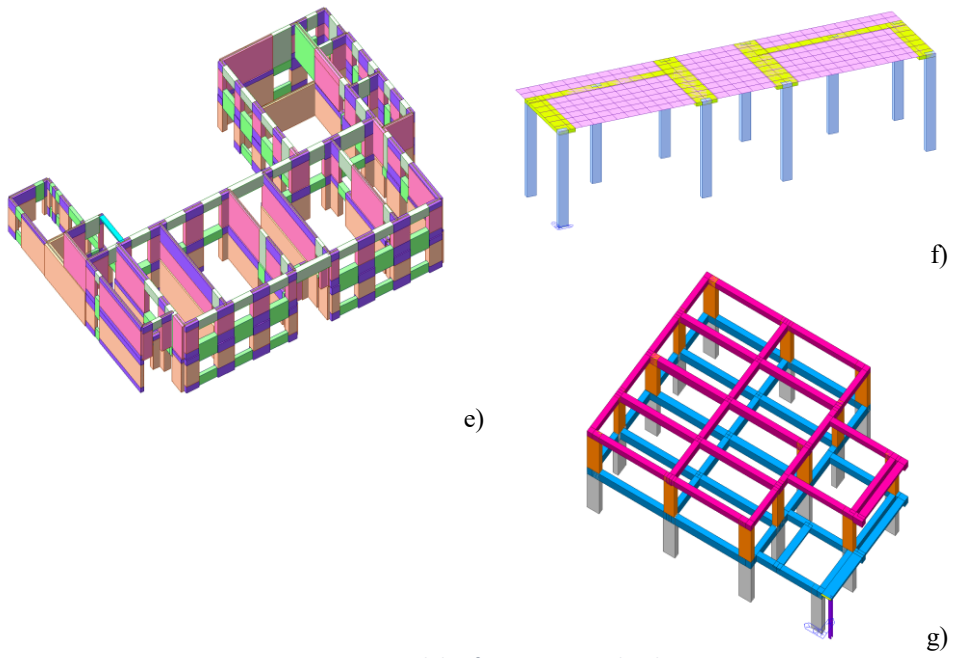
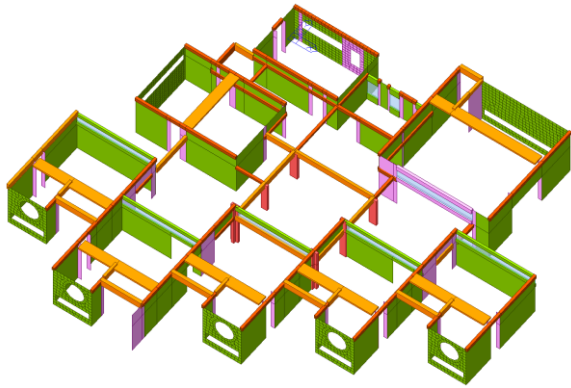
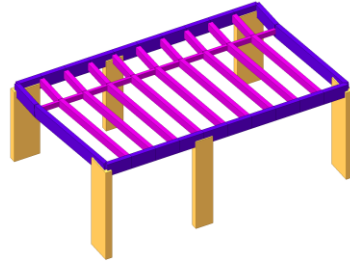


Figure 5.5 Models of G. Marconi school.

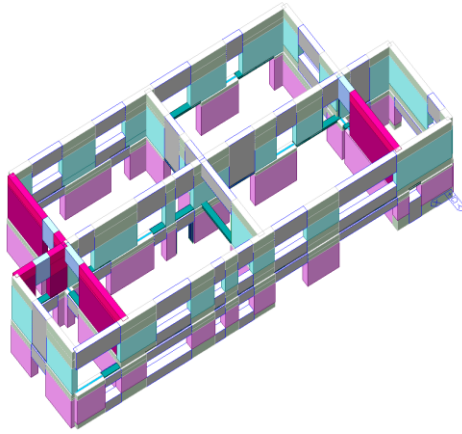


h)

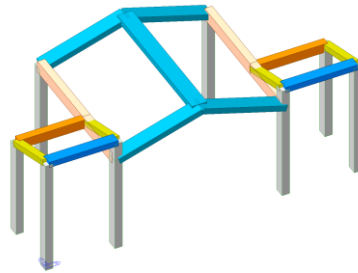


i)

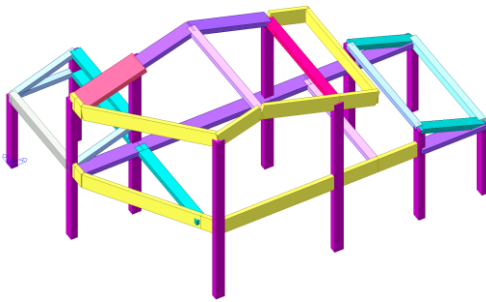
Figure 5.6 Models of Peter Pan school.



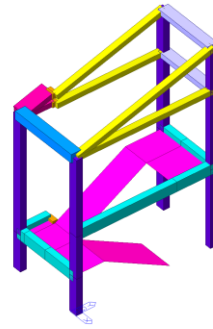
l)



m)



n)



o)

Figure 5.7 Models of Il Piccolo Principe school.

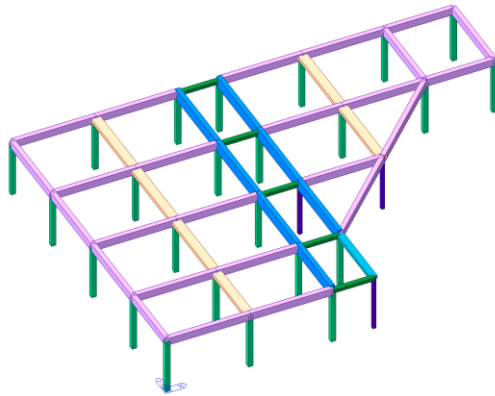
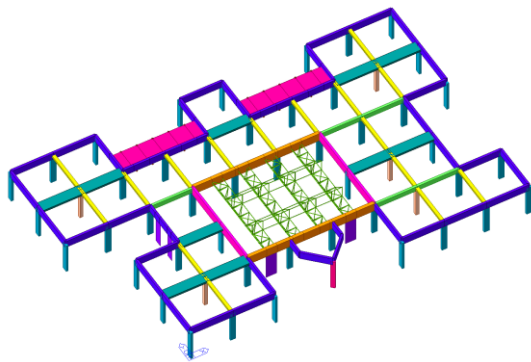
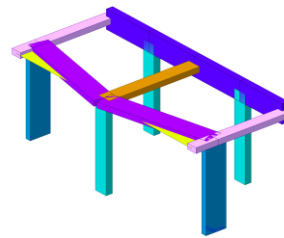


Figure 5.8 Models of Il Girasole school.

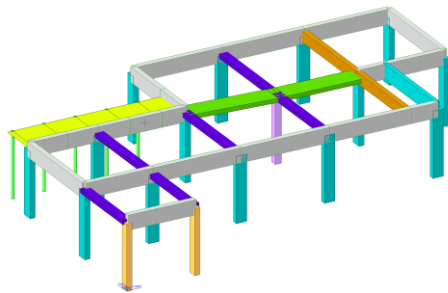
p)



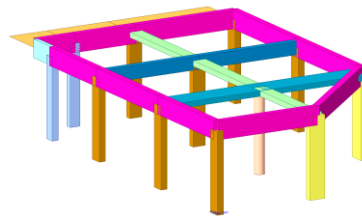
q)



r)



s)



t)

Figure 5.9 Models of La Carica dei 101 school.

5.3 Distributed Plasticity Model (Fibre Model)

In this second type of modelling, plasticity is distributed throughout the structural element, both transversely and longitudinally.

Structural elements are discretised in control sections with a considerable number of fibres (Figure 5.10), which only deform axially, using a force-based element formulation [70].

Each section is discretised into parts (fibres) to which the relationship between stress and strains of the corresponding material (hysteretic behaviour) is assigned. A fibre model allows to correctly describe the interaction between the axial force and the two components of bending moment. Especially, it has the advantage of considering the movement of neutral axis due to axial force. This model type does not require a great experience of the operator since plasticization can occur anywhere in the element.

When a fibre model is used, the moment curvature relationship of a section can be rather accurately traced, based on the assumption of the stress-strain relationship of the fibre material and the distribution pattern of sectional deformation.

If the number of fibres is sufficiently high, the distribution of the mechanical nonlinearities due to the materials on the surface of the section is accurately modelled, even in the strongly inelastic field, unlike a model with a lumped plasticity that is less accurate.

In the current version available in the most widespread calculation codes, a fibre model is not suitable for representing nonlinear phenomena such as the buckling of rebars and bond strength between bars and concrete and shear failure, etc. Usually, the models with fibre sections are characterised by very long calculation times compared to lumped plasticity models.

A distributed plasticity approach - less constrained to initial assumptions - suffers the absence of an interaction between bending (M), shear (V) and axial force (N) just like the lumped plasticity approach.

The assumption in fibre models considered are:

- 1) The section remain plane in the process of deformation and is assumed to be perpendicular to the axis of the beam. Accordingly, bond-slip between reinforcing bars and concrete is not considered.
- 2) The centroidal axis of the section is assumed to be a straight line throughout the entire length of the beam element.

In a fibre model, the status of each fibre is assessed by axial deformations corresponding to the axial and bending deformations of the fibre. The axial force

and bending moments of the section are then calculated from the stress of each fibre.

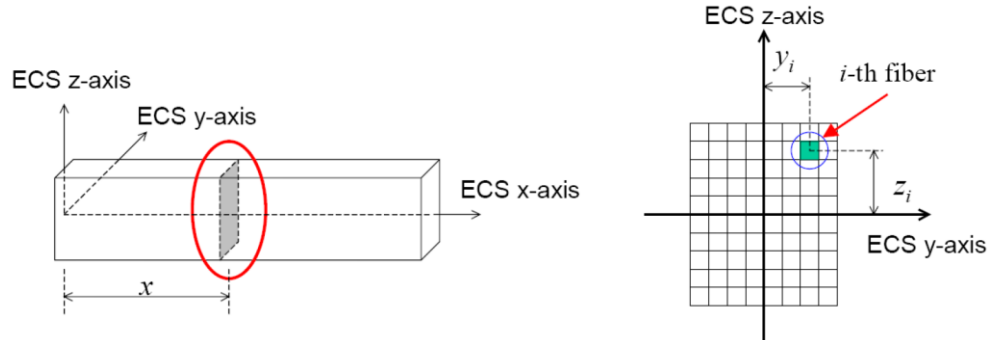


Figure 5.10 Discretisation of a section in a fibre model [71]

Based on the basic assumptions stated above, the relationship between the deformations of fibre and the deformation of the section is given below.

$$\varepsilon_i = [-z_i - y_i \mathbf{1}] \begin{Bmatrix} \phi_y(x) \\ \phi_z(x) \\ \varepsilon_x(x) \end{Bmatrix} \quad (5.14)$$

where,

x : location of a section

$\phi_y(x)$: curvature of the section about y -axis in Element Coordinate System at the location x

$\phi_z(x)$: curvature of the section about z -axis in Element Coordinate System at the location x

$\varepsilon_x(x)$: deformation of the section in the axial direction at the location x

y_i : location of the i -th fibre on a section

z_i : location of the i -th fibre on a section

ε_i : deformation of the i -th fibre

The properties of nonlinear behaviour of a section in a fibre model are defined by the stress-strain relationship of nonlinear fibres.

The literature proposes a lot of examples, based on experimental tests, for the behaviour of concrete subjected to cyclic loads [72]. In particular, the Kent and Park model [73], which is refined to take into account the confinement contribution of the stirrups, was used. For the nonlinear behaviour of steel, Menegotto and Pinto model as modified by Filippou et al. [74] was adopted. These constitutive models are explained in the next sections.

5.3.1 Steel fibre constitutive model

Steel fibre constitutive model basically retains the curved shapes approaching the asymptotes defined by the bilinear kinematic hardening rule. The transition between two asymptotes corresponding to the regions of each unloading path and strain-hardening retains a curved shape. The further the maximum deformation point in the direction of unloading is from the intersection of the asymptotes, the smoother the curvature becomes in the transition region. The constitutive model is thus defined by the equation below.

$$\hat{\sigma} = b \cdot \hat{\varepsilon} + \frac{(1-b) \cdot \hat{\varepsilon}}{(1-\hat{\varepsilon}^R)^{1/R}} \quad (5.15)$$

where

$$\hat{\varepsilon} = \frac{\varepsilon - \varepsilon_r}{\varepsilon_0 - \varepsilon_r}$$

$$\hat{\sigma} = \frac{\sigma - \sigma_r}{\sigma_0 - \sigma_r}$$

$$R = R_0 - \frac{a_1 \cdot \xi}{a_2 + \xi}$$

ε : Strain of steel fibre

σ : Stress of steel fibre

$(\varepsilon_r, \sigma_r)$: Unloading point, which is assumed to be (0, 0) at the initial elastic state

$(\varepsilon_0, \sigma_0)$: Intersection of two asymptotes, which defines the current loading or unloading path

b : Stiffness reduction factor

R_0, a_1, a_2 : Constants

ξ : Difference between the maximum strain in the direction of loading or unloading and ε_0 (absolute value).

However, the initial value of the maximum strain is set to $\pm(F_y/E)$ (refer to Figure 5.11).

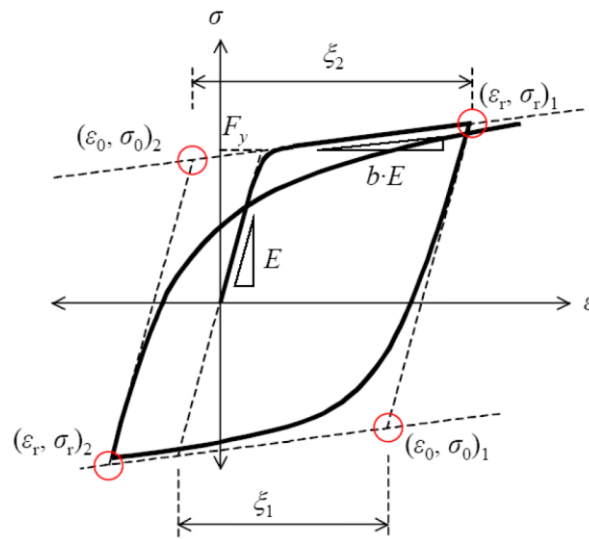


Figure 5.11 Steel fibre constitutive model – Menegotto and Pinto

5.3.2 Concrete fibre constitutive model

it is possible to use the equation of envelope curve proposed by Kent and Park (Figure 5.12) [73] for the concrete fibre constitutive model of concrete under compression. Tension strength of concrete is ignored. The equation of the envelope curve for compression is noted below. This is a well-known material model for considering the effect of increased compression strength of concrete due to lateral confinement.

$$\sigma_c = \begin{cases} Kf'_c \left[2 \left(\frac{\varepsilon}{\varepsilon_0} \right) - \left(\frac{\varepsilon}{\varepsilon_0} \right)^2 \right] & \text{for } \varepsilon \leq \varepsilon_0 \\ Kf'_c [1 - Z(\varepsilon - \varepsilon_0)] \geq 0.2 Kf'_c & \text{for } \varepsilon_0 \leq \varepsilon \leq \varepsilon_u \end{cases} \quad (5.16)$$

where

ε : Strain of concrete fibre

σ : Stress of concrete fibre

ε_0 : Strain at maximum stress

ε_u : Ultimate strain

K : Factor for strength increase due to lateral confinement

Z : Slope of strain softening

f'_c : Compressive strength of concrete cylinder (MPa)

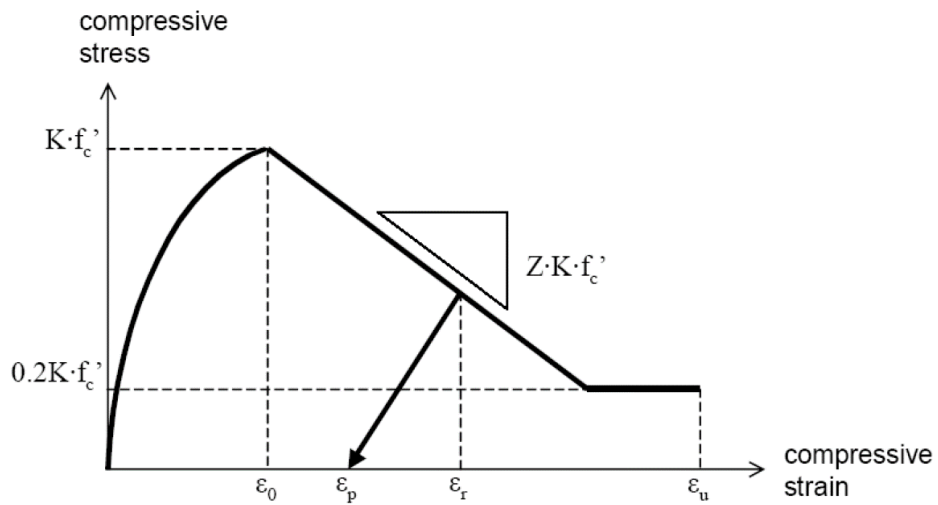


Figure 5.12 Concrete fibre constitutive model Kent & Park.

The concrete, which has exceeded the ultimate strain, is assumed to have arrived at crushing, and as such it is considered unable to resist loads any longer. Kent and Park suggested the following equation in order to calculate the parameters defining the above envelope curve for a rectangular column section.

$$\varepsilon_0 = 0.002K \quad (5.17)$$

$$K = 1 + \frac{\rho_s f_{yh}}{f'_c} \quad (5.18)$$

$$Z = \frac{0.5}{\frac{3 + 0.29 f'_c}{145 f'_c + 1000} + 0.75 \rho_s \sqrt{\frac{h'}{s_h}} - 0.002K} \quad (5.19)$$

where

f_{yh} : Yield strength of stirrups

ρ_s : Reinforcing ratio of stirrups = Volume of stirrups / Volume of concrete core

h' : Width of concrete core (longer side of a rectangle)

s_k : Spacing of stirrups.

Scott et al. (1982) proposed the following equation of ultimate strain for a laterally confined rectangular column.

$$\varepsilon_u = 0.004 + 0.9\rho_s(f_{yh}/300) \quad (5.20)$$

When unloading takes place on the above envelope curve, the unloading path is defined by the equations below, pointing towards a point $(\varepsilon_p, 0)$ on the strain axis. When the strain reaches this point, it moves to the tension zone following the strain axis.

$$\frac{\varepsilon_p}{\varepsilon_0} = 0.145 \cdot \left(\frac{\varepsilon_r}{\varepsilon_0}\right)^2 + 0.13 \cdot \left(\frac{\varepsilon_r}{\varepsilon_0}\right) \quad \text{for } \left(\frac{\varepsilon_r}{\varepsilon_0}\right) < 2 \quad (5.21)$$

$$\frac{\varepsilon_p}{\varepsilon_0} = 0.707 \cdot \left(\frac{\varepsilon_r}{\varepsilon_0} - 2\right) \quad \text{for } \left(\frac{\varepsilon_r}{\varepsilon_0}\right) \geq 2 \quad (5.22)$$

ε_r : Strain at the start of unloading

ε_p : Strain at the final point of unloading path

If the compressive strain increases again, the load follows the previous unloading path and reaches the envelope curve.

5.3.3 Distributed plasticity (fibre) model of Building C (G. Marconi school complex, Monterado)

The basic model consists of the same beams and columns geometries as well as the previous lumped plasticity model, with the same assigned loads and constraint conditions (Figure 5.13 a).

Each beam element is discretised in sections with a considerable number of fibres. In order to carry out a nonlinear analysis using fibre elements, beam cross-sections are appropriately divided into fibre cells (Figure 5.13 b). Such fibre cells are assigned various nonlinear material properties representing stress-strain hysteresis models for concrete, steel, etc. For each reinforced concrete element, it was possible to define the cover concrete, the core concrete and reinforcing steel bars.

The fibre model considers the distributed nonlinearity unlike the lumped plasticity model; the non-linearity of the material allows to derive the behaviour of the element through an integration of the response in the section. Therefore, each change of the geometry in the section in reinforcement or otherwise, a different fibre section must be assigned.

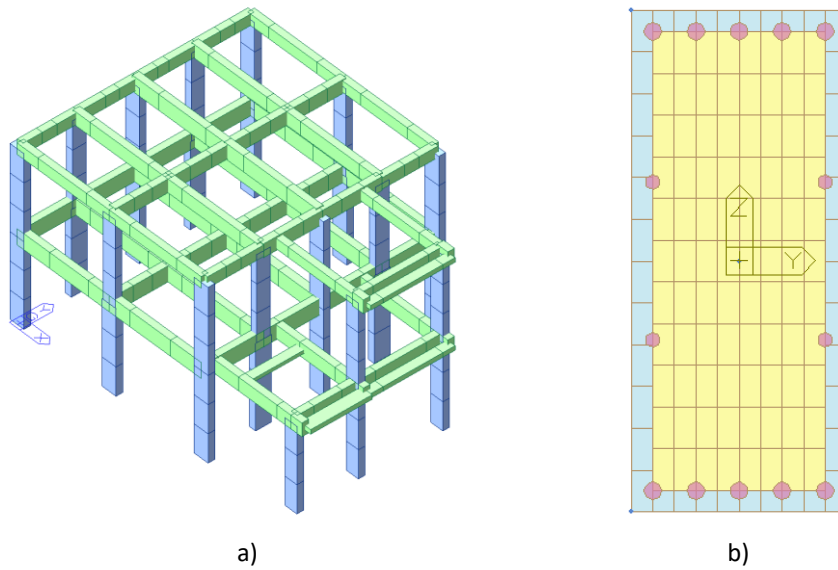


Figure 5.13 Model of G. Marconi school, Building C a), discretisation of each section by fibres b)

The nonlinear analyses were performed assuming a rigid ground foundation (fixed base model) with 200 increment steps and the static load cases were applied order in sequential loading with a time forcing function.

5.4 3D Continuum FE model using a smeared approach for the fracture energy

The proposed numerical model used to study the in-plane behaviour of concrete elements is based on a smeared crack approach. The smeared crack concept itself offers a variety of possibilities, ranging from fixed single to fixed multi-directional and rotating crack approaches. Since smeared crack modelling approaches do not require re-meshing of the Finite Element (FE) model after occurrence of cracks or a priori definition of possible locations of cracks, they were widely used in FE modelling. The smeared crack models are practice-oriented due to the limited data required. A Continuum FE models utilised for masonry structures were realised in [75][76][77].

5.4.1 Concrete crack model

Analysis models for concrete cracking can be classified into a discrete crack model (discontinuum model) and a smeared crack model (continuum model) (see Figure 5.14). The discrete crack model uses finite elements at which concrete cracks are separately represented as boundaries. In the smeared crack model, concrete cracks are assumed to be scattered and distributed, such that discrete elements are not used at the crack locations.

The smeared crack model assumes that locally generated cracks are evenly scattered over a wide surface. This model is known to be suitable for reinforced concrete structures with reasonable amount of reinforcement, and its finite element modelling is relatively simple. The smeared crack model can be classified into orthogonal and non-orthogonal crack models depending on the assumption of angles of crack development. The orthogonal crack model assumes orthogonal crack directions, whereas the non-orthogonal crack model assumes non-orthogonal directions of cracks. Also, depending on the numerical analysis methods for cracks, the smeared crack model is further classified into various models such as a decomposed-strain model and a total strain model.

The decomposed-strain model in the smeared crack model calculates the total strain in terms of material strain and crack strain. The material strain is quite versatile in its expandability since it can include elastic strain, plastic strain, creep strain, thermal strain, etc. The crack strain also can be expanded into a non-orthogonal multi-directional crack model as it can include a number of crack strains at different angles. However, its disadvantages exist in that the algorithm is

complex; selection of material properties is difficult; and convergence may become an issue.

The total strain model in the smeared crack model can be rather simply formulated using total strain without having to decompose it into the strain components. In addition, its algorithm is easy to understand because the total strain model uses only one stress-strain relationship for tensile behaviour including cracks and one for compressive behaviour. It is also more practical since the input for material properties for defining nonlinear behaviours is relatively simple enough.

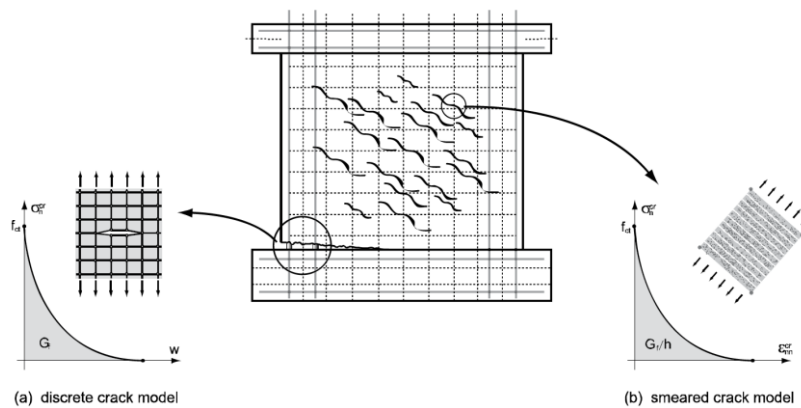


Figure 5.14 Concrete crack models.

The smeared crack concept itself offers a variety of possibilities, ranging from fixed single to fixed multi-directional and rotating crack approaches. Here, the distinction lies in the orientation of the crack, which is either kept constant, updated in a stepwise manner, or updated continuously.

The following parameters need to be defined in order to analyse the Total Strain Crack Model.

It was chosen the *fixed crack model* to accurately simulate the physical behaviours of concrete cracks.

General Concrete Properties

The required material properties to analyse crack models were defined using CEB-FIP 1990 [78].

CEB-FIP 1990 uses f_{cd} and D_{max} to calculate the Young's modulus, mean compressive strength, mean tensile strength and fracture energy.

The mean compressive strength is expressed by,

$$f_{cm} = f_{ck} + \Delta f \quad (5.23)$$

where $\Delta f = 8 \text{ MPa}$

The Young's modulus is expressed in terms of the mean compressive strength (f_{cm}),

$$E_c = E_{c0} \left(\frac{f_{cm}}{f_{cm0}} \right)^{1/3} \quad (5.24)$$

where $E_{c0} = 2.15 \times 10^4 \left(\frac{\text{N}}{\text{mm}^2} \right)$ and the reference mean compressive strength, f_{cm0} is $10 \left(\frac{\text{N}}{\text{mm}^2} \right)$.

The fracture energy is related to the compressive strength and the maximum aggregate size, D_{\max} , which uses the following equation:

$$G_f = G_{f0} \left(\frac{f_{cm}}{f_{cm0}} \right)^{0.7} \quad (5.25)$$

f_{cm0} is $10 \left(\frac{\text{N}}{\text{mm}^2} \right)$. Table 5.1 shows the values of G_{f0} corresponding to the maximum size of aggregates.

$D_{\max} \text{ (mm)}$	$G_{f0} \text{ (J/m}^2\text{)}$
8	25
16	30
32	58

Table 5.1 G_{f0} corresponding to D_{\max} CEB-FIP 1990 [78].

The concrete parameters used for the case study are summarised below.

MATERIAL 1									
		f_{cm}	E	w	v	Ft	Gr	h	KL3
		(Mpa)	(Mpa)	(N/mm ³)	-	(Mpa)	(N/mm)	(mm)	1
Concrete	Average value from the tests	34.58	32512.23	2.14839E-05	0.20			DIM MESH	
	KL3	34.58	32512.23	2.14839E-05	0.20	2.69	0.072	150	

Table 5.2 Concrete parameters.

Tensile Behaviour: Hordijk Model

Hordijk, Cornelissen & Reinhardt proposed an expression for the softening behaviour of concrete (Figure 5.15), which also results in a crack stress equal to zero at a crack strain.

Tensile strength: $f_t > 0.0$

Tensile fracture energy: $G_f^I > 0.0$

Crack band width: $h > 0.0$

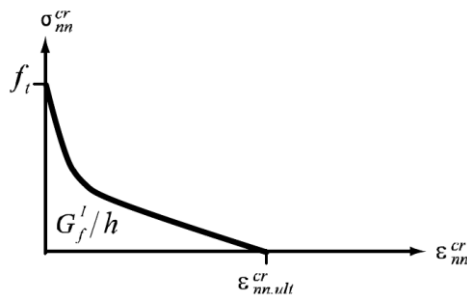


Figure 5.15 Nonlinear tension softening.

Compressive Behaviour: Thorenfeldt Model

Concrete subjected to compressive stresses shows a pressure-dependent behaviour, i.e., the strength and ductility increase with increasing isotropic stress. Due to the lateral confinement, the compressive stress–strain relationship is modified to incorporate the effects of the increased isotropic stress. Furthermore, it is assumed that the compressive behaviour is influenced by lateral cracking. To model the lateral confinement effect, the parameters of the compressive stress–

strain function, f_{cf} and ϵ_p , are determined with a failure function. The failure function gives the compressive stress, which causes failure as a function of the confining stresses in the lateral directions. Thorenfeldt Model was chosen (Figure 5.16); it uses the value of compressive strength as, $f_c > 0.0$

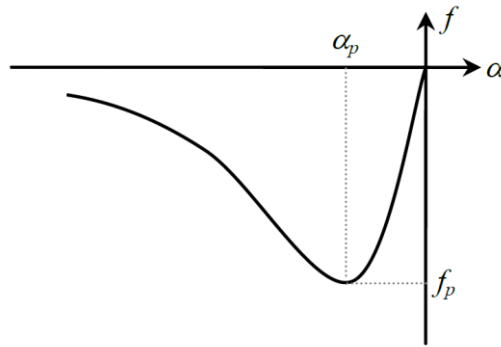


Figure 5.16 Thorenfeldt compression curve.

Shear Behaviour

The modelling of the shear behaviour is necessary in the fixed crack concept where the shear stiffness is usually reduced after cracking. A constant shear stiffness reduction was used:

$$G^{cr} = \beta G \quad (5.26)$$

where, β the shear retention factor, $0 \leq \beta \leq 1$.

Here, a constant value equal to 0.05 was adopted.

Lateral Influences

The lateral crack effect and the confinement effect were considered by the formulation of Vecchio and Collins [79] and Selby and Vecchio [80].

5.4.2 Steel model

The constitutive model type selected for the analyses was Von Mises model. The parameters are summarised in the Table 5.3 below.

MATERIAL 2						
		f_{ym}	E	w	v	KL3
		(Mpa)	(Mpa)	(N/mm ³)	-	1
Steel Reinforcement	Average value from the tests	543.49	210000	7.698E-05	0.30	
	KL3	543.49	210000	7.698E-05	0.30	

Table 5.3 Steel parameters for rebar.

5.4.3 3D Continuum FE model of Building C (G. Marconi school complex, Monterado)

The numerical model was built to accurately reproduce the geometry of the structure, focusing on the use of 1D mesh elements to represent the steel reinforcement embedded. The adopted mesh size is 150 mm. After meshing, the Continuum FE model is reported in Figure 5.17.

The main characteristics of the mesh in terms of number of elements and degrees of freedom (d.o.f.) are reported in Table 5.4.

	Elements	Degrees of freedom
FEM	86824	88968

Table 5.4 Main characteristics of meshed elements.

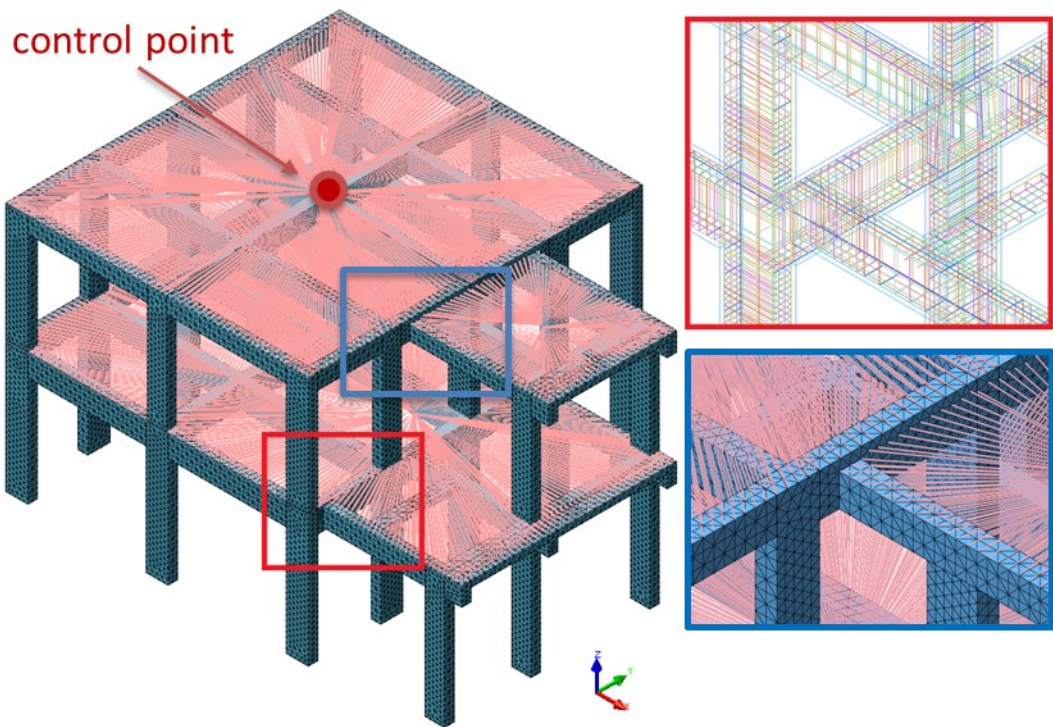


Figure 5.17 Finite element models of the Building C of G. Marconi complex.

The nonlinear analyses, whose results are reported in the next Chapter 6, were performed assuming a rigid ground foundation (fixed base model) and the following parameters were adopted during the analyses:

- maximum number of iterations of load increment: 100;
- maximum analysis number of substeps: 500;
- minimum analysis number of substeps: 5;
- initial load factor 0.1.

The hypothesis of rigid floor slab (in its plane) is the most used, since this is the closer to the real case. It is possible to see rigid links in correspondence of reinforced concrete slabs.

The nonlinear system of equations was solved by an incremental nonlinear static analysis with the Arc-length iteration procedure with the Initial Stiffness Method, and an energy norm with a tolerance of 10^{-2} was requested. It is noteworthy to point out that the computing time required by each pushover analysis was heavy.

6 Chapter - Results

6.1 Overview of the structural performances of school buildings located in Trecastelli

The considered building belongs to the “Class III” (i.e., school buildings) in the Italian Seismic Code. This implies that the Limit State of Significant Damage (SLSD or SLV in Italian) is associated to a recurrence period ($T_{R,D}$) of 712 years, which corresponds to an expected Peak Ground Acceleration (PGA) equal to 0.214g.

The seismic behaviour of each structure was investigated by using a nonlinear static (pushover) analysis with lumped plasticity models. According to code requirements, the horizontal forces were applied separately in two orthogonal directions, in order to determine the structure capacity in these directions. Such forces, not acting simultaneously, were evaluated taking into account two load distributions. The first one is directly proportional to the product of the masses and the displacements of the corresponding first modal shape (PushMode), the second one is proportional to the masses of the structures (PushMass). These two load distributions could be considered as two limit cases for the building capacity.

From a first evaluation carried out on the school building stock of the municipality of Trecastelli, it was found that the brittle mechanisms, and in particular those of the beam-column joints, are the most problematic phenomena based on the results of the safety verifications.

The Figure 6.1 shows that more than two thirds of the school buildings analysed exhibit brittle risk indexes less than 0.4 absolutely not appropriate also for the function of public interest that they host.

Since in reality the shear crisis is the decisive cause of collapse, whether it precedes the damage due to a flexural mechanism, or which occurs as a result of a reduction in shear strength due to cyclic flexural deformation, it is therefore appropriate to try to better understand the structural behaviour of these building using also other types of more refined models and comparing the results obtained.

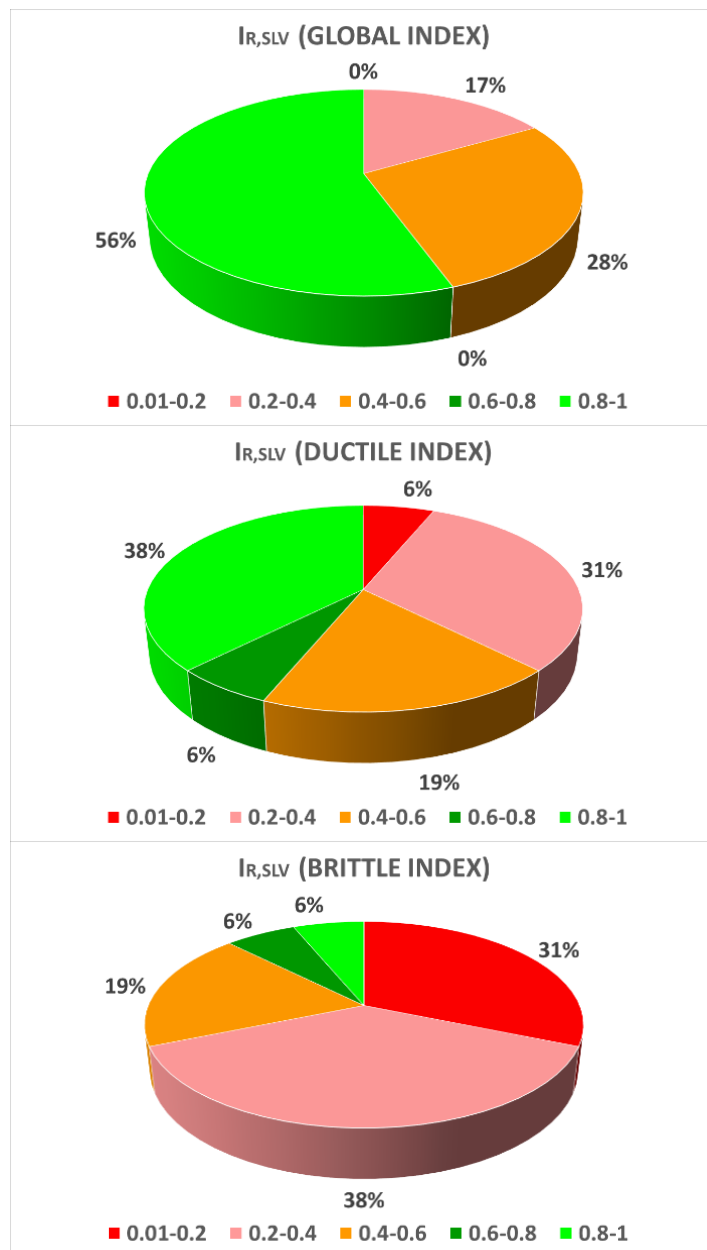


Figure 6.1 Global risk indexes for the school buildings of the municipality of Trecastelli.

6.2 Comparison of results for the three different models

In order to assess the dynamic characteristics of the structure, modal analyses were initially performed. The natural periods with the corresponding participation masses are reported in *Table 6.1* for the lumped plasticity model, in *Table 6.2* for the fibre model and in *Table 6.3* for the 3D continuum FE model.

From all FE models, the same principal modes are detected. As expected, the participation masses of the principal modes are higher than 75% in both directions (due to the rigidity of the floor).

The results of modal analyses for the three models are reported in *Figure 6.2* for a) LPM, b) FM and c) CM models.

Mode n°	Period [sec]	Frequency		TRAN-X		TRAN-Y		ROTN-Z	
		[rad/sec]	[cycle/sec]	Mass(%)	Sum(%)	Mass(%)	Sum(%)	Mass(%)	Sum(%)
1	0.1931	32.5311	5.1775	0.0252	0.0252	87.9586	87.9586	1.4581	1.4581
2	0.1753	35.8417	5.7044	84.666	84.6912	0.072	88.0306	0.7561	2.2142
3	0.1515	41.4676	6.5998	0.7099	85.401	1.3849	89.4155	85.2355	87.4497
4	0.0808	77.7542	12.375	0.0023	85.4034	10.1844	99.5999	0.3842	87.8339
5	0.0642	97.7963	15.5648	13.8341	99.2375	0.0326	99.6325	0.8006	88.6345
6	0.0616	102.0763	16.246	0.7625	100	0.3675	100	11.3655	100

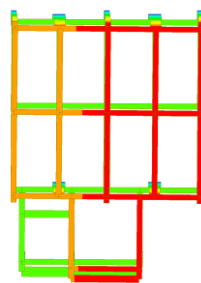
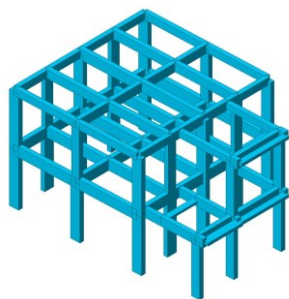
Table 6.1 Periods and modal effective masses for transversal, longitudinal and vertical directions for the principal modes of Lumped plasticity model.

Mode n°	Period [sec]	Frequency		TRAN-X		TRAN-Y		ROTN-Z	
		[rad/sec]	[cycle/sec]	Mass(%)	Sum(%)	Mass(%)	Sum(%)	Mass(%)	Sum(%)
1	0.1922	32.6958	5.2037	0.0192	0.0192	86.9859	86.9859	1.016	1.016
2	0.1744	36.0366	5.7354	83.486	83.5052	0.0462	87.0321	0.5297	1.5457
3	0.1454	43.2141	6.8777	0.4821	83.9872	0.9682	88.0003	84.0944	85.6401
4	0.079	79.4977	12.6525	0.0018	83.989	10.2112	98.2116	0.2655	85.9056
5	0.0629	99.8996	15.8995	14.1977	98.1868	0.0094	98.2209	0.2482	86.1537
6	0.0581	108.1769	17.2169	0.1957	98.3825	0.2945	98.5154	11.7349	97.8887

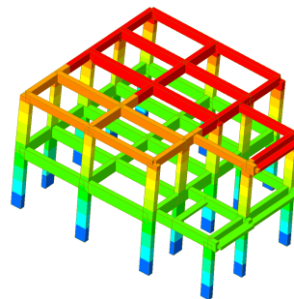
Table 6.2 Periods and modal effective masses for transversal, longitudinal and vertical directions for the principal modes of Fibre model.

Mode n°	Period [sec]	Frequency		TRAN-X		TRAN-Y		ROTN-Z	
		[rad/sec]	[cycle/sec]	Mass(%)	Sum(%)	Mass(%)	Sum(%)	Mass(%)	Sum(%)
1	0.17898	35.10545	5.587206	0.02	0.02	90.4	90.4	2.35	2.35
2	0.154355	40.70601	6.478562	89.61	89.63	0.01	90.41	0.01	2.35
3	0.136624	45.989	7.319376	0.02	89.65	0.84	91.25	61.79	64.14
4	0.07162	87.72921	13.96254	0	89.65	5.13	96.38	0.25	64.39
5	0.060687	103.534	16.47794	6.85	96.5	0.04	96.42	0.33	64.73
6	0.053811	116.7645	18.58365	0.41	96.91	0.61	97.04	4.14	68.87

Table 6.3 Periods and modal effective masses for transversal, longitudinal and vertical directions for the principal modes of 3D Continuum FE model.

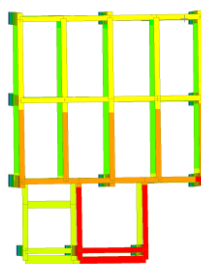


MODE N° 2

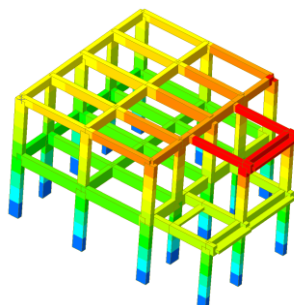


MODE N° 2 X-DIR.: 84.67%

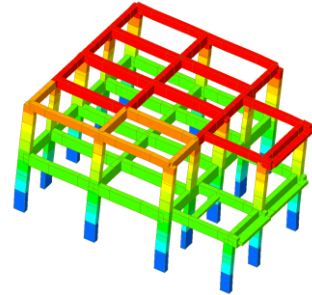
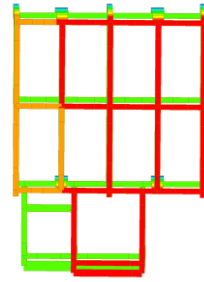
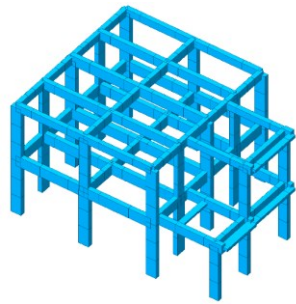
MODE N° 1 Y-DIR.: 87.96%



MODE N° 1



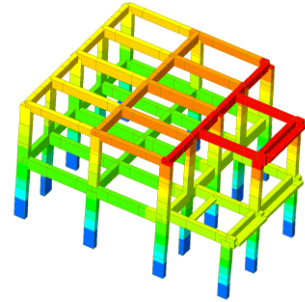
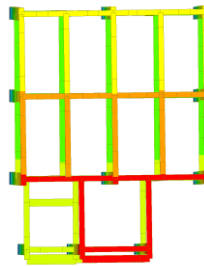
a)



MODE N° 2

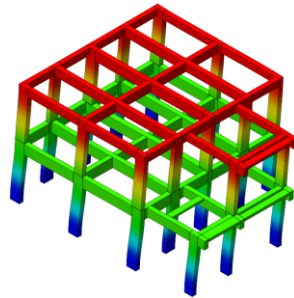
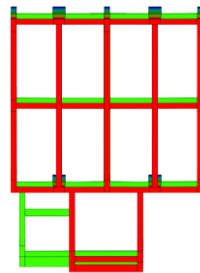
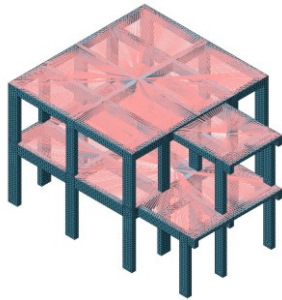
MODE N° 2 X-DIR.: 83.49%

MODE N° 1 Y-DIR.: 86.99%



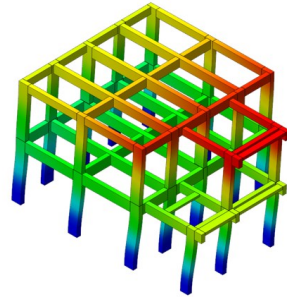
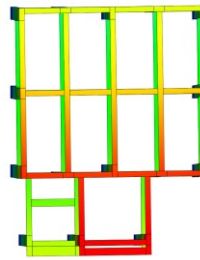
MODE N° 1

b)



MODE N° 2 X-DIR.: 89.61%

MODE N° 1 Y-DIR.: 90.40%

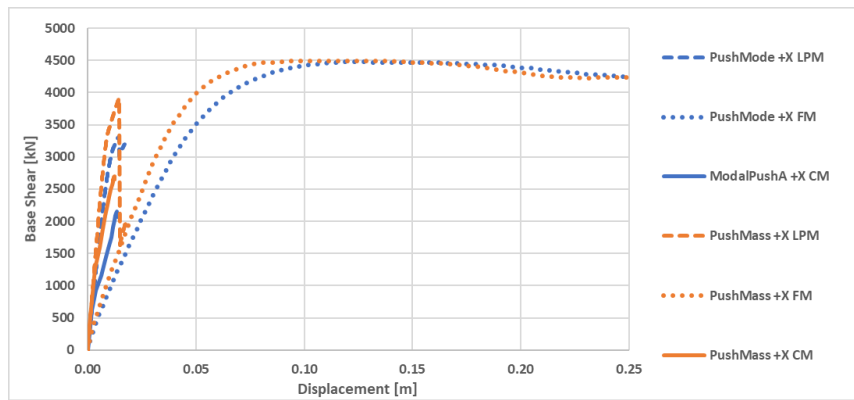


c)

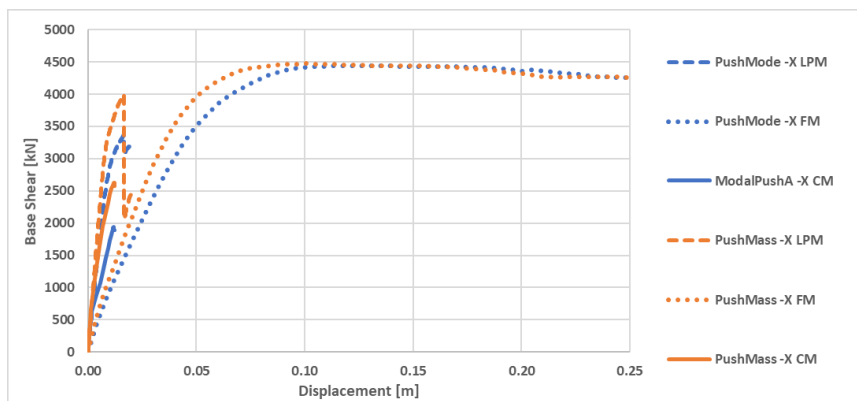
Figure 6.2 Modal analyses results for the three models: a) LPM, b) FM, c) CM.

The pushover curves obtained with the Italian Seismic Code formulation are reported in Figure 6.3 with dashed lines for the PushMode and PushMass distributions of the lumped plasticity model (LPM) and with dotted lines for the fibre model (both implemented in Midas Gen) for each direction.

In the same Figure 6.3 are reported with continuous lines the analogous pushover curves obtained for the 3D Continuum FE Model (CM) with smeared approach modelled in Midas FEA [81] (Modal pushover analyses and PushMass analyses for each direction).



a)



b)

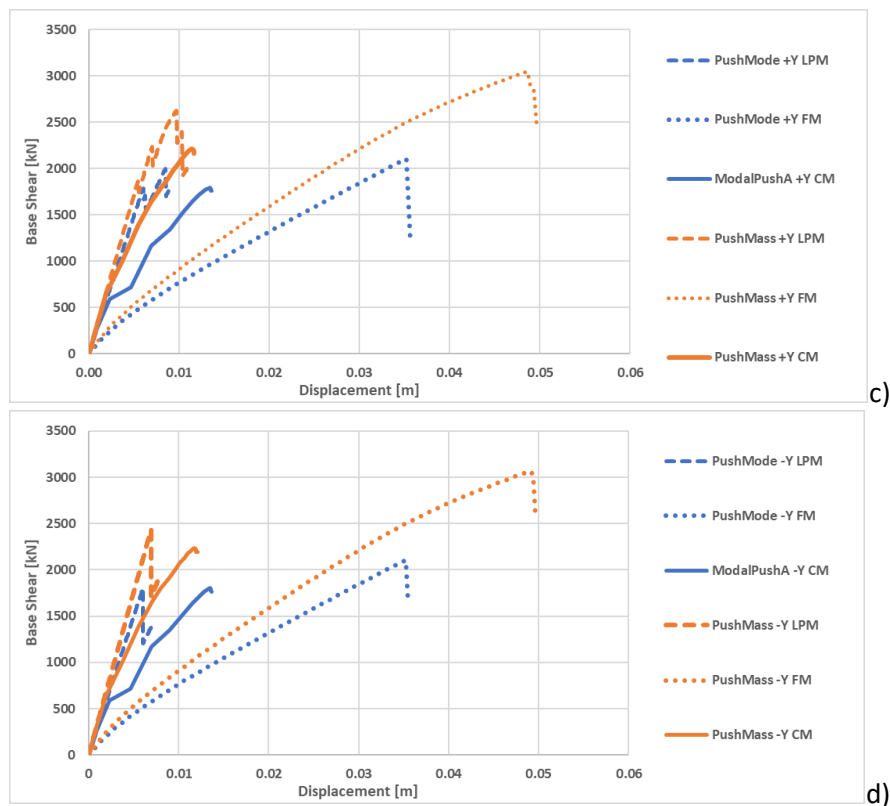


Figure 6.3 Pushover curves for the three models.

The capacity curves highlight a brittle global behaviour (i.e., when the vertical drop in the capacity curve is clear), mainly in -Y/+Y directions.

These low building performances are due to the brittle mechanisms localised on the beams of the first floor (with misalignments of structural elements) positioned between the classrooms block and the common area and toilets (Figure 6.4).

From a global point of view, it is possible to evaluate the T_R of the seismic action that corresponds to a clear drop of the base shear on the capacity (pushover) curves or, alternatively, when the shear decreases of about 15% with respect to the maximum value.

For the lumped plasticity model, the action producing a global mechanism is for $T_R=150$ years ($I_R=0.53$).

Comparing this result with those of the local checks of the safety verifications of brittle members, evaluated as explained in the previous Chapter 5 in terms of I_R ,

the global mechanism is gained immediately after the local failure for brittle mechanism ($T_R=140$ years, $I_R=0.51$).

As regards the prediction of the beam-column joint behaviour, using expressions reported in the Italian Code, the failure of most joints occurs (see Figure 6.5) for $T_R=20$ years ($I_R=0.23$).

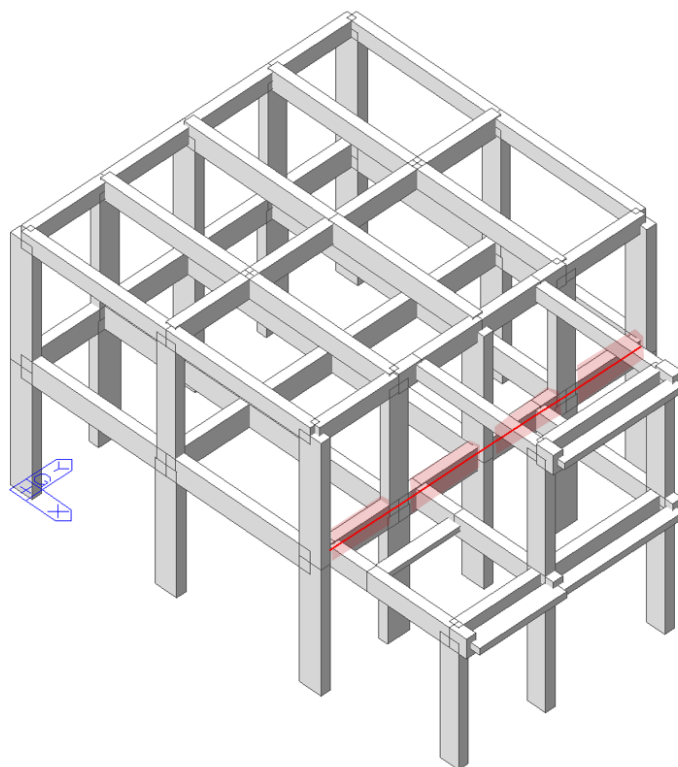


Figure 6.4 Brittle mechanisms due to the failure of the beams highlighted.

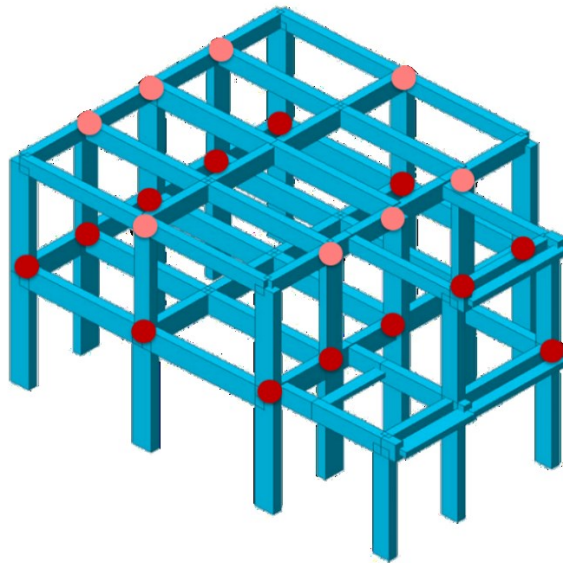


Figure 6.5 Failure of beam-column joints (red and pink dots for, respectively, the 1° floor and the 2° floor).

The consistency of the results obtained with the lumped plasticity model was checked by a comparison with the pushover curves of the fibre model (Figure 6.6). First of all, regarding the global behaviour, the initial elastic stiffness of the capacity curves of the lumped plasticity model (LPM) is markedly different than the corresponding curves of fibre model (FM).

It is known that elastic stiffness is influenced by the choice of the plastic hinge type and location: a stiffer behaviour is observed if the plastic behaviour is concentrated at the end of the element as in the lumped plasticity model [63]

It is worth noting that the use of a lumped plasticity model with a phenomenological approach implies the localisation of inelastic hinges at the beam ends and the shear span L_v ($L_v=M/V$, where M and V are the bending moment and the shear demand) that has a constant value equal to $L/2$ (where L is the element length). Furthermore, with the lumped approach, the interaction of axial-bending-shear forces during the transversal loading increment on the global and local assessment is purely numeric and is delegated to the Finite Element solver.

These quantities are a function of the shear span, which is always constant during the loading increment: this assumption can lead to under- or over-estimate the capacity of the element. This means that the capacity curve obtained from this

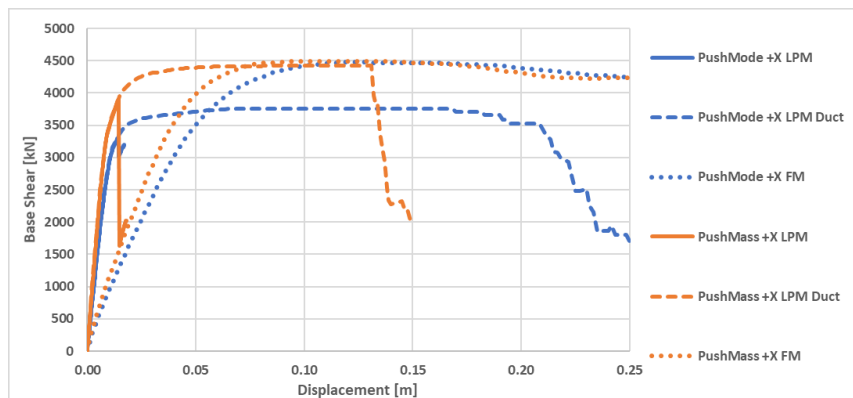
model type is not sufficient to evaluate the capacity of the structure and this explains the need for local checks.

Furthermore, as mentioned in the previous chapter, the fibre model with the formulation available in the most widespread calculation codes, is not suitable for representing nonlinear phenomena such as the buckling of rebars and bond strength between bars and concrete and shear failure.

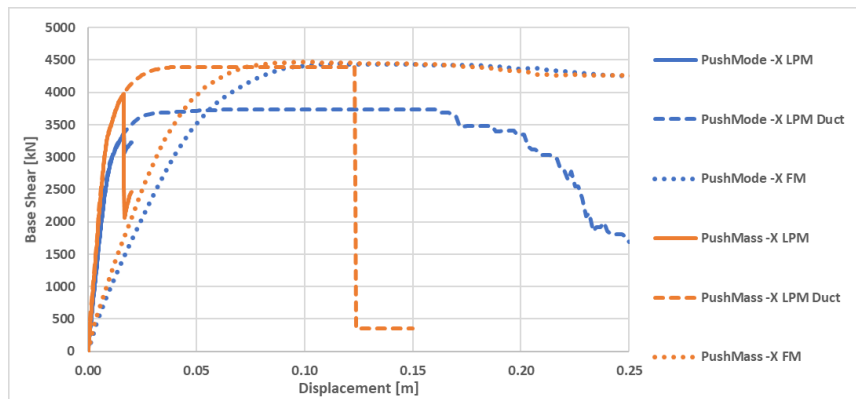
In Figure 6.6 is reported also the capacity curves obtained with the lumped plasticity model only using the bending and axial hinges (LPM Duct). The capacity curves of the LPM Duct (dashed lines) and the Fibre Model (dotted lines) are now comparable (in terms of base shear and displacement), confirming the poor representativeness of the fibre model for structures subject to shear problems.

Then, the concomitance of bending (M), shear (V) and axial force (N) and the interaction between them in the inelastic response remain the most relevant phenomena treated in an approximate and incomplete way with both types of modelling.

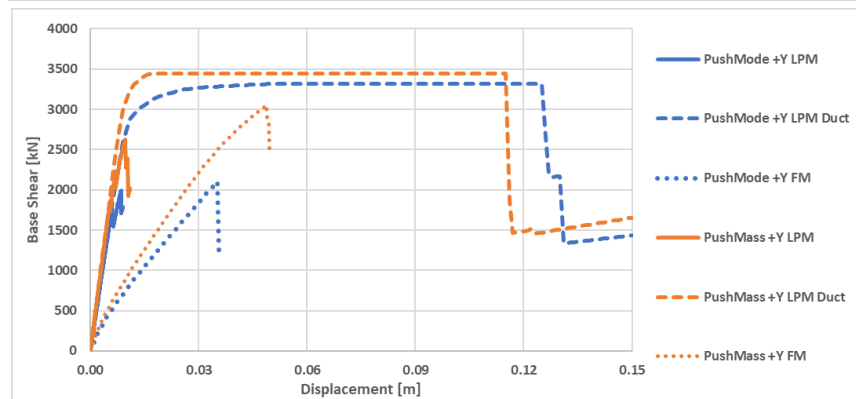
Otherwise, for example in Clementi et al. [82] and in Pierdicca et al. [72], fibre models were representative of the behaviour of analysed industrial buildings since they mainly triggered ductile-type mechanisms.



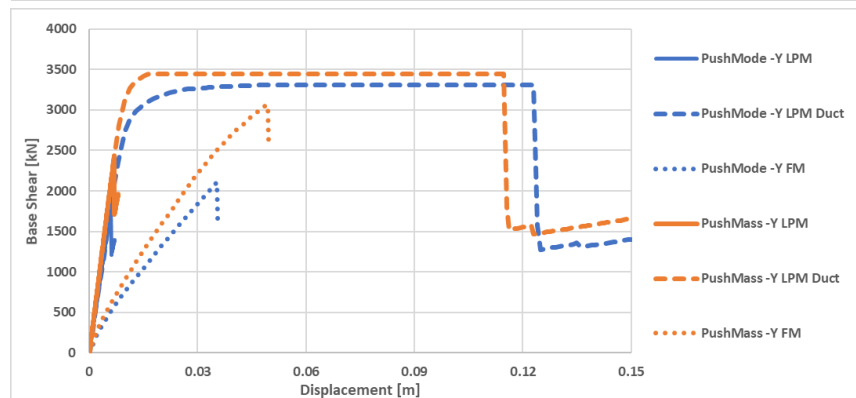
a)



b)



c)



d)

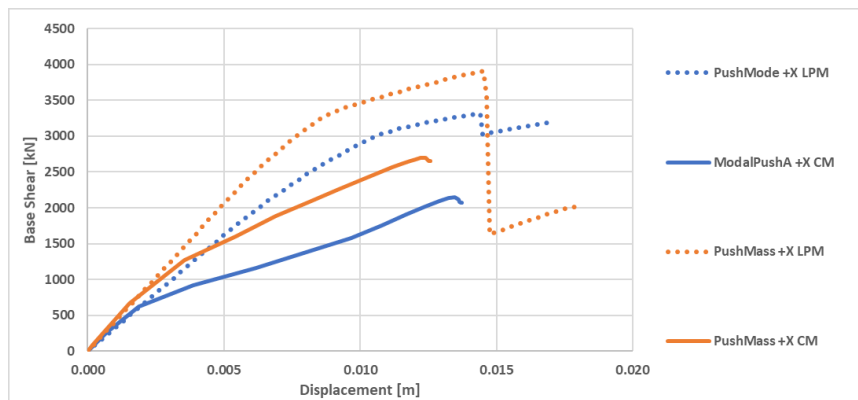
Figure 6.6 Pushover curves for the lumped plasticity model (LPM), the LPM only with axial-bending hinges and the Fibre Model (FM).

Finally, the comparison of the 3D Continuum FE model (CM) with the Lumped Plasticity model was performed indeed, for this specific building, LP model is more

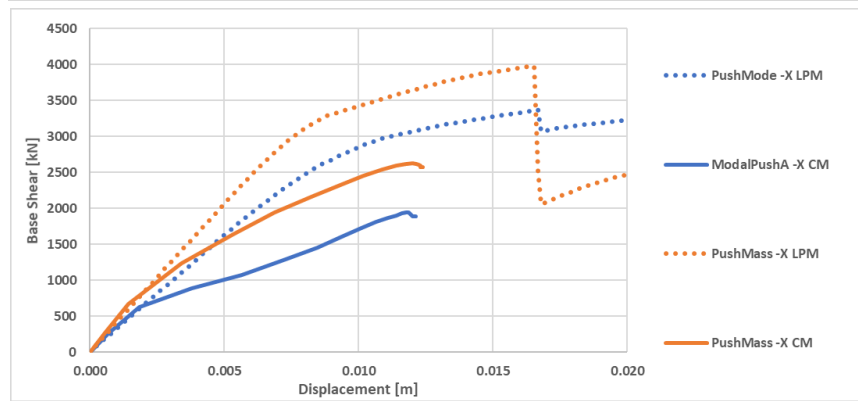
significant than the one with a distributed plasticity that does not adequately consider brittle mechanisms.

Through the continuum model is possible to evaluate together the states of stress (axial bending and shear), offering a representation of the phenomena much more realistic, as well as stresses on the beam-column joints.

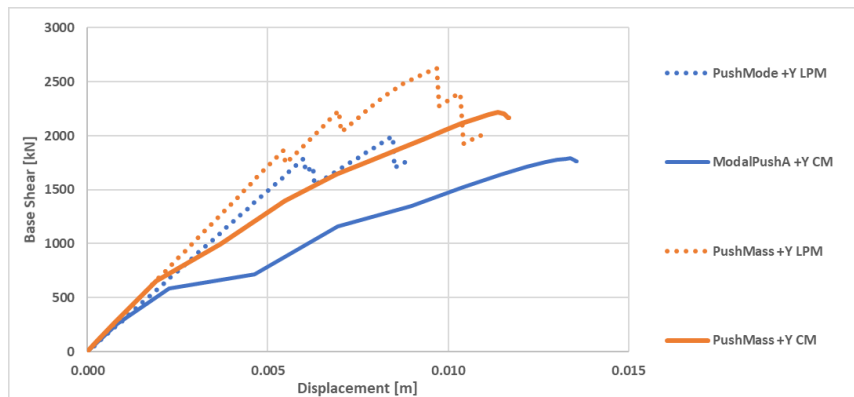
The comparison of the curves shown in Figure 6.7 shows that the capacities in terms of displacement of the curves in the most disadvantaged + -Y directions, very limited in the LPM model, tend to be much larger in the CM model. Also, it is possible to note the variation of the slope of the CM capacity curves, after a first initial elastic part overlapped on the LPM curves.



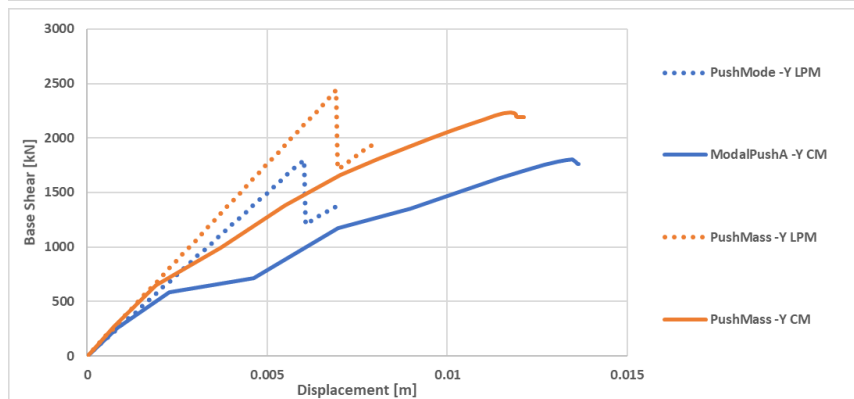
a)



b)



c)



d)

Figure 6.7 Pushover curves for the lumped plasticity model (LPM) and for the 3D Continuum Model (CM).

In Figure 6.8 below it is possible to see the cracking pattern, in particular that it spreads mainly on the beam-column joints, which are the most stressed elements together with the base of the columns. It is also possible to notice the damaged beam which can also be seen in the lumped plasticity model.

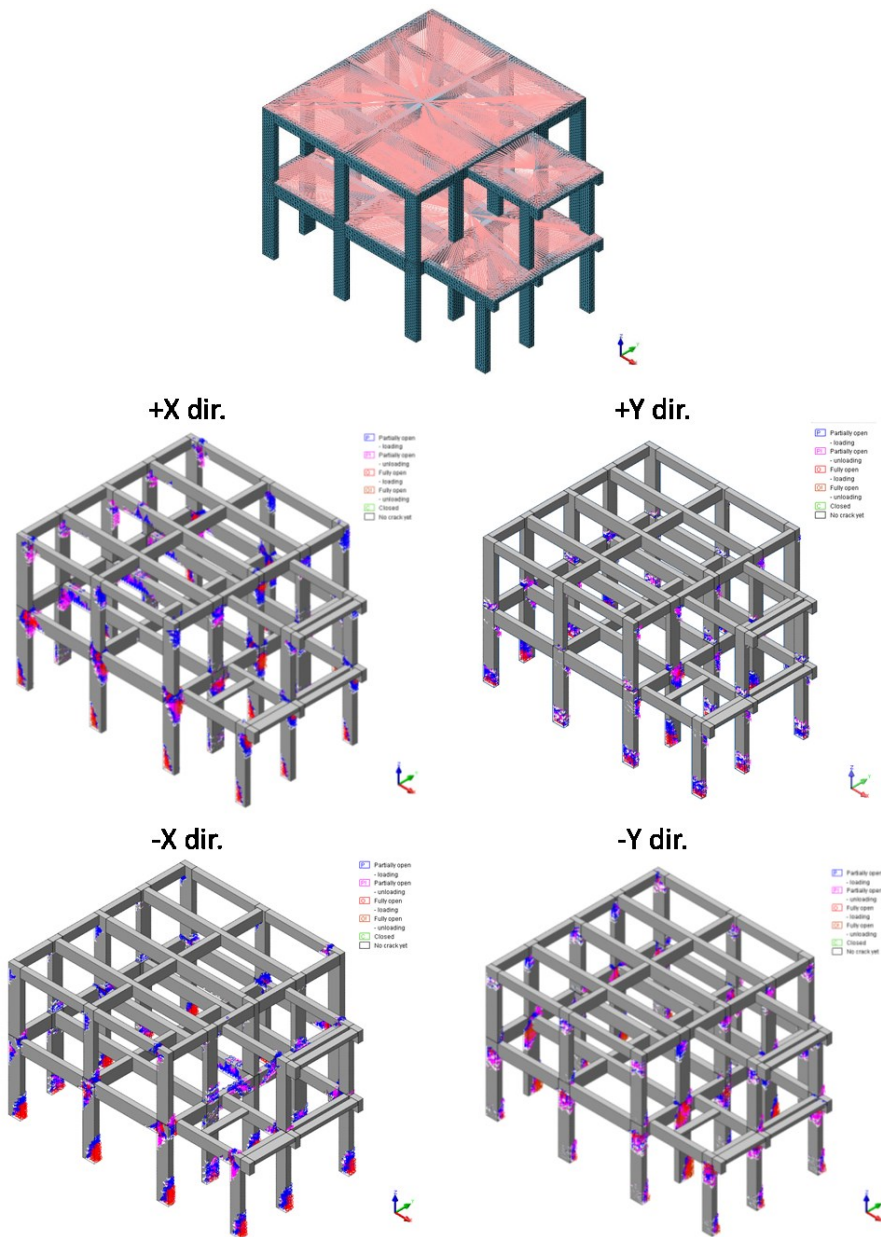


Figure 6.8 Modal pushover analyses for all directions: Crack patterns for 3D Continuum FE model with the smeared approach.

A reliable evaluation of strength and deformability of beam-column joints is a crucial aspect in the framework of performance-based design or evaluation of Reinforced Concrete (RC) buildings, as confirmed by recent experimental activities and damage observations from recent earthquakes [83].

As shown by many experimental programs, the failure of joint panels is induced usually by shear or bond flaws. The stress distribution due to flexural and shear forces transferred through the joint produces a wide diagonal crack pattern in the panel leading to a crushing failure of the compressed strut and consequently to strength and stiffness deterioration. The cyclic deterioration of bond performance, on one side, yields to reduced flexural strength and ductility of framing elements, while it yields, on the other, to a noticeable increase in the story drift.

In this case study, most of the joints subject to failure identified in the LP model confirm to be damaged in the 3D Continuum model; in some cases, the simplified lumped plasticity model tends to be too restrictive as it can be seen in the rear joints (see -X dir. on the right of Figure 6.9). In some cases, such as those on figures enlargements (Figure 6.9), it is observable the triggering of brittle mechanisms with diagonal crack pattern, while on the right of Figure 6.9 (see -X dir.) there are mechanisms of a different nature not attributable to a well-defined type of failure. In Figure 6.10 3D element strains for 3D Continuum FE model for +Y and -Y directions are shown.

Nowadays, a large consensus has not been found on a single joint modelling technique neither in the scientific literature nor in the Codes, in spite of the fact that many research groups worldwide, during the last three decades, performed wide experimental and theoretical studies on this topic to evaluate the cyclic behaviour of beam-column joints.

Due to the limited number of tested specimens, accurate numerical simulations are required to get a more reliable proof of the effectiveness of code expressions.

In this context, with a continuum approach the approximations (e. g. geometric) are limited, it should be noted that, even if the structure is simple with some negligible irregularities, there will probably be the absence of a type of mechanism that can be ascribed only to bending or to shear behaviour.

Of course, it is that the information given by the model is much more accurate about the mechanisms developed in the joints which are very complex and combined.

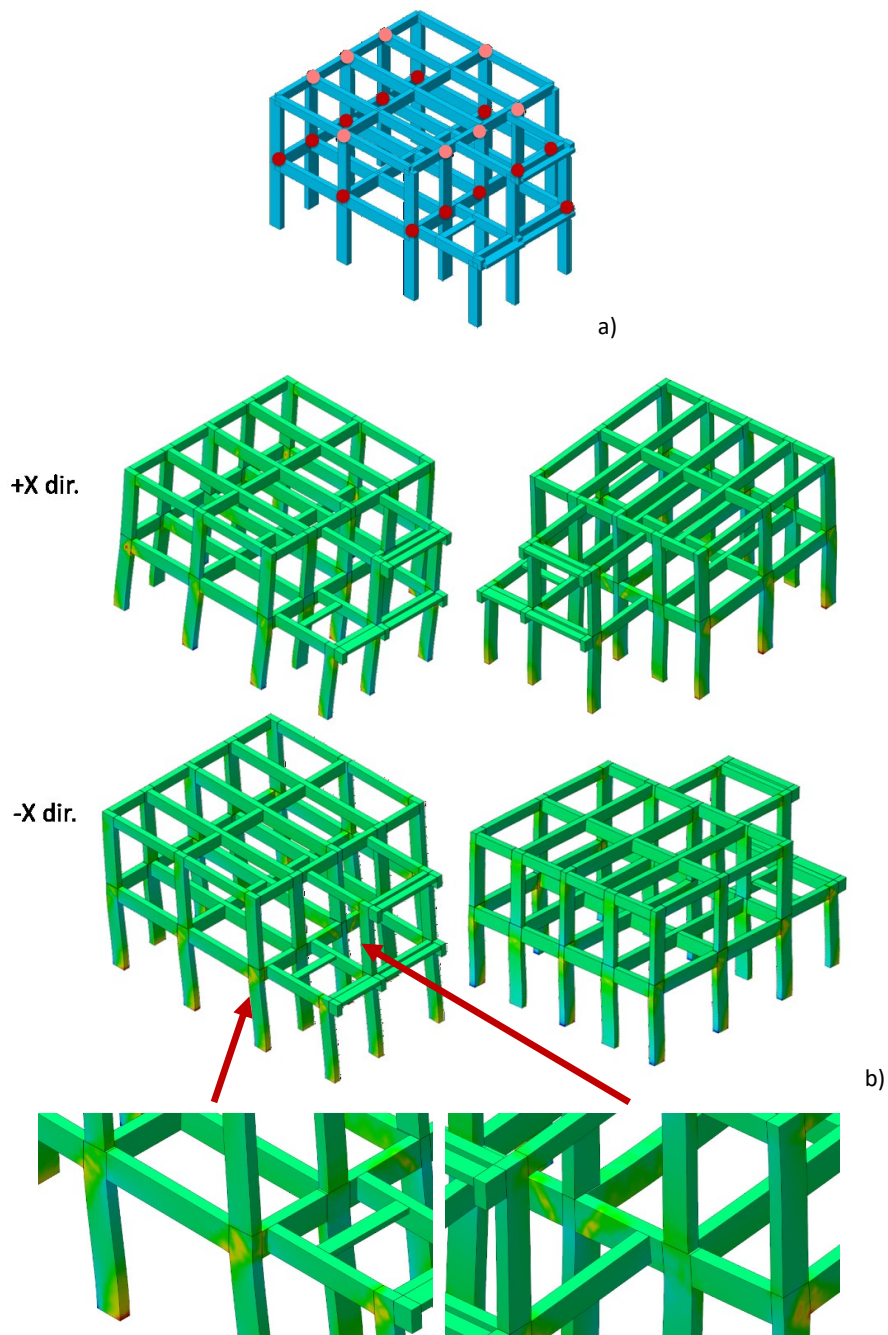


Figure 6.9 3D element strain for 3D Continuum FE model (+X, -X directions).

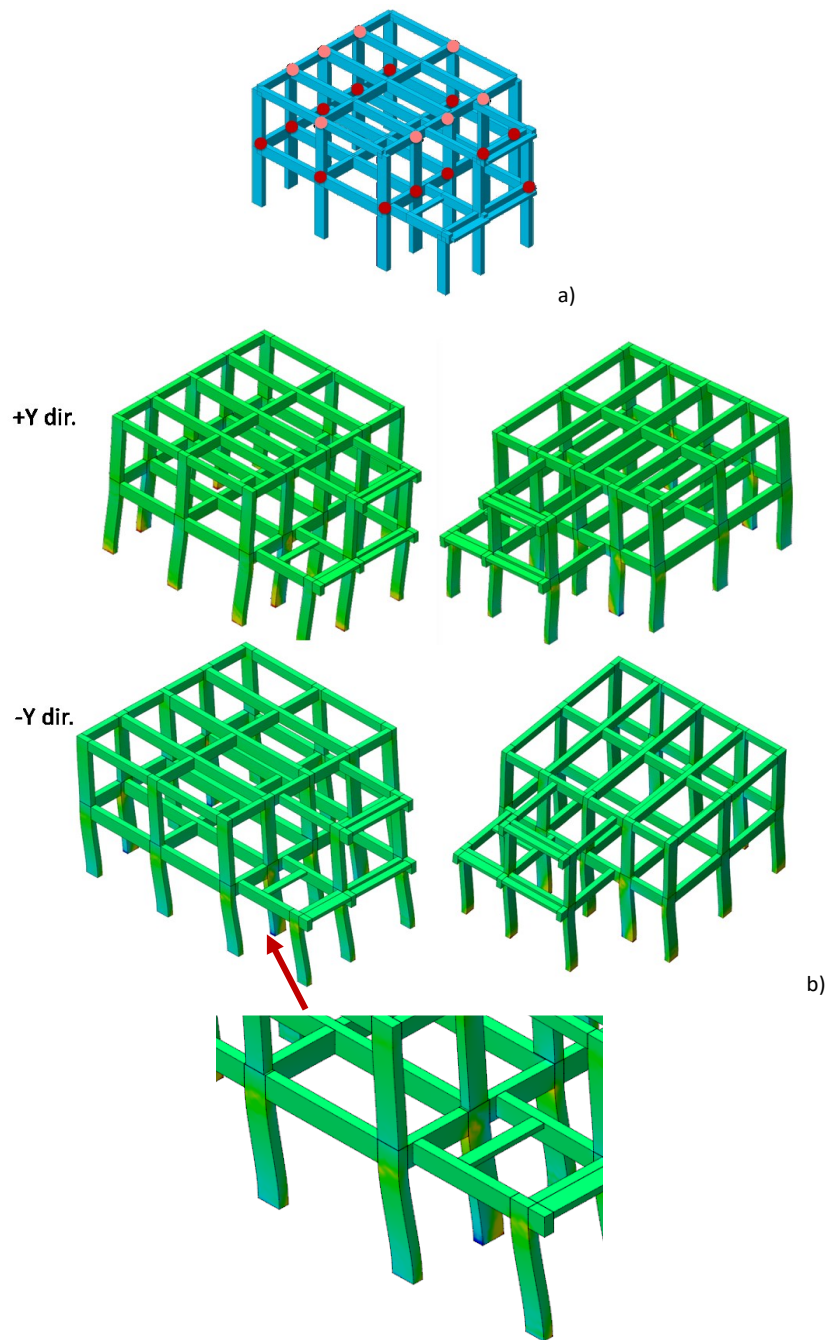


Figure 6.10 3D element strains for 3D Continuum FE model (+Y, -Y directions).

6.3 General consideration and estimate of results for buildings not investigated in detail

The complete knowledge of an existing building is not fully achievable, and it requires the structural engineer skills to compensate for the lack of information, formulating hypotheses on the structure.

Moreover, with the same information acquired and hypotheses made on the structure, the modelling and analysis method choices are significantly reflected on the results of a verification, in particular as regard as the quality of the operator, as well as his calculation tools.

The current state of knowledge about the ultimate capabilities of structural components not designed to respond to seismic actions is still underdeveloped and models are characterised by considerable dispersion (DT212). Furthermore, for each mechanism, generally, alternative models built on comparable empirical bases are available. The choice of one of them, as well as the introduction of uncertainties of the corresponding model, influences the variability of results.

The assessment process begins with the acquisition of a first level of knowledge of the geometric features of the structure to which the seismic resistance is entrusted, including the non-structural parts that may have a significant influence on the response of the structure. Through this first activity it is possible to create a preliminary model to evaluate the mechanical and geometrical parameters and the modelling hypothesis of structural response. The results of this first evaluation can be useful for drawing up the investigation plan and to complete the information already available.

The preliminary analysis is intended to determine approximately the state of the structure and its possible critical areas, where it is more important to check carefully construction details and materials.

The knowledge of the placement of the reinforcements within each element is a data of considerable importance for the reliability of the evaluation result of a RC building. This offers the possibility to proceed with the accurate modelling of the reinforcements, in particular for solid modelling.

Finally, the investigation must also be extended to unconfined beam-column joints. Generally, for beam-column joints, confined internal ones do not present critical issues. Otherwise, the external joint, and in particular those of construction before the introduction of modern seismic codes, represent critical elements for the building response.

The modelling of joints did not reach a development comparable with that of the beam-column elements and the practicable solutions are referred to rotational springs to describe the shear deformation of joints.

Note that the only type of modelling that provides accurate information on the stresses of beam-column joints is 3D Continuum FE model.

The confinement of unconfined joints is always advisable if the building is designed with the absence of stirrups in joints and with inadequate anchoring details of the reinforcement in beams and in vertical reinforcements between two building elevations.

As already mentioned, beams and columns are subject to concomitant bending, shear and axial stresses and the interaction between these is one of the most relevant phenomena in the inelastic response near the collapse of RC structures. Shear crisis represents in most cases the cause of the collapse.

In this work, the vulnerability assessment of the building has required nonlinear analyses to obtain the response of the structure.

The models used for determining the nonlinear response of beam and column available in the most common calculation codes belong to the following categories:

- Lumped plasticity models with "plastic hinges";
- Distributed plasticity models with fibre models;
- Continuum FE model with 3D solid elements for the concrete.

Obviously, the nonlinearities to be included in models are mechanical and geometric ones.

Lumped plasticity models can be used when the possibility of forming plasticized areas within the element can be excluded.

The fibre models allow to correctly describe the interaction between the axial stress and the two components of bending moment for cyclic loads.

A fibre model that describe the nonlinear flexural behaviour of elements, such as the one used for the comparison in this work, provide a basis for more advanced models that describe both bending and shear behaviours.

In the most common codes, these models are not, however, adequate to detect the degradation phenomena associated with high levels of deformation, such as bond strength between bars and concrete, rebar buckling and poor confinement.

Therefore, the fibre section models must be considered models without degradation, i.e. the constitutive law for materials or section/element for modelling

the mechanical nonlinearities of the elements are without resistance degradation caused by shear.

The phenomenon of degradation (both stiffness and resistance) is very relevant for RC elements not designed according to modern seismic protection criteria.

Rigorous models that describe both bending and shear phenomena with a necessary generality are still theoretical and experimental research topics [84] [85]. Currently, several models are available whose overall section response (NMV) is obtained joining the axial-bending behaviour of the fibre section to a uniaxial shear model independent of M and N or models composed by an element that describes the bending behaviour with NM interaction (fibre section) and one or two zero-length elements at the ends in which the shear behaviour, the axial behaviour and eventually the effect of bond strength between bars and concrete are represented. Then, the distributed approach with fibres without the addition of elements to take into account the shear behaviour is not suitable for the assessment of structures built before 1974; these constructions represent most of the building stock in Italy and they have problems about brittle mechanisms due to the high spacing stirrups, the lack of any design rule attributable to the so-called capacity design and the effect of the non-control of damage to the secondary elements.

The results obtained by the first analysis of the school building stock of Trecastelli (Section 6.1) show that many buildings assessed are characterised by brittle mechanisms and shear failures for beams, column and joints and this results in a poor applicability of the fibre approach without the addition of elements describing the shear behaviour.

The only buildings for which significant results could be obtained by using the fibre approach are Building B of G. Marconi school complex – Monterado (Section 4.4.2) and Building A of Il Girasole school complex - Ripe (Section 4.4.5), both characterised by ductile mechanisms of the columns.

7 Chapter - Reduction of seismic vulnerability of buildings by FRP local retrofit strengthening of RC Beam-Column Joints

The recent seismic events have demonstrated that the high vulnerability of existing RC structures is often related to the joint shear failure which may lead to the collapse of the entire building.

Field observation of structures damaged by L'Aquila earthquake strongly confirmed that premature failure of partially confined beam-column joints is one of the main causes limiting the global structural seismic capacity [86].

Joints damage and the greater demand of ductility in the columns are usually located in the external joints and columns, in particular the corner ones, for the following reasons.

First of all, as regards the joints, they are not confined on at least one or two faces; moreover, joints and columns are subjected to the infill strut force which is not compensated by another wall in the opposite side and finally the structural elements may be subject to greater deformations due to torsional effects that can occur on the structure. In addition, particular situations can be identified that may favour shear failure mechanisms, as can be seen where misalignments of the supporting structure occur.

However, most of the available computer software do not properly account for this aspect.

The Guidelines for repairing and strengthening of structural elements [87], infill walls and partitions developed by the ReLUIS Consortium and the Civil Protection Department agree with interventions foreseen in the OPCM 3779. The repetitiveness of some collapse mechanisms, highlighted on the earthquakes occurred, requires interventions to eliminate or reduce the original lack of the design such as, for example, the weaknesses of the external beam-column joints in the RC frames and the fragility and poor connection of the infill walls to the frame. The elimination of constructive deficiencies and typical vulnerabilities is the prerequisite for achieving the desired level of safety.

For RC buildings, the recent Guidelines for the classification of seismic risk of constructions in Annex A of DM65 7-3-2017 which modifies DM58 28-2-2017 "Sismabonus" Decree [88] [89] provide for the possibility of switch to the next higher Class of Seismic Risk for a construction, performing only local strengthening interventions and also in the absence of a prior attribution of the Class of Risk.

This is only possible if the structure was originally conceived with the presence of RC frames in both directions and if all the following interventions are carried out:

- confinement of all the unconfined peripheral panel joints of the building;
- prevention of the overturning of the peripheral infill panels on the facades;
- restoration of damaged and/or deteriorated areas.

After the assessment of the vulnerabilities and the identification of the deficiencies, the definition of local interventions to confine all the unconfined peripheral panel joints must be carried out with the most appropriate techniques to the case study, under the economic and technological aspects and with reference to the geometric characteristics of the elements to be reinforced and interaction with the rest of the structure.

Focusing on the unconfined beam-column joints, among the possible techniques that can be chosen to reinforce them, the most widespread solutions also analysed by the Guidelines [87] are based on the steel jacketing, on plating, on wrapping with composite materials and on the CAM system.

In particular, fibre reinforced polymer (FRP) systems have gained popularity as a strengthening solution because they are light weight, durable and easy to install. Many experimental tests were carried out to investigate the seismic performance of beam-column joints strengthened with FRP systems. They pointed out the effectiveness of FRP systems to improve the strength and deformation capacity of beam-column subassemblies. Recent tests and analytical studies on typical existing RC buildings demonstrated that the adoption of FRP materials as a local strengthening is a cost effective solution to improve the global seismic capacity [90].

By choosing the composite materials, it is possible to refer to the instructions of CNR-DT200 [91] and to the Guidelines of the Supreme Council responsible for overseeing public works [92].

For the instruction reported in CNR-DT200 [91], the calculation of the increase in tensile strength achievable in the panels of the unconfined joints must be carried out taking into account the contribution of the fibre-reinforced composite in the direction of the main tensile stresses and limiting the maximum deformation in the composite to the value of 4 ‰. The intervention is effective only if the ends of the reinforcement are properly anchored with the adoption of appropriate construction details. Otherwise reinforcement cannot be considered effective.

This chapter deals with the evaluation of benefits of the FRP local strengthening in the seismic assessment of RC systems designed without proper seismic details in the joint panel.

Using the previously realised 3D continuum FE model with a smeared crack approach of the same case study (Building C of the school complex of Monterado) it's possible to account for the joint nonlinear behaviour and the fibre reinforced polymer (FRP) strengthening in the finite element method (FEM). The predicted structural performances and structural damages observable before and after the retrofit intervention were compared and the benefits of the joint FRP strengthening on the global seismic performances were assessed.

7.1 Numerical model of the school building with FRP strengthening

The basic numerical model of the construction built using the software MIDAS FEA is the same shown in Chapter 5. The nonlinear behaviour of the concrete is represented by a Total Strain Crack Model based on the fixed stress-strain law concept. The incremental/iterative solution procedure employed is an Arc Length approach. The compression and the tension behaviours were the same of the previous model.

The shear capacity increase of each beam-column joint can be achieved through the application of composites with fibres placed along the principal tensile stresses. In this case, two crossed quadriaxial CFRP sheets with a unit weight of 1.75 g/cm², a thickness of dry fibre of 0.106 mm, a Young modulus of 270GPa were used for joint panel strengthening (Figure 7.1).

They were externally bonded on the joint panel with fibres in the directions 0°, ±45° and 90° respect to the beam axis.

The CFRP overlapped sheets were modelled using 3D solid elements directly connected to the nodes of the concrete meshes of the joint panels without using interface elements between the FRP and the concrete support (Figure 7.2). Thus, perfect adhesion between concrete joint and FRP was considered: this assumption reflects the use of proper anchorage solution with anchors made from fibre-reinforced polymer (FRP) composites to delay the premature FRP debonding and enhance the deformability of FRP-to-concrete interfaces.

The CFRP sheets were considered not able to carry compression loads (compressive strength almost zero) and the tensile behaviour was represented with a stress-strain relationship reported in Figure 7.1a).

The intervention was hypothesised to be less invasive as possible and only to confine the unconfined joint panel, with the idea of understanding how the FRP

strengthening modifies the global behaviour and the transverse stiffness of the structure.

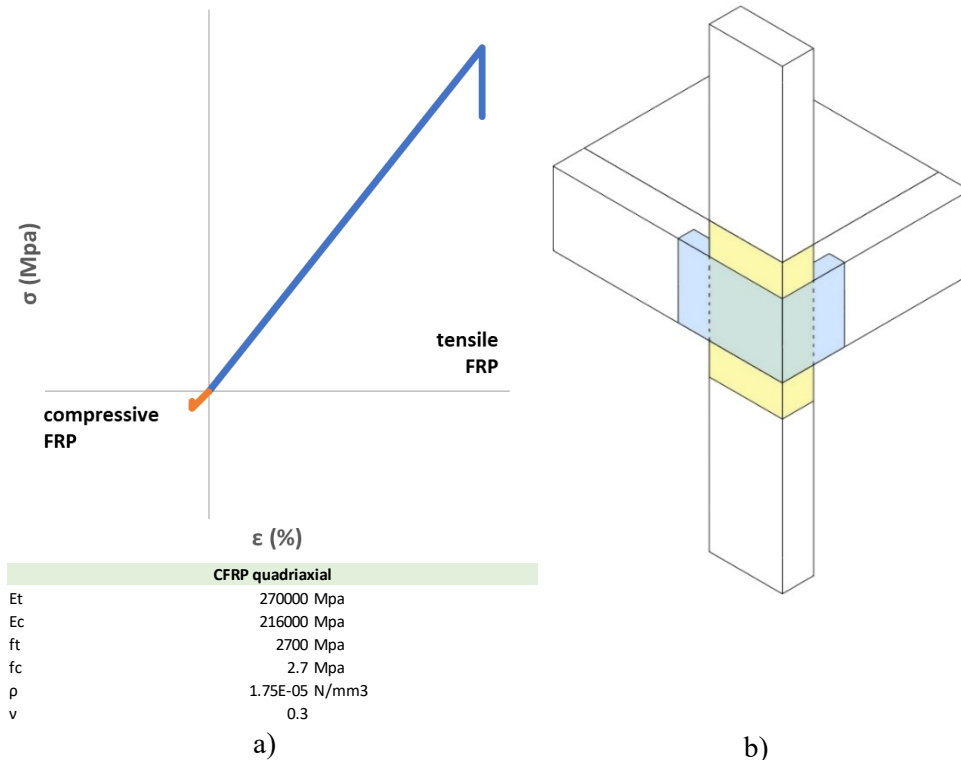


Figure 7.1 Tensile and compressive behaviours of the CFRP strengthening a) and system details b)

It is emphasised that this objective can only be achieved with sophisticated models because on simplified models the node is over strength with respect to the rest of the structure rather than subjected to the real stresses.

In fact, in the lumped plasticity approach, where the deformation capacity of the joint panels is not considered in the model and only safety checks on the joint shear strength are performed, the frame deformation capacity is dramatically low. This is because, according to the current seismic codes, the frame capacity at the ultimate limit state is limited at the joint first cracking.

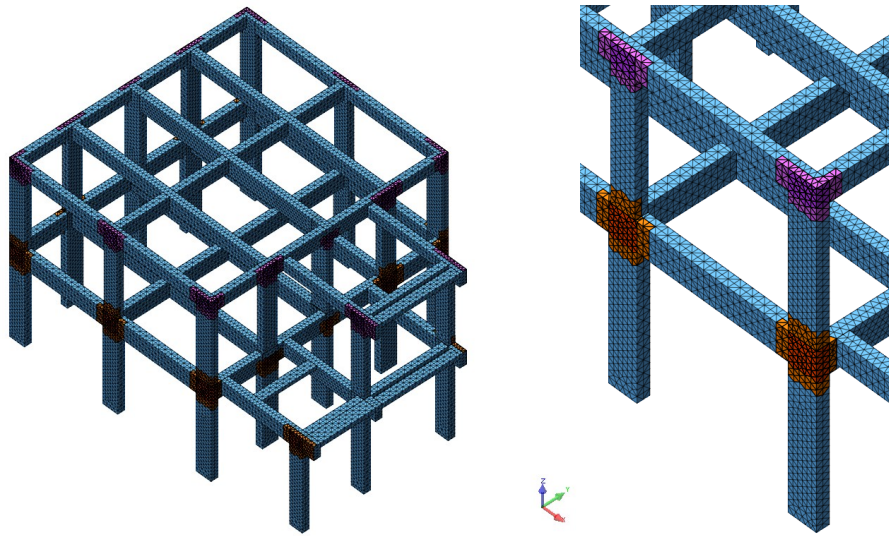
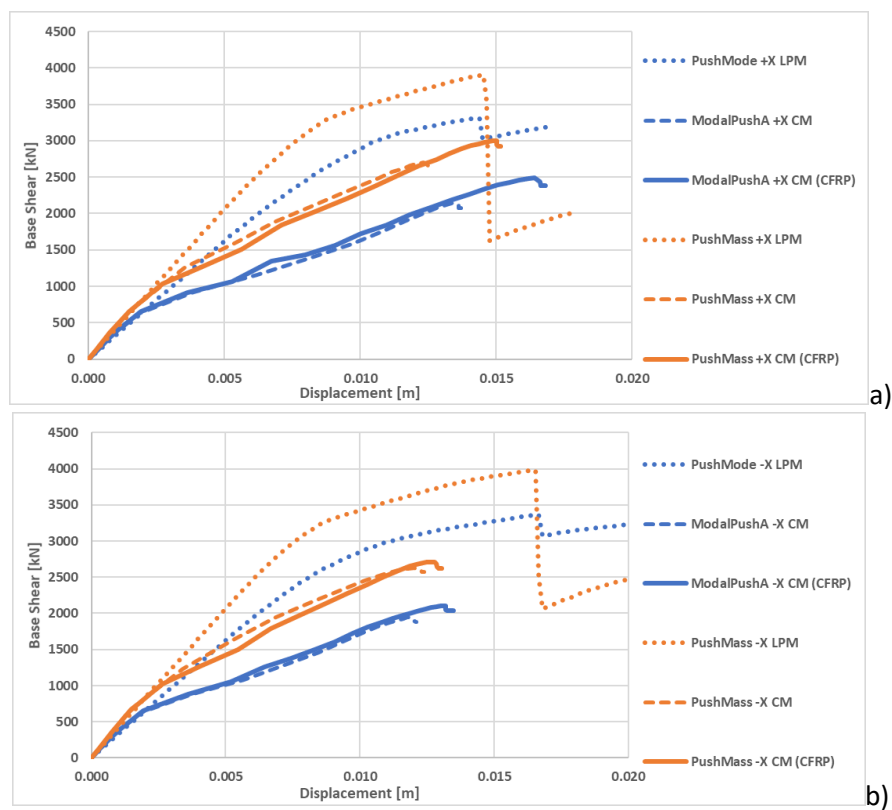


Figure 7.2 3D Continuum FE Model with FRP strengthening on beam-column joints.

7.2 Comparison of the numerical results of both unreinforced and reinforced models

Nonlinear static (pushover) analyses were carried out on unreinforced and reinforced structures, separately for the positive and negative X and Y directions. Comparing the pushover curves in Figure 7.3, the joint panel FRP strengthening improves the global displacement capacity.

Moreover, the initial stiffness does not change substantially for all directions analysed.



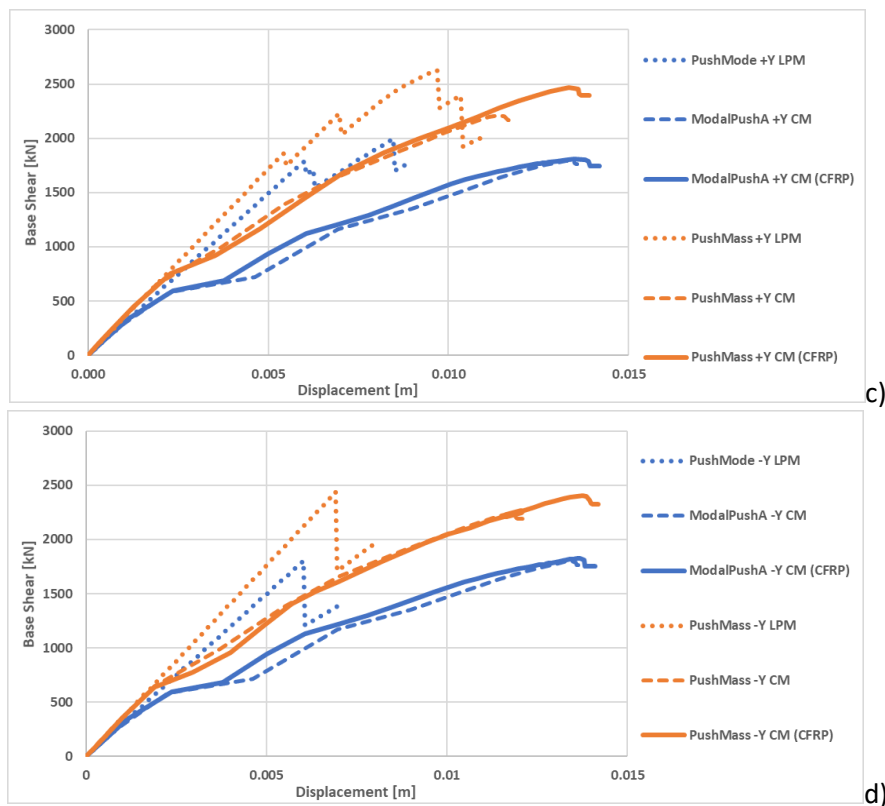


Figure 7.3 Pushover curves for the lumped plasticity model (LPM) and for the 3D Continuum FE Model (CM) without/with FRP retrofit intervention.

For +X direction, the FRP strengthening intervention increases the maximum displacement capacity of the structure of about 20% in both PushMode and PushMass analyses. For the other directions the increases vary from 5 to 20%.

The use of a local strengthening solution by means of FRP fabrics externally bonded on the exterior beam-column joints may improve the frame seismic performances of the school building that does not significantly change the stiffness of the structure.

The local strengthening of beam-column joints with a proper amount of FRP fabric prevents the joint panel shear failure promoting a more ductile failure mode with a higher displacement capacity and higher seismic performances.

Indeed, Figure 7.4 c) d) points out major flexural cracks on the beam and columns instead of joint panel shear cracks.

it is also possible to see in Figure 7.5 the comparison between the strain distributions in joint panels before and after the intervention.

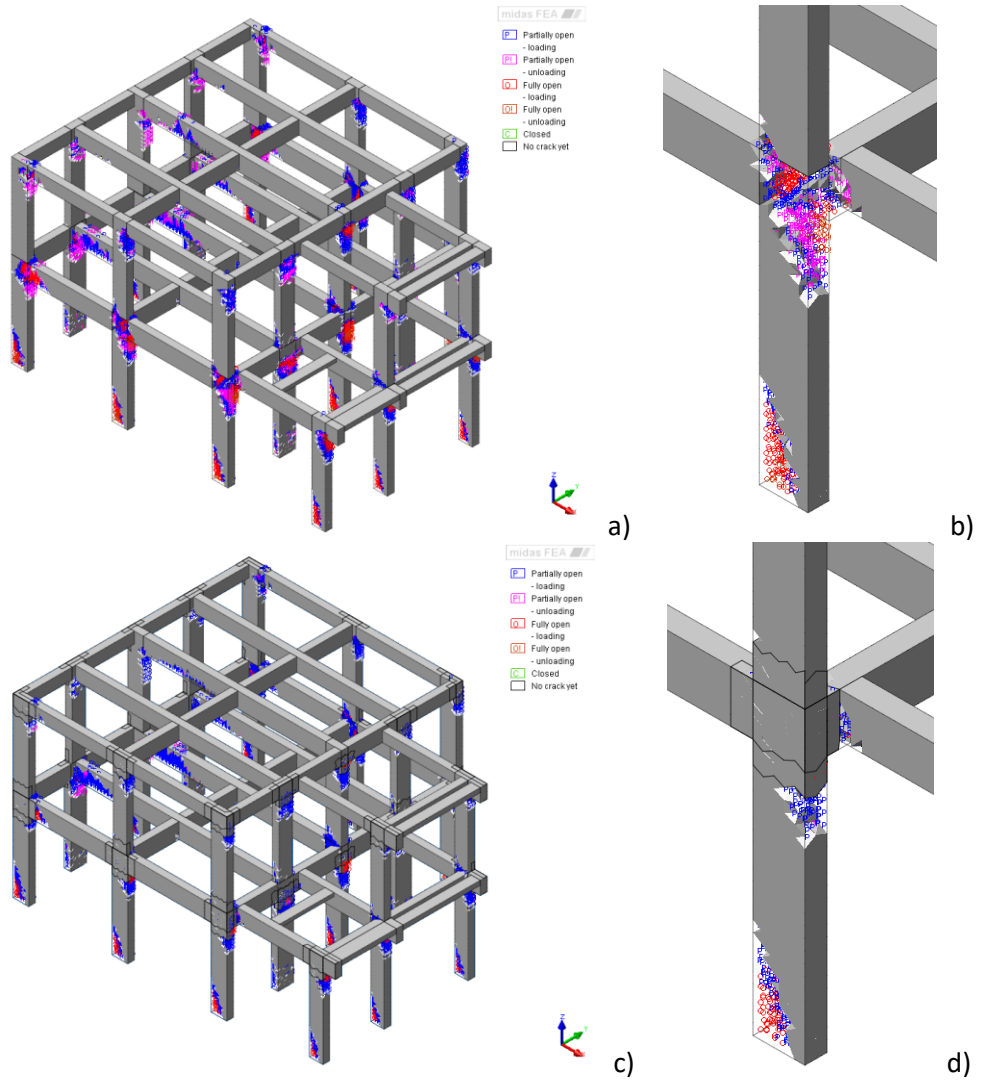


Figure 7.4 Crack patterns for 3D Continuum FE model before a), b) and after c), d) FRP strengthening intervention (+X direction).

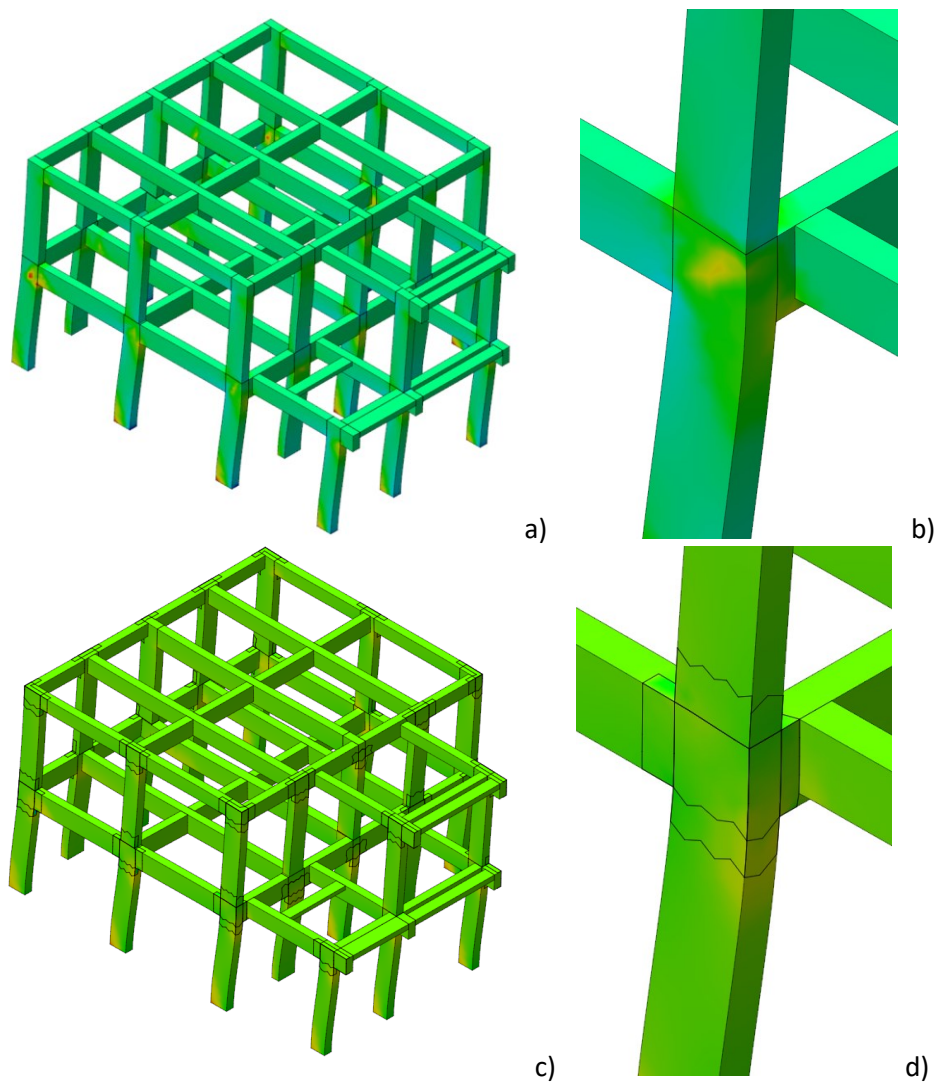


Figure 7.5 3D element strain for 3D Continuum FE model before a), b) and after c), d) FRP strengthening intervention (+X direction).

These evaluations could be extended in the future by considering further FRP strengthening configurations and alternative intervention techniques mentioned at the beginning of the chapter and comparing them with current results.

8 Conclusions and Remarks

This thesis has investigated the influence of FE modelling on typical and specific vulnerabilities of school buildings, in particular for RC constructions belonging to the lower levels of the Italian educational system.

It has been seen that architectural layouts of school buildings, with their spatial configurations result in more or less irregular structures with unfavourable seismic behaviour. Specific and typical vulnerabilities for RC school building built before the current Seismic Code were identified.

Firstly, in order to quickly evaluate the performance of school buildings, the vulnerability of each school building belonging to the municipality of Trecastelli was assessed adopting a lumped plasticity approach and a nonlinear static procedure after reaching an appropriate level of knowledge of them according to DM2018 [51].

From this first assessment carried out on the school building stock of the municipality of Trecastelli, it was found that the brittle mechanisms, and in particular those of the beam-column joints, are the most problematic phenomena based on the results of the safety verifications.

To evaluate the effects due to irregularities, misalignments, functional layouts and inadequate construction details, the RC building C of the school complex of Monterado was chosen to consider additional information provided by a more accurate modelling approach (which the mechanical nonlinearities are accurately represented) than a simpler one.

With the aim of quantifying the effective influence of these vulnerabilities detected on the global seismic behaviour, three different models were implemented correspond to as many different approaches affected by various limitations in the representativeness respect to the reality.

Nonlinear static (pushover) analyses were performed following the N2 method, with two distributions, one proportional to the fundamental mode and the other to the mass.

The capacity curves of the three models highlights a brittle global behaviour, mainly in -Y/+Y directions, due to the brittle mechanisms localised on beams of the first floor positioned between the classrooms block and the common area, even if the most severe phenomena in terms of I_R for structural performances are located in the beam-column joints.

Firstly, the consistency of the results obtained with the lumped plasticity model was checked with the pushover curves of the fibre model, denoting a markedly difference between the initial elastic stiffness of the respective capacity curves.

It is clear that elastic stiffness is influenced by the choice of the plastic hinge type and location: a stiffer behaviour is observed when the plastic behaviour is concentrated at the end of the element as in the lumped plasticity model.

It is worth noting that the use of a lumped plasticity model with a phenomenological approach implies the localisation of inelastic hinges at the beam ends and the shear span L_v has a constant value equal to $L/2$ (where L is the element length). Furthermore, with the lumped approach, the interaction of axial-bending-shear forces during the transversal loading increment on the global and local assessment is purely numeric and is delegated to the Finite Element solver.

Moreover, the fibre model with the formulation available in the most widespread calculation codes, is not suitable for representing nonlinear phenomena such as the buckling of rebars and bond strength between bars and concrete and shear failure. By making a comparison between the capacity curves obtained from the Lumped Plasticity model only using the bending and axial hinges (LPM Duct) and the Fibre Model, it is confirmed the poor representativeness of the fibre model for structures subject to shear problems.

The concomitance of bending (M), shear (V) and axial force (N) and the interaction between them in the inelastic response remain the most relevant phenomena treated in an approximate and incomplete way with both types of modelling (LPM and FM).

Finally, the comparison of the 3D Continuum FE model (CM) with the Lumped Plasticity model was performed indeed, for this specific building, LP model is more significant than the one with a distributed plasticity that does not adequately consider brittle mechanisms.

Through the continuum model is possible to evaluate together the states of stress (axial, bending and shear), offering a representation of the phenomena much more realistic, as well as stresses on the beam-column joints.

The comparison of the curves shows that the capacities in terms of displacement of the curves in the most disadvantaged $+ -Y$ directions, very limited in the LPM model, tend to be much larger in the CM model.

The cracking pattern of the 3D Continuum FE model, observables mainly on the beam-column joints together with the base of the columns and some beams of the first floor, confirms enough the results of the LPM evaluation.

In this case study, most of the joints subject to failure identified in the LP model confirms the damage in the 3D Continuum FE model; in some cases, the simplified

lumped plasticity model tends to be too restrictive as it can be seen in the rear joints. In some cases, the triggering of brittle mechanisms with diagonal crack pattern is observable, while in others there are mechanisms of a different nature not attributable to a well-defined type of failure.

In this context, with a continuum approach the approximations (e.g. geometric) are limited, it should be noted that, even if the RC frame structure is simple with some negligible irregularities, there will probably be the absence of a type of mechanism that can be ascribed only to bending or shear behaviour.

Of course, the information given by the model is much more accurate about the mechanisms developed in the joints, which are very complex and combined.

The repetitiveness of some collapse mechanisms, highlighted on the earthquakes occurred, requires interventions to eliminate or reduce the original lack of the design such as, for example, the weaknesses of the external beam-column joints in the RC frames and the fragility and poor connections of the infill walls to the frame. For RC buildings, the recent Guidelines for the classification of seismic risk of constructions (DM65 7-3-2017) which modifies (DM58 28-2-2017 "Sismabonus" Decree) [88] [89] provide for the possibility of switch to the next higher Class of Seismic Risk for a construction, performing only local strengthening interventions for structure equipped with RC frames in both directions, among which the confinement of all the unconfined peripheral panel joints of the building stands out. After the assessment of the vulnerabilities and the identification of the deficiencies, the definition of local interventions was carried out with the CFRP strengthening system.

Using the previous 3D Continuum FE model with a smeared crack approach of the same case study it was possible to account for the joint nonlinear behaviour and the fibre reinforced polymer (FRP) strengthening in the finite element method (FEM).

The intervention was hypothesised to be less invasive as possible and only to confine the unconfined joint panel, following the idea of understanding how the FRP strengthening modifies the global behaviour and the transverse stiffness of the structure.

The predicted structural performances and structural damages observable before and after the retrofit intervention were compared and the benefits of the joint FRP strengthening on the global seismic performances were assessed.

CFRP overlapped quadriaxial sheets were modelled considering perfect adhesion between concrete joint and FRP: this assumption reflects the use of proper anchorage solution with anchors made from fibre-reinforced polymer (FRP)

composites to delay the premature FRP debonding and enhance the deformability of FRP-to-concrete interfaces.

It is emphasised that this objective can only be achieved with sophisticated models because on simplified models the node is over strength with respect to the rest of the structure rather than subjected to the real stresses.

In fact, in lumped plasticity approach, where the deformation capacity of the joint panels is not considered in the model and only safety checks on the joint shear strength are performed, the frame deformation capacity is dramatically low.

Nonlinear static (pushover) analyses were performed out on unreinforced and reinforced structures, for each push direction, and comparing the capacity curves it's clear that the joint panel FRP strengthening improves the global displacement capacity.

The use of a local strengthening solution by means of FRP fabrics externally bonded on the exterior beam-column joints may improve the frame seismic performances of the school building that does not significantly change the stiffness of the structure, promoting a more ductile failure mode with a higher displacement capacity.

In conclusion, with this study it is remarked that, due to the limited number of tested specimens, accurate numerical simulations are required to get a more reliable proof of the effectiveness of code expressions.

Finally, these evaluations could be extended in the future by considering further FRP strengthening configurations and alternative intervention techniques such as steel jacketing, plating and CAM system.

References

- [1] Dolce M. Seismic safety of schools in Italy. Proc Ad Hoc Expert Gr Meet Earthq Saf Sch 2004:52–63.
- [2] Di Ludovico M, Digrisolo A, Moroni C, Graziotti F, Manfredi V, Prota A, et al. Remarks on damage and response of school buildings after the Central Italy earthquake sequence. Bull Earthq Eng 2018;1–22. doi:10.1007/s10518-018-0332-x.
- [3] Grant DN, Bommer JJ, Pinho R, Calvi GM, Goretti A, Meroni F. A prioritization scheme for seismic intervention in school buildings in Italy. Earthq Spectra 2007;23:291–314. doi:10.1193/1.2722784.
- [4] Lupo V. L'idea di scuola: didattica e tipologia (in Italian) 1996.
- [5] Carbonara P, Cicconcelli C. Architettura pratica. volume terzo. composizione degli edifici. sezioni 5-8, 2 tomi 1958.
- [6] Reza M, Kakavand A, Neuner M, Schreter M. A 3D continuum FE - model for predicting the nonlinear response and failure modes of RC frames in pushover analyses. Bull Earthq Eng 2018;16:4893–917. doi:10.1007/s10518-018-0388-7.
- [7] Antonio MP. Ph.D Thesis 2017.
- [8] Ministero dei Lavori Pubblici. Decreto Ministeriale 14 Gennaio 2008. "Norme tecniche per le costruzioni" 2008.
- [9] Vittorio Emanuele III. Regio Decreto 18 aprile 1909 n.193 1909.
- [10] Regio Decreto. Norme per l'esecuzione delle opere conglomerato cementizio semplice od armato - 2229/39 1939.
- [11] Presidente della Repubblica. Legge 2 Febbraio 1974, n. 64. "Provvedimenti per le costruzioni con particolari prescrizioni per le zone sismiche". 1974.
- [12] Presidente della Repubblica. Legge 5 agosto 1975 n.412 1975.
- [13] Ministro dei lavori pubblici e per la pubblica istruzione. D.M. 18 dicembre 1975 1975.
- [14] Ministero dei Lavori Pubblici. D.M. 3 giugno 1981 n.515 1981.
- [15] Regione Marche. Legge Regionale 3/11/1984 1984:1–5.
- [16] Presidente della Repubblica. Legge 11/01/1996 n.23 1996.
- [17] Presidente della Repubblica. D.L. 31/03/1998 n.112 1998.
- [18] Ordinanza Presidente del Consiglio dei Ministri. Ord. P.C.M. 20 marzo 2003 n. 3274 "Primi elementi in materia di criteri generali per la classificazione sismica del territorio nazionale e di normative per le costruzioni in zona sismica". 2003.

- [19] Ordinanza Presidente del Consiglio dei Ministri. opcm 3519 28/04/2006 2006.
- [20] Circolare Ministero dei Lavori Pubblici. Circolare LL.PP. 2 febbraio 2009 , n. 617 "Istruzioni per l'applicazione delle «Nuove norme tecniche per le costruzioni» di cui al Decreto Ministeriale 14 Gennaio 2008 2009.
- [21] Presidente della Repubblica. D.L. 6/12/2011 2011.
- [22] Chen C, Cheng L, Sui L, Xing F, Li D, Zhou Y. Design method of end anchored FRP strengthened concrete structures. *Eng Struct* 2018;176:143–58. doi:10.1016/j.engstruct.2018.08.081.
- [23] Ministero dell'istruzione. D.Dirett. 10-10-2013 n.267 2013.
- [24] Ministro dell'Istruzione dell'Università e della R. D.M. 5/11/2013 2013:131. doi:http://dx.doi.org/10.4236/ojo.2014.48035.
- [25] Presidente della Repubblica. Legge 24/06/2009 n.77 2009. doi:10.1109/BIBM.2013.6732455.
- [26] Presidente della Repubblica. D.L. 12/09/2014 n.133 2014.
- [27] Progetto SAVE. SCHEDA DI CENSIMENTO DEI DATI DI "LIVELLO 0" PER GLI EDIFICI STRATEGICI AI FINI DELLA PROTEZIONE CIVILE O RILEVANTI IN CASO DI COLLASSO A SEGUITO DI EVENTO SISMICO n.d.
- [28] Baggio C, Bernardini a., Colozza R, Corazza L, Della Bella M, Di Pasquale G, et al. Manuale per la compilazione della scheda di primo livello di rilevamento danno, pronto intervento e agibilità per edifici ordinari nell'emergenza post-sismica (AEDES) 2009:113.
- [29] INGV. Rilevamento della vulnerabilità sismica degli edifici n.d.
- [30] INGV - Progetto SAVE. CARATTERISTICHE TIPOLOGICHE DEGLI EDIFICI PER L'ISTRUZIONE E LA SANITÀ 2002.
- [31] Formisano A, Florio G, Gamardella F. Terremoto dell'Emilia Romagna – Maggio 2012 Report Preliminare sui Danni Riscontrati in Alcuni Edifici Pubblici dei Comuni di San Pietro in Casale (BO), Bondeno (FE) e Bomperto (MO) in Seguito agli Eventi Sismici del 20 e 29 Maggio 2012 2012:1–19.
- [32] Legambiente. Ecosistema scuola XVI rapporto di LEGAMBIENTE 2014.
- [33] Cosentino N, Manieri G, Benedetti A. A brief review of school typologies in Italy: Specific vulnerability and possible strategies for seismic retrofitting. *Keep Sch Safe Earthquakes* 2004:187–96.
- [34] Augenti N, Cosenza E, Dolce M, Manfredi G, Masi A, Samela L. Performance of school buildings during the 2002 Molise, Italy, earthquake. *Earthq Spectra* 2004;20:257–70. doi:10.1193/1.1769374.
- [35] Borzi B, Pinho R, Crowley H. Simplified pushover-based vulnerability analysis for large-scale assessment of RC buildings. *Eng Struct* 2008;30:804–20.

doi:10.1016/j.engstruct.2007.05.021.

- [36] Ceci AM, Contento A, Fanale L, Galeota D, Gattulli V, Lepidi M, et al. Structural performance of the historic and modern buildings of the University of L'Aquila during the seismic events of April 2009. *Eng Struct* 2010. doi:10.1016/j.engstruct.2009.12.023.
- [37] Augenti N, Parisi F. Learning from Construction Failures due to the 2009 L'Aquila, Italy, Earthquake. *J Perform Constr Facil* 2010;24:536–55. doi:10.1061/(ASCE)CF.1943-5509.0000122.
- [38] Rodgers J. Why Schools are Vulnerable to Earthquakes. *litkAcIn* 2012;1–27.
- [39] Clementi F, Quagliarini E, Maracchini G, Lenci S. Post-World War II Italian school buildings: Typical and specific seismic vulnerabilities. *J Build Eng* 2015;4:152–66. doi:10.1016/j.job.2015.09.008.
- [40] Al-chaar G. Evaluating Strength and Stiffness of Unreinforced Masonry Infill Structures. 2002. doi:10.1016/j.ijproman.2014.06.002.
- [41] DECANINI L, MOLLAIOLI F, MURA A, SARAGONI R. Seismic Performance of Masonry Infilled R/C Frames. 13th World Conf Earthq Eng 2004:Paper No. 165.
- [42] Fiore A, Porco F, Raffaele D, Uva G. About the influence of the infill panels over the collapse mechanisms activated under pushover analyses: Two case studies. *Soil Dyn Earthq Eng* 2012;39:11–22. doi:10.1016/j.soildyn.2012.02.004.
- [43] Fiore A, Netti A, Monaco P. The influence of masonry infill on the seismic behaviour of RC frame buildings. *Eng Struct* 2012;44:133–45. doi:10.1016/j.engstruct.2012.05.023.
- [44] Chrysostomou CZ, Asteris PG. On the in-plane properties and capacities of infilled frames. *Eng Struct* 2012;41:385–402. doi:10.1016/j.engstruct.2012.03.057.
- [45] Asteris PG, Cotsovos DM, Chrysostomou CZ, Mohebkah A, Al-Chaar GK. Mathematical micromodeling of infilled frames: State of the art. *Eng Struct* 2013;56:1905–21. doi:10.1016/j.engstruct.2013.08.010.
- [46] Di Trapani F, Macaluso G, Cavaleri L, Papia M. Masonry infills and RC frames interaction: Literature overview and state of the art of macromodeling approach. *Eur J Environ Civ Eng* 2015;19:1059–95. doi:10.1080/19648189.2014.996671.
- [47] Asteris PG, Cavaleri L, Di Trapani F, Tzaris AK. Numerical modelling of out-of-plane response of infilled frames: State of the art and future challenges for the equivalent strut macromodels. *Eng Struct* 2017;132:110–22. doi:10.1016/j.engstruct.2016.10.012.

- [48] O'Reilly GJ, Perrone D, Fox M, Monteiro R, Filiatrault A. Seismic assessment and loss estimation of existing school buildings in Italy. *Eng Struct* 2018;168:142–62. doi:10.1016/j.engstruct.2018.04.056.
- [49] Bilgin H, Uruçi R. Effects of Structural Irregularities on Low and Mid-Rise Rc Building Response 2018;4:33–44.
- [50] Masi A, Vona M, Università AM, Università MV. Estimation of the in-situ concrete strength: provisions of the European and Italian seismic codes and possible improvements. RELUIS - Eurocode 8 Perspective from Italian Standpoint Work 2009.
- [51] Ministero dei Lavori Pubblici. Decreto Ministeriale per aggiornamento delle "Norme Tecniche per le Costruzioni" - NTC 2018 2018:1–198.
- [52] Ministero dei Lavori Pubblici. Decreto Ministeriale 9 Gennaio 1996 "Norme tecniche per il calcolo, l'esecuzione ed il collaudo delle strutture in cemento armato, normale e precompresso e per le strutture metalliche." 1996:1–135.
- [53] Ministero dei Lavori Pubblici. Decreto Ministeriale 16 Gennaio 1996 "Norme tecniche per le costruzioni in zone sismiche". 1996.
- [54] Decanini LD, De Sortis A, Goretti A, Liberatore L, Mollaioli F, Bazzurro P. Performance of reinforced concrete buildings during the 2002 Molise, Italy, earthquake. *Earthq Spectra* 2004;20:1765107. doi:10.1193/1.1765107.
- [55] Ricci P, de Luca F, Verderame GM. 6th April 2009 L'Aquila earthquake, Italy: Reinforced concrete building performance. *Bull Earthq Eng* 2011;9:285–305. doi:10.1007/s10518-010-9204-8.
- [56] Verderame GM, Iervolino I, Ricci P. Report on the damages on buildings following the seismic event of 6th of April 2009, V1.20 2009:17.
- [57] Salvatore W, Caprilli S, Barberi V. Rapporto dei danni provocati dall'evento sismico del 6 Aprile sugli edifici scolastici del centro storico dell'Aquila (in Italian) 2009.
- [58] Di Ludovico M, Digrisolo A, Graziotti F, Moroni C, Belleri A, Caprilli S, et al. The contribution of ReLUIS to the usability assessment of school buildings following the 2016 central Italy earthquake. *Boll Di Geofis Teor Ed Appl* 2017;58:353–76. doi:10.4430/bgta0192.
- [59] Poiani M, Gazzani V, Clementi F, Milani G, Valente M, Lenci S. Iconic crumbling of the clock tower in Amatrice after 2016 center Italy seismic sequence: advanced numerical insight. *CINPAR 2018 - XIV Int Conf Build Pathol Constr Repair* 2018;11:314–21. doi:10.1016/j.prostr.2018.11.041.
- [60] Gazzani V, Poiani M, Clementi F, Milani G, Lenci S. Modal parameters identification with environmental tests and advanced numerical analyses

for masonry bell towers: a meaningful case study. *Procedia Struct Integr* 2018;11:306–13. doi:10.1016/j.prostr.2018.11.040.

- [61] Quagliarini E, Clementi F, Maracchini G, Monni F. Experimental assessment of concrete compressive strength in old existing RC buildings: A possible way to reduce the dispersion of DT results. *J Build Eng* 2016;8:162–71. doi:10.1016/j.jobe.2016.10.008.
- [62] Masi A, Chiauzzi L. An experimental study on the within-member variability of in situ concrete strength in RC building structures. *Constr Build Mater* 2013. doi:10.1016/j.conbuildmat.2013.05.102.
- [63] Clementi Francesco, Di Sciascio Giovanni, Di Sciascio Sergio LS. INFLUENCE OF THE SHEAR-BENDING INTERACTION ON THE GLOBAL CAPACITY OF REINFORCED CONCRETE FRAMES A brief overview of the new perspectives 2016.
- [64] Fajfar P, Gašperšič P. The N2 method for the seismic damage analysis of RC buildings. *Earthq Eng Struct Dyn* 1996. doi:10.1002/(SICI)1096-9845(199601)25:1<31::AID-EQE534>3.0.CO;2-V.
- [65] Chopra AK, Goel RK. A modal pushover analysis procedure for estimating seismic demands for buildings. *Earthq Eng Struct Dyn* 2002;31:561–82. doi:10.1002/eqe.144.
- [66] Biskinis DE, Roupakias GK, Fardis MN. Degradation Of Shear Strength Of Reinforced Concrete Members With Inelastic Cyclic Displacements. *ACI Struct J* 2004:773–83.
- [67] CEN (Comité Européen de Normalisation). Eurocode 8 - Design of structures for earthquake resistance - Part 3: Assessment and retrofitting of buildings - EN 1998-3 2005.
- [68] CNR. DT 212/2013: Istruzioni per la valutazione affidabilistica della sicurezza sismica di edifici esistenti 2013. doi:CNR-DT 212/2013.
- [69] Applied Technology Council. NEHRP guidelines for the seismic rehabilitation of buildings: FEMA 273. 1997. doi:10.6028/NIST.GCR.16-917-41.
- [70] Spacone E, Filippou FC. Fibre beam column model for non linear analysis of RC frames.pdf 1996.
- [71] Midas GEN. Analysis Manual 2018.
- [72] Pierdicca A, Clementi F, Maracci D, Isidori D, Lenci S. Damage detection in a precast structure subjected to an earthquake : A numerical approach. *Eng Struct* 2016;127:447–58. doi:10.1016/j.engstruct.2016.08.058.
- [73] Dudley Charles Kent and Robert Park. Flexural Members with Confined Concrete.pdf. *J Struct Div* 1971. doi:10.1017/S000748530002229X.
- [74] FILIPPOU F, POPOV E, BERTERO V. Effects of Bond Deterioration on

Hysteretic Behaviour of Reinforced Concrete Joints. 1983. doi:<https://doi.org/10.1016/j.jad.2016.08.040>.

- [75] Clementi F, Gazzani V, Poiani M, Antonio Mezzapelle P, Lenci S. Seismic Assessment of a Monumental Building through Nonlinear Analyses of a 3D Solid Model. *J Earthq Eng* 2018. doi:10.1080/13632469.2017.1297268.
- [76] Clementi F, Gazzani V, Poiani M, Lenci S. Assessment of seismic behaviour of heritage masonry buildings using numerical modelling. *J Build Eng* 2016. doi:10.1016/j.jobe.2016.09.005.
- [77] Clementi F, Quagliarini E, Monni F, Giordano E, Lenci, S. Cultural Heritage and Earthquake: The Case Study of “Santa Maria della Carità” in Ascoli Piceno. *Open Civ Eng J* 2017. doi:10.2174/1874149501711011079.
- [78] Structural C-FIF for. *Structural Concrete: Textbook on Behaviour, Design and Performance: Updated Knowledge of the CEB/FIP Model Code 1990. Bulletin* 2009. doi:10.1017/CBO9781107415324.004.
- [79] Vecchio FJ, Collins MP. PREDICTING THE RESPONSE OF REINFORCED CONCRETE BEAMS SUBJECTED TO SHEAR USING MODIFIED COMPRESSION FIELD THEORY. *ACI Struct J* 1988. doi:10.14359/10416.
- [80] Selby RG, Vecchio FJ. A constitutive model for analysis of reinforced concrete solids. *Can J Civ Eng* 1997. doi:10.1139/cjce-24-3-460.
- [81] Midas FEA. *Analysis and Algorithm* 2015.
- [82] Clementi F, Scalbi A, Lenci S. Seismic performance of precast reinforced concrete buildings with dowel pin connections. *J Build Eng* 2016;7:224–38. doi:10.1016/j.jobe.2016.06.013.
- [83] Prota A, Nanni A, Manfredi G, Cosenza E, Nani A, Manfredi G, et al. Seismic upgrade of beam-column joints with FRP reinforcement. *L’Industria Ital Del Cem* 2000;70:1–17. doi:10.1190/1.3587220.
- [84] Mehanny Gendy SSF, Ayoub A. Displacement and mixed fibre beam elements for modelling of slender reinforced concrete structures under cyclic loads. *Eng Struct* 2018;173:620–30. doi:10.1016/j.engstruct.2018.07.008.
- [85] Lee CS, Han SW. Computationally effective and accurate simulation of cyclic behaviour of old reinforced concrete columns. *Eng Struct* 2018;173:892–907. doi:10.1016/j.engstruct.2018.07.020.
- [86] Prota A, Di Ludovico M, Balsamo A, Moroni C, Dolce M, Manfredi G. FRP local retrofit of non-conforming RC beam-column joints. *Geotech. Geol. Earthq. Eng.*, 2014. doi:10.1007/978-3-319-00458-7_14.
- [87] ReLUIS. *LINEE GUIDA PER RIPARAZIONE E RAFFORZAMENTO DI ELEMENTI STRUTTURALI, TAMPONATURE E PARTIZIONI* 2012.

- [88] Ministro delle infrastrutture e dei trasporti. DM 58 28-2-2017 SISMABONUS 2017.
- [89] Ministro delle infrastrutture e dei trasporti. DM 65 del 07-03-2017 SISMABONUS 2017.
- [90] Vecchio C Del, Ludovico M Di, Prota A, Manfredi G. Modelling beam-column joints and FRP strengthening in the seismic performance assessment of RC existing frames. *Compos Struct* 2016;142:107–16. doi:10.1016/j.compstruct.2016.01.077.
- [91] CNR. CNR-DT 200: “CNR–Advisory Committee on Technical Recommendations for construction” 2013.
- [92] Consiglio superiore dei lavori pubblici. Linea Guida per la identificazione, la qualificazione ed il controllo di accettazione di compositi fibrorinforzati a matrice polimerica (FRP) da utilizzarsi per il consolidamento strutturale di costruzioni esistenti 2018:1–17. doi:10.1109/ChiCC.2015.7260208.